Numerical Methods for Weather Derivatives Pricing

by

CLARINDA VITORINO NHANGUMBE
STUDENT NUMBER: NHNCLA001

Thesis submitted in fulfilment of

the requirements for the degree of Doctor of Philosophy

in

Department of Mathematics and Applied Mathematics
Faculty of Sciences
UNIVERSITY OF CAPE TOWN

SEPTEMBER 2, 2024

SUPERVISOR: Dr. Ebrahim Fredericks
Department of Mathematics and Applied Mathematics, University of Cape Town

CO-SUPERVISOR: Dr. Betuel Canhanga
Departament of Mathematics and Informatic, Universidade Eduardo Mondlane

Declaration of Authorship

I, Clarinda Vitorino Nhangumbe, hereby declare that the work on which this thesis is based is my original work (except where acknowledgements indicate otherwise) and that neither the whole work nor any part of it has been, is being, or is to be submitted for another degree in this or any other university.

I empower the university to reproduce for the purpose of research either the whole or any portion of the contents in any manner whatsoever,

Signed: Clarinda Nhangumbe

Date: 2023/12/15

"All truths are easy to understand once they are discovered, the point is to discover them. "

(Galileo Galilei)

UNIVERSITY OF CAPE TOWN

Abstract

Faculty of Sciences

Department of Mathematics and Applied Mathematics

Doctor of Philosophy

Numerical Methods for Weather Derivatives Pricing

by
Clarinda Vitorino Nhangumbe

Weather derivatives are financial products used to hedge non-catastrophic weather risks with a weather index as an underlying asset. Mispricing these contracts poses a significant risk due the nature of weather variable. On rainfall derivatives pricing, the rainfall process is considered to be a stochastic, consisting of two random variables: one representing frequency, which is a two state Markov Chain, and the other representing the rainfall amount. Generally, these variables are modelled separately. The frequency is modelled by the discrete models and the rainfall amount by the continuous models. However, the debate on how to model the dynamics of rainfall amounts still open. The main objective of this thesis, is to price rainfall based derivatives using only monthly rainfall amount. The monthly rainfall amount are modeled by Ornstein-Uhlenbeck process. Then, applying the Feynman-Kac theorem we derive the partial differential equations that govern the price of an European derivative option. Since the partial deferential equation does not admit analytical solutions, we use the numerical methods to solve it. The explicit numerical methods that are special cases of finite-difference schemes and nonstandard finite difference combined with the operator splitting approaches, are proposed. The methods are effective on handling with convection dominant condition and preserve the positivity. The positivity and stability conditions are established and the numerical solutions are simulated. Furthermore, we propose the boundary conditions which have financial interpretation that are also compatible with the mathematical view points.

Keywords - Finite differences, nonstandard schemes, operator splitting, partial differential equation, stochastic models, weather derivatives.

Acknowledgements

Firstly, I would like to sincerely thank the Almighty GOD for everything in my life, including protection, wisdom, and perfect guidance, as well as the chance and capacity to work on this project.

I am enormously grateful to my supervisors, Dr. Ebrahim Fredericks and Prof. Betuel Canhanga, for their unwavering support throughout my studies and all insights which improved my research.

I would like to express my gratitude to Prof. Ercília Sousa, for the friendly guidance since the internship project in numerical methods, sponsored by Calaoust Gulbenkian Foundation. This research project would not have been possible without your support and commitment throughout these years.

I would like to thank the University of Cape Town, Faculty of Science, Department of Mathematics and Applied Mathematics, for hosting me during the research period and creating an excellent research and educational environment. The UCT Educare center, for providing a trusted and lovely environment to educate and take care of my baby, Akani Matusse. Thank you for your kindly assistance.

This work was financially supported by the Swedish SIDA Foundation International Science Program and the Eduardo Mondlane University, Faculty of Sciences, Department of Mathematics and Informatics. I would like to express my gratitude and warm regards for trusting me and investing in my studies. Prof. João Paulo Munembe, as the represent of the program, I would like to express gratitude for all support during this period.

I would like to extend my gratitude to Calaoust Gulbenkian Foundation for the financial support that allowed me to initiate this research project on numerical methods which was the base for my PhD research.

My lovely father and mother, all family and friends for unwavering love and support, thank you. I love you so much. You are always in my heart.

Last but not least, the completion of this dissertation would not have been possible without the love and support given by my family. I am so blessed to have you, Americo Matusse as my colleague, friend and husband. Such wonderful and sad moments we have been sharing. Thank you so much. For you, my always little baby, Akani Matusse, I did my best to give you all the love as your mom. Several times I had to sacrifice my attention on my research project for you. We did it together. I want you to always consider it as inspiration to achieve your goals. With love, any journey is easier and very pleasant. Love is everything!

May GOD Bless You All !!!

Contents

Abstract **iii**

1 Introduction **1**

2 Theoretical background **4**
2.1 Products and fundamentals of financial mathematics 4
2.1.1 Financial derivatives 4
2.1.2 Self financing portfolio 8
2.1.3 Market Completeness 10
2.2 Stochastic differential equations 13
2.2.1 The Itô process 13
2.2.2 The generator of Itô formula 16
2.2.3 The Feynman-Kac formula 18
2.2.4 Girsanv's theorem 19

3 Weather derivatives and the market **21**
3.1 Overview of weather derivatives 21
3.2 Rainfall index 25

4 Rain weather derivatives models and pricing **27**
4.1 Rain weather derivatives model 27
4.1.1 Overview of rainfall modelling 27
4.1.2 Rainfall dynamics 29
4.1.3 Parameter estimation 34
4.2 From the Ornstein-Uhlenbeck process to the PDE model 36
4.2.1 The PDE model 36
4.2.2 Boundary conditions 39

5 An explicit numerical method for the PDE model **44**
5.1 The generalities of finite difference methods 44
5.2 Computational domain 49
5.3 Numerical method I 50
5.3.1 Convergence analysis 52
5.3.2 Test problem: stability and convergence rate 58

5.4 Case studies with weather data 60
5.4.1 Case study with Tempelhot (Germany) data 61
5.4.2 Case study with Tofo (Mozambique) data 65
5.5 Numerical method II 70
5.5.1 Comparative results 72

6 A splitting finite difference method for the PDE model 76
6.1 The generalities of splitting methods 76
6.2 Strang splitting with upwind and Lax-Wendroff 79
6.2.1 Convergence analysis 81
6.2.2 Test problem: stability and convergence rate 84

7 Nonstandard finite differences for the PDE model 87
7.1 The generalities of nonstandard numerical methods 87
7.1.1 Foundations 88
7.1.2 Nonstandard modeling rules 91
7.1.3 Best finite difference schemes 92
7.1.4 The nonstandard methods for PDEs 93
7.2 The nonstandard numerical method for the PDE model 95
7.2.1 Convergence analysis 101
7.2.2 Test problem: stability and convergence rate 103

8 Final remarks 106
8.1 Future work 107

References 109

With love to my family . . .

Chapter 1

Introduction

Weather derivatives are financial instruments, structured as futures, options, or swaps, that facilitate the trading of weather-related risks. Unlike standard financial derivatives, which are based on tradable assets, these types of derivatives are based on specific weather indices like temperature, precipitation, wind, snow, or frost. The primary goal of employing the weather derivatives is to covering non-catastrophic weather events, which mean that, weather derivatives cover low-risk, high-probability events. For instance, companies can utilize the rainfall derivatives, which will be the focus of this work, to hedge against variations in their revenue due to dry spells or periods of heavy rain.

The weather market is still in developing. Many investors have been reluctance to participate actively. The primary cause can be the challenge of appropriately pricing the traded financial products, originated by the complexities of effectively modelling the underlying meteorological variables. It's also thought that most investors are unaware of the weather market's existence and the advantages it offers. The temperature derivatives is the most dominant market. Then, a number of studies on pricing models for weather derivatives with payouts based on temperature index Alaton et al., 2002. There is evidence of a growing demand for precipitation weather derivatives particularly by farmers, tourism industry, and hydroelectric producers Alexandridis and Zapranis, 2013. However, the literature on the pricing of rainfall derivatives has increased significantly since the introduction of rainfall derivatives at the Chicago Mercantile Exchange in 2010.

The evolution of precipitation is far more erratic and uneven than that of temperature. First of all, it is a binary event. That is, on each day precipitation may or may not be observed. Second, the rainfall is a type of local weather event and, even two locations are near together, rain at one does not always indicate that another will be raining too. This fact implies that each place needs to be modeled separately. Despite these realities, recently some approaches have been developed for modelling precipitation and pricing rainfall weather derivatives.

The rainfall is typically modeled based on cumulative of daily or monthly average amount of rainfall Emmerich et al., 2005; Nhangumbe et al., 2020; Odening et al., 2007. There are several developed methodologies. Both Carmona and Diko, 2005; Leobacher and Ngare, 2011 use the utility indifference pricing approach to price rainfall derivatives, and Markov processes are taken into account for the stochastic dynamics of the underlying precipitation. The two-stage method for the rainfall process is used in Cabrera et al., 2013; Wilks, 1998. The rainfall amount process is assumed to follow a mixed exponential distribution, and the occurrence process is modelled as a first-order two-state Markov process. A multiplicative stochastic process comprising three elements, seasonal average rain, noise, and an indicator function for modelling the probability of rain, is adopted as the rainfall model in Benth and Saltyte-Benth, 2012. Subsequently, the authors use the Escher transform and Monte Carlo simulations, to compute the prices of rainfall derivatives. A stochastic model is proposed in Noven et al., 2015 to characterise the temporal and distributional properties of rainfall. The accumulated rainfall is modelled as an integral of a continuous time ARMA (CARMA) process driven by Lévy process. Then, the authors use Fourier methods to determine the price of rainfall futures.

This work, provide contribute to the ongoing discussion around rainfall weather derivative pricing, which is still in its early stages. The dynamics of rainfall in the rainfall model, will be governed by an Ornstein-Uhlenbeck process. Then, based on this model and the cumulative index, is developed a pricing model for European option contract based on partial differential equation approach. The numerical solutions of the model are studied and the choice of boundary conditions is discussed, according to the necessity of having a well-posed problem, and boundary conditions with financial interpretation.

This thesis provides a selection of continuous time stochastic models for the valuation of rainfall derivatives contracts. The real rainfall data is used. The pricing model is developed on the partial differential equation approach. It leads to the convection-diffusion equation and it is convection dominant. Then, we study the numerical methods to approximate the convection dominant partial differential equations. The thesis consists of 8 chapters. In Chapter 2, we give an introduction to the theoretical background of financial mathematics and stochastic differential equation. Here are outlined some relevant concepts, fundamental results and techniques of financial mathematics and stochastic differential equations, used throughout the later chapters.

Chapter 3, provides general considerations about the concept of weather derivatives, the history of and evolution of the weather derivative market. The specification of weather derivative is outlined, and the relevant formulae are provided, with principal focus on rain weather derivatives. In Chapter 4, we focus on modeling

the dynamics of rainfall process, and we discuss how the models can be used to develop a rainfall pricing model based on apartial differential approach.

Chapter 5 involves the numerical evaluation of weather derivatives. First, we provide a review on finite difference methods where relevant concepts are defined. Is proposed an explicit numerical method in order to deal efficiently with the different choices of the coefficients involved in the equation, that depend on the rainfall deficit (or excess) and on the precipitation (amount of rain). Being an explicit numerical method, it will be conditionally stable. Then, we discuss the stability region of the numerical method and its order of convergence. In the end, two test cases are examined where the parameters of the model presented are estimated based on real precipitation data.

In Chapter 6 we develop an alternative numerical method based on a splitting approach for the rainfall pricing model. The two-dimensional problem is decomposed into a sequence of simpler two one-dimensional problems. Then, the numerical schemes are applied to one dimensional equations, including the analysis of stability and accuracy. Then, are implemented in such a way to produce the solution of the original equation. Such implementation has the advantage of reducing the cost of direct extensions of finite difference methods.

Chapter 7, we develop the numerical method for the European rainfall options based on nonstandard methodology. The numerical solutions are evaluated based on the concept of exact schemes and nonstandard modeling rules which tend to preserve all the underlying physical properties for the corresponding underlying problem. The nonstandard modeling rules also include the use of more complicated denominator functions, allowing us to take large time steps without sacrificing the solution's accuracy of the numerical method. We end with Chapter 8, the closing chapter. Then, the results of the thesis are summarized and provide several directions for future works.

Chapter 2

Theoretical background

In this chapter, we covered some concepts and methods of stochastic processes and financial mathematics that are pertinent to pricing financial derivatives.

2.1 Products and fundamentals of financial mathematics

In this section, we give an overview of financial tools used to manage financial risks. We give the concepts used for evaluation of financial derivatives which will be used during this thesis and are based on the literature Alexandridis and Zapranis, 2013; Björk, 2009; Cerny, 2009; Delbaen and Schachermayer, 2006; Hull, 2009, 2012; Iacus, 2011; Miyahara, 2011; Nhangumbe et al., 2020; Wilmott, 2013.

2.1.1 Financial derivatives

The value of financial derivative is contingent on the evolution of the underlying products and is called contingent claims. The mathematical definition is given under assumption of arbitrage free.

Definition 2.1.1 (of contingent claims)
A contingent claim-T, also known as a T-claim, is a contract that pays its holder a stochastic amount $X = \Phi(Z)$ at time T. The random variable X is $\mathcal{F}_T$-measurable, Z is the stochastic variable driving the stock price process, and T is the contingent claim's exercise time or contract maturity.

From the definition above, we can understand that a contingent claim represents a stochastic amount of money which the holder of the contract will obtain at the final time. Then, the main problem is to determine the price at the initial time of the contract, for a given claim X in such a way that there are no arbitrage opportunities. In order to do this, the characteristics of the market have to be investigated first. The underlying asset of the derivative and the type of financial products that will be traded are what define the financial market. Every contingent claim describes a particular financial market. For example:

- stock markets: include the stock exchange markets such as New York, London, Tokyo, Milan;
- bond markets: fixed-return securities typically issued by the central banks;
- foreign exchange, also known as currency markets: is where currencies and their values are set;
- markets for commodities: places where the fixed prices of goods like gold and oil are found;
- market derivatives such as futures, forwards, swaps, and options, are derived based on one or more underlying products, usually found in the stock, bond, currency, and commodities markets.

The market of financial derivatives consists of futures, forwards, swaps and options markets and can be classified according to the underlying asset. For instance, on the power derivative market, the underlying asset is power. For the oil derivatives market, the underlying asset is oil. And on the weather derivatives market, the underlying asset is the weather indexes. The contingent claims may be structured, exotic, or standard products. The exotic products are made to specifically address the needs of the business treasure.

Generally, financial derivatives can be traded in two types of market: the over-the-counter market (OTC) and the exchange-traded market. The OTC markets are not organized markets. Then, the term of the contract do not have to be those set forth by an exchange. Market players are free to negotiate any agreement that appeals to both parties. On the other hand, the exchange-traded market is a structured market in which the participants' contracts and their trading are both clearly defined. The exchange arranges the exchange-traded market so that traders can be certain that the deals they accept will be carried out. Below we define some of the most popular and traded contingent claims traded in these markets.

- **Forward contract**
  A forward contract on the T-claim X, made at time t, is a contract which stipulates that the holder of the contract pays the deterministic amount K at the delivery date T, and receives the stochastic amount $\mathcal{X} = \Phi(S_T)$ at delivery date T. One of the parties to this agreement takes a long position, committing to purchase the underlying asset at a predetermined price at a future date. Additionally, the opposing party takes a short position, agreeing to sell the asset at the same price on the same date. Typically, these contracts are traded on the over-the-counter (OTC) market.
- **Futures contracts**
  The futures contracts have the same setup as the forwards contracts in the

sense that they are written on the T-claim X at time t and stipulates the delivery date T. However, there is a difference in payments. On future contracts, all the payments, from the holder of the contract to the underwriter, are no longer made at delivery T, but are made continuously over time. The futures contracts are standardized contracts and are traded on an exchange market. The exchange defines the features of the contract such as, the amount of the underlying asset, the delivery date, the delivery product. The contract can be closed before the delivery date is reached.

- **Swaps**
  The term swaps refer to a fixed payment. In this contract, an agreement is made to exchange cash flows for a set of fixed future payments (the fixed leg). The agreement defines the features of the contract, such as, the start and end dates of the payments, the fixed leg, and how it has to be calculated. One could think of the forward contracts as swap contracts. In actuality, cash flow exchanges under forward contracts occur on a single future date, but cash flow exchanges under swaps occur on multiple future dates.

- **Options**
  Options is a financial contract that gives the holder the option or right (as opposed to the obligation) to buy or sell some underlying asset, and are called respectively a *call option* and a *put option*. The holder of a *call option* is granted the right to purchase the underlying asset at a predetermined price, known as the *exercise price* or *strike price*, and on a fixed date, known as the *expiration date* or *maturity*. The holder of a *put option* is granted the right to sell the underlying asset at a fixed price and on a maturity date. The options contracts can be split in respect of the exercise date, that is, *American option* and *European options*. The *European options* is a financial contract that can be exercised only on the expiration date. A financial contract known as an *American options* may be exercised at any moment prior to its expiration date. The options contracts can be traded on both exchanges and OTC markets.

  The term "at-the-money," "out-of-the-money," and "in-the-money" refers to the status of the option contract on the exercise date, based on how closely the strike price matches the price of the underlying asset. An option is considered to be "at-the-money" if its strike price is near to the cost of the underlying asset. A "*call option* with a strike price above the underlying asset price or a *put option* with a strike price below the underlying asset price is known as a "out-of-the-money option". A call option with a strike price below the underlying asset price or a put option with a strike price above the underlying asset price is referred to as an "in-the-money option".

The Option contracts when compared to other financial contracts (forwards, futures, and swap) is quit distinct. The option grants the holder the rights, with some cost associated with taking a position. However, the holder is under no obligation to sell or purchase the underlying asset. The other hedging instruments (forward, futures, or swaps contracts), which do not impose a cost associated with taking a position, provide an obligation to sell or purchase the underlying asset. A hedger can obtain exposure at a specific point in time through forward and futures contracts. This kind of hedging gives the holder the flexibility to terminate the agreement before the maturity date. However, due to basis risk, the uncertainty surrounding the difference between the futures price and the spot price on the close-out date, may cause the hedge's performance to be reduced. Conversely, the swaps contracts offer hedging for cash flows that are scheduled to happen on a regular basis over a predetermined length of time. Then, we can say that an option offers insurance and swaps provide the prices for upcoming sales.

The main idea behind these contingent claims is to catch up with market pricing. It will, however, be contingent upon both the time t and the underlying asset's price $S(t)$. At maturity T, the requirement $X \in \mathcal{F}_T$ in The **Definition** 2.1.1 ensures that the value to be paid can be ascertained. The corresponding payoff function, $\Phi(\cdot)$, is computed at the asset price at maturity, S_T. Let's now look at an example of visual representation of the payoff function for a European call option,

$$\Phi(S_T) = (S_T - K, 0)^+,$$

and for a European put option,

$$\Phi(S_T) = (K - S_T, 0)^+,$$

where K, represents the strike price.

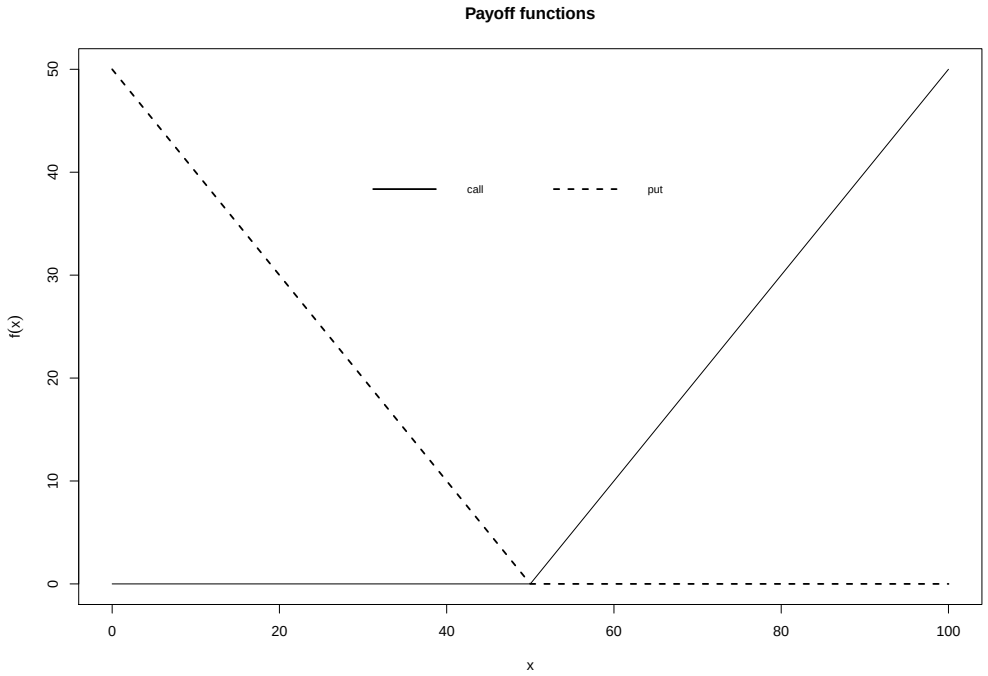

FIGURE 2.1: The payoff functions of European call and put options.

A call option holder can profit in the **Figure** 2.1 if the spot price is greater than the strike price $K = 50m.u.$ at maturity S_T. The payoff is then $(S_T - K, 0)^+ = (55m.u - 50m.u, 0)^+ = 5m.u.$ if the spot price is $S_T = 55m.u.$ Alternatively, we will have the payoff $(S_T - K, 0)^+ = 0$ if $S_T - K \leq 0$. In contrast, the holder of a put option will profit if, at maturity, the spot price is less than the strike price K. In this case, we would obtain $(K - S_T, 0)^+ = (50m.u - 45m.u, 0)^+ = 5m.u$ if $S_T = 45m.u.$ On the other hand, we will obtain $(K - S_T, 0)^+ = 0$ if the spot price at maturity is greater than the strike price, that is, $K - S_T \leq 0$.

One of the problems in financial mathematics is to study and develop the pricing models for financial asset which are also called financial derivatives. The most popular is Black-Scholes formula. The Black-Scholes model is developed under some assumptions that allow us to determine the unique price of the option. However, these assumptions are not generally true in the real world, where we can find in the market diversified asset. The principals assumptions considered in the theory of the Black-Scholes include the concepts of self-financing portfolio, free arbitrage and market completeness. These concepts are used as a starting point in the theory of financial investments and to investigate the practical problems of pricing financial asset.

2.1.2 Self financing portfolio

Definition 2.1.2 (of self financing portfolio)
Let us consider the price process $\{S(t),\ t \geq 0\}$:

- a portfolio strategy is any $\mathcal{F}_t-$ adapted $N-$dimensional process

$$\{h(t),\ t \geq 0\}$$

. $h_i(t)$ is the number of shares of the type i held during the period $[t, t + \Delta t]$;

- assuming that $S_i(t)$ is a stock price of the underlying asset to the share i at time t, the formula

$$V^h(t) = \sum_{i=1}^{N} h_i(t) S_i(t), \tag{2.1}$$

provide the value process V^h that corresponds to the portfolio h;

- a consumption process is any $\mathcal{F}_t-$adapted one- dimensional process;
- the term "self-financing" refers to a portfolio-consumption pair (h, c) where the value V^h meets the requirements of

$$dV^h(t) = h(t)dS(t) - c(t)dt. \tag{2.2}$$

Definition 2.1.3 (of risk free asset)
If the price process, S, has the dynamics

$$dS(t) = r(t)S(t)dt, \tag{2.3}$$

where r is any adapted process, then the price process S is a risk-free asset.

According to the definition of a risk-free asset, a stochastic term does not control the asset's dynamics. It may be equivalent to the price of a bond for a deterministic constant rate r, or to a bank deposit with a short interest rate r.

Definition 2.1.4 (of arbitrage)
In a financial market, an arbitrage opportunity is a self-financing portfolio h such that

$$V^h(0) = 0,\ \ P(V^h(T) \geq 0) = 1,\ \ P(V^h(T) > 0) > 0. \tag{2.4}$$

If there are no opportunities for arbitrage (absence of arbitrage), a market is said to be arbitrage free.

One way to understand the arbitrage opportunities is as a way to make positive money values without taking any risks. This is a significant issue with the financial market. Then, even though this is typically untrue in the real world, it is assumed that the market is efficient if there are no opportunities for arbitrage.

Theorem 2.1.1 (no arbitrage condition)
Assume that a self-financing portfolio h exists with the dynamics of the value process V^h given by

$$dV^h(t) = k(t)V^h(t)dt, \tag{2.5}$$

where k is an adapted process. Then, for all t, either $k(t) = r(t)$, or arbitrage opportunities exist.

The main idea behind this theorem is to consider the following: for $k > r$, we can borrow money at the rate r from the bank and immediately invest in the portfolio strategy h. It will grow at the rate k so that, from zero initial investment, we get profit at any time $t > 0$ (it means that we have the possibility of arbitrage). On the other hand, if we assume that $r > k$, we would sell the portfolio h (short) and promptly deposit the proceeds in a bank, thus creating another opportunity for arbitrage. The detailed proof of this theorem can be found in Björk, 2009.

2.1.3 Market Completeness

Enough commodities must be present in the markets for a system of markets to be considered complete. When every asset can be replicated in a portfolio, the market is considered complete. However, since time and uncertainty are part of the definition of the whole market, such markets do not exist in the real world. It is possible for certain commodities to be non-tradable, in which case the market is deemed incomplete. The concept of completeness holds great significance as it enables the evaluation of a market's inefficiencies, enabling the implementation of specific mechanisms for making such markets less incomplete. Because the martingale measure is not unique as it is in complete markets, the no-arbitrage theory of valuation, which is based on the idea of a self-financing replicating portfolio, is not applicable in incomplete markets Björk, 2009; Delbaen and Schachermayer, 2006. The Meta-theorem can be used to determine whether a market is complete:

Theorem 2.1.2 (Meta-theorem)
Let R represent the number of random sources and M represent the total number of underlying assets in the model excluding the risk-free asset. In general, the following relationships are true:

1. The model is arbitrage free if and only if $M \leq R$,
2. The model is complete if and only if $M \geq R$,
3. The model is complete and arbitrage free if and only if $M = R$.

The ideas of completeness and absence of arbitrage (arbitrage free) operate counter to one another in the meta-theorem. The theory is that an arbitrage portfolio can be created by increasing the number of underlying assets while fixing the number of random sources. Thus, the number of underlying assets must be less than the number of random sources in order to prevent an arbitrage free market. However, by including a new underlying asset in the model, we are able to replicate a particular contingent claim in new ways. In order for the market to be considered complete, there must be more underlying assets than random sources.

The meta theorem is also applied to non-tradable asset problems. For instance, we have one underlying asset and one risk asset ($M = 1$) in the Black-Scholes model. One Wiener process ($R = 1$) drives the model, ensuring that the number of underlying assets and random sources are equal. Then, the Black-Scholes model is in a complete market that is free of arbitrage, according to the meta-theorem.

Theorem 2.1.3 (First fundamental theorem in mathematical finance)
The presence of the martingale measure of the underlying asset process is a necessary and sufficient condition for the absence of arbitrage opportunities.

This theorem's proof is done in two steps: one step is to prove the sufficiency and the other step to prove the necessity. It has been demonstrated that the presence of an equivalent martingale measure is a prerequisite for the absence of arbitrage. To ensure integrability, the demonstration assumes that all asset price processes are bounded. As a result, the arbitrage is understood to be "bounded arbitrage". In order to convert the $P-$measure into a Q martingale measure, we must demonstrate the existence of a Radon-Nikodyn derivative L in $\mathcal{F}_T$, according to the Girsanov theorem. This is achieved by taking into account that $L \in L^1 = L^1(\Omega, \mathcal{F}_T, P)$ and the duality between the spaces L^1 and $L^m = L^\infty(\Omega, \mathcal{F}_T, P)$. However, this is not a general assumption (a full explanation of this can be found in Björk, 2009). Now we define the sets

$$\begin{aligned} \mathcal{K} &= \mathcal{K}_0 \cap L^\infty, \\ L^\infty_+ &= \text{the set of non-negative random variables in } L^\infty, \\ C &= \mathcal{K} - L^\infty_+. \end{aligned} \tag{2.6}$$

$\mathcal{K}$ represents all bounded claims which are reachable by a self-financing portfolio at zero initial cost.$\mathcal{K}_0$ denotes the space of all claims which can be reached by a self-financing portfolio at zero initial cost. C consists of claims in $\mathcal{K}$ that can be reached by self-financing portfolio with zero initial cost if the investor also permits himself to throw away the money. We conclude that $C \cap L^\infty_+ = \{0\}$ and that L^∞_+ and C are

convex sets in L^m with a single common point, assuming that there is no arbitrage assumption. The random variable $L \in L^1$, which is nonzero, such that

$$\begin{aligned} (a): \quad & E^P[LX] \geq 0, \ \ \forall X \in L^{\infty}_{+} \ \text{ and} \\ (b): \quad & E^P[LX] \leq 0, \ \ \forall X \in C \end{aligned} \tag{2.7}$$

is guaranteed by the convex separation. By scaling L so that $E^P[L] = 1$, one can determine that $L \geq 0$ from (2.7(a)) and use L as a Radon-Nikodym derivative to define a new measure Q by $dQ = LdP$ in $\mathcal{F}_T$. Q is a prime candidate as a martingale measure.

The existence of a martingale measure Q implies the absence of arbitrage, which is how sufficiency is demonstrated. First, we assume that Q exists, and then we apply the Girsanov theorem to show that all price processes can be expressed with zero drift under Q. Moreover, the non-arbitrage possibility is demonstrated by supposing the existence of a uniformly bounded, self-financing process h. Then, it is required that,

$$P(V(T,h) \geq 0) = 1 \ \ \wedge \ \ P(V(T,h) > 0) > 0, \tag{2.8}$$

where $V(T,h)$ represents the process h's value at T's maturity. Given that h may be a possible arbitrage portfolio according to the condition (2.8), we must demonstrate that $V(0,h) > 0$ in order to ensure that there is no arbitrage. This is derived by taking into account that under Q, we also obtain the condition (2.8) from $Q \sim P$. On the other hand, it is demonstrated that $V(t,h)$ is $Q-$martingale since h is self-financing and bounded, meaning that $V(0,h) = E^Q[V(T,h)]$ and $V(0,h) > 0$, Since (2.8) under Q implies that $E^Q[V(T,h)] > 0$.

Theorem 2.1.4 (Second fundamental theorem in mathematical finance)
Consider that there are no opportunities for arbitrage. Then, the necessary and sufficient requirement for the market's completeness is the uniqueness of the martingale measure.

The demonstration of this theorem is made in two stages. Assuming that the martingale measure Q is unique in the sufficiency, $M = \{Q\}$ implies that Q is trivially an extreme point of M. Consequently, the stochastic integral of the form

$$M(t) = x + \sum_{i=1}^{N} \int_0^t h_i(s) dZ_i(s), \tag{2.9}$$

can be used to represent every $Q-$ martingale M, where x represents the initial value of the portfolio, N the number of shares, $Z_i(s)$ the price of each share. The

expression (2.9), suggests that M can be hedged in the $S-$ economy, proving the completion of the model. The requirement is derived from the idea that, in the event that the market is complete, each claim X can be duplicated, resulting in a hedging portfolio h,

$$V(t,h) = E^Q[e^{-\int_t^T r(s)ds} X|\mathcal{F}_t].$$

Björk, 2009 contains further information regarding the proof of the first and second fundamental theorems in mathematical finance. These two theorems allow one to ascertain the financial market's completeness and arbitrage-free conditions from a martingale perspective. Thus, under the assumption of arbitrage free principle and a complete market, the unique price $\pi(S)$ of a risk-free contingent claim S can be found using the following formula:

$$\pi(S) = E^Q[e^{-rT}S] \tag{2.10}$$

where r is the risk-free asset's interest rate and Q is the unique martingale measure. The price $\pi(S)$ is expected to fall within the interval

$$\pi(S) \in \left[inf_{Q\in\mathcal{M}} E^Q[e^{-rT}S], sup_{Q\in\mathcal{M}} E^Q[e^{-rT}S]\right]. \tag{2.11}$$

In this scenario, the set of all equivalent martingale measures is denoted by $\mathcal{M}$.

2.2 Stochastic differential equations

In this section we introduce terminology and fundamental ideas of stochastic calculus in continuous time, which are necessary for pricing financial derivatives Karatzas and Shreve, 1988, 1998; Klebaner, 2005; Nhangumbe et al., 2020; Oksendal, 2000.

2.2.1 The Itô process

More realistic mathematical models of various phenomena are obtained by allowing randomness in some of the coefficients of differential equations. In financial mathematics, one of the well known models is the famous Black and Scholes option price formula. This formula was developed by Fischer Black and Myron Scholes (1973), when they used stochastic analysis and an equilibrium argument to compute a theoretical value for the price of a European call option. This formula has become to be an indispensable tool for mathematical modeling in finance and the authors were awarded the Nobel prize in Economics in 1997 for their work related to this formula.

The random quantity added to the differential equation is mathematically called a random variable, which we define next.

Definition 2.2.1 (of random variable)
A random variable X is an $\mathcal{F}-$ measurable function $X : \Omega \to \mathbb{R}^n$, where Ω is a topological space.

Definition 2.2.2 (of stochastic process)
Let us define the probability space $(\Omega, \mathcal{F}, P)$. A stochastic process also called random processes is a parametrized collection of random variables $X = \{X_t\}_{0 \leq t < \infty}$ on $(\Omega, \mathcal{F}, P)$, having values in $\mathbb{R}^n$.

Every stochastic process realization, also known as the stochastic process sample path, is a function of time t. It can be categorized based on the time it takes or the values it can accept. For both classifications we have two forms, the discrete or continuous. The combination of time class and the type of values lead to the following 4 categories:

- discrete time-discrete variable,
- discrete time-continuous variable,
- continuous time-discrete variable,
- continuous time- continuous variable.

The stochastic process consists of two components, that are, the deterministic component and an Brownian component. The category of "continuous time-continuous variable", can be thought of as an extension of differential equations that are produced by adding a random term $\sigma(t, X_t)W_t$ to the differential equation,

$$\frac{dX_t}{dt} = b(t, X_t) \tag{2.12}$$

to get,

$$\frac{dX_t}{dt} = b(t, X_t) + \sigma(t, X_t)W_t. \tag{2.13}$$

Here, the stochastic process is denoted by $X_t \in \mathbb{R}^n$. The drift rate of the stochastic process X_t per unit time is $b(t, X_t) \in \mathbb{R}^n$. The "White noise" is indicated by $W_t \in \mathbb{R}^m$, and the variance rate of the stochastic process X_t, or the intensity of the noise at variable X_t per unit time, is indicated by $\sigma(t, x) \in \mathbb{R}^{n \times m}$. According to the equations (2.13), an unknown rate (the "white noise") combined with a known rate (the deterministic term) can explain variations in the variable over short time periods. The Itô formula or process provides one of the possible interpretations of

equation (2.13), that is,

$$dX(t) = b(t, X(t))dt + \sigma(t, X(t)dW_t \tag{2.14}$$

In order to obtain the Itô equation, substitute $W_t = \frac{dB_t}{dt}$ for the component W_t in the equation (2.13) and we multiply the resulting equation by dt. In this case, the deterministic coefficient b is referred to as the drift coefficient and the stochastic coefficient σ is referred to as the diffusion coefficient.

The forms of the diffusion $\sigma(t, x)$ and drift $b(t, X_t)$ components determine the types of stochastic differential equations (2.14). For example, if X_t has a constant drift rate equal to b and constant variance equal to σ^2 per unit time, then (2.14) yields the following form:

$$dX_t = bdt + \sigma dW_t. \tag{2.15}$$

By assuming in (2.14) that both the drift rate and variance rate are functions of X_t, that is, change over time, we define the well-known geometric Brownian motion model. The geometric Brownian motion is primarily used to model stock price changes. The expected proportional change in a short period of time stays constant, while the expected absolute change in a short period of time varies with time, and the uncertainty about the magnitude of future changes in the variable is proportional to the variable,

$$dX_t = bX_t dt + \sigma X_t dW_t. \tag{2.16}$$

The Itô process, then, can be understood as a generalization of the Wiener process or Brownian motion, with b and σ being functions expressed in general form (2.14) of the underlying variable X and time t. Such a stochastic process is called Itô diffusions Oksendal, 2000 if the solution of (2.14) is understood as a representation of the mathematical trajectory of the motion of a small particle in a moving fluid. In the sense of the Markov property, the Itô diffusion possess the property of being time-homogeneous, meaning that the Itô diffusion's future behaviour remains independent of its past. Is usual to assume that in (2.13) that the process W_t has the following properties:

i for $t_1 \neq t_2$ implies that the noise terms W_{t_1} and W_{t_2} are independent;

ii the noise term $\{W_t\}$ is stationary. It means that the joint distribution of $W_{t_1+t} \ldots$, W_{t_k+t}, does not depend on t;

iii $E(W_t) = 0$ for all t.

However, many stochastic processes do not satisfy the properties *i* and *ii*. And for such noise term W_t we do not have continuous paths. However, the noise term

W_t can be represented as a generalized stochastic process called the white noise process or just rewrite equation (2.13) in a form that suggests a replacement of the noise term W_t by a proper stochastic process. The assumptions *i*, *ii* and *iii* on the noise term W_t suggest to have stationary independent increments with mean zero, when consider the discrete version of stochastic process (2.13). Then, such process with continuous paths is only the Brownian motion B_t. Thus, the Itô integral is defined as the random variable

$$I_t(X) = \int_0^t X_s dB_s = \lim_{n\to\infty} \sum_{i=1}^{n-1} X(s_i)(B(s_{i+1}) - B(s_i)). \tag{2.17}$$

It has been figured out that the Itô process (2.14), which was previously expressed in differential form, can also be rigorously expressed in integral form.

Definition 2.2.3 (Itô integral)
The Brownian motion in $(\Omega, \mathcal{F}, P)$ is denoted by B_t. For a stochastic process X_t in $(\Omega, \mathcal{F}, P)$, an Itô process (also called an Itô stochastic integral) has the form

$$X_t = X_0 + \int_0^t b(s,w)ds + \int_0^t \sigma(s,w)dB_s, \tag{2.18}$$

here, $\sigma \in \mathcal{W}_{\mathcal{F}} = \bigcap_{T\geq 0} \mathcal{W}_{\mathcal{F}}(0,T)$, $\mathcal{W}_{\mathcal{F}}(0,T)$ is the class of process $\sigma(t,w) \in \mathbb{R}$ satisfying the following properties:

- $(t,w) \to \sigma(t,w)$ is $\mathcal{B} \times \mathcal{F}$- measurable ($\mathcal{B}$ denotes the Borel σ-algebra on $[0,\infty)$);
- Exists an increasing family of σ-algebras $\mathcal{F},\ t \geq 0$ in which σ is $\mathcal{F}_t$-adapted and B_t is a martingale with respect to $\mathcal{F}_t$;
- $$P\left[\int_0^t \sigma^2(s,w)ds < \infty \text{ for all } t \geq 0\right] = 1, \tag{2.19}$$

$b(s,w)$ is $\mathcal{F}_t-$adapted and

$$P\left[\int_0^t |b(s,w)|ds < \infty \text{ for all } t \geq 0\right] = 1. \tag{2.20}$$

2.2.2 The generator of Itô formula

Theorem 2.2.1 (the Itô formula)
Taking into account the Itô process X_t, which can be expressed as follows:

$$dX_t = b(t,x_t)dt + \sigma(t,X_t)dB_t, \tag{2.21}$$

and the process $f(t,x)$, which is twice continuously differentiable on $[0,\infty)\times\mathbb{R}$. As a result, $Y_t = f(t,X_t)$ is also an Itô process, and its stochastic differential equation process is given by

$$dY_t = \frac{\partial f}{\partial t}(t,X_t)dt + \frac{\partial f}{\partial x}(t,X_t)dX_t + \frac{1}{2}\frac{\partial^2 f}{\partial x^2}(t,X_t)(dX_t)^2, \tag{2.22}$$

where $(dX_t)^2 = (dX_t)(dX_t)$ is calculated following rules

$$dtdt = dtdB_t = dB_t dt = 0, \;\; dB_t dB_t = dt. \tag{2.23}$$

By using the definition of an Itô process, we can demonstrate that the $f(t,X_t)$ process admits the representation,

$$\begin{aligned} f(t,X_t) &= f(0,X_0) + \int_0^t \sigma_s \frac{\partial f}{\partial x}(s,X_s)dB_s + \\ &\quad + \int_0^t \left(\frac{\partial f}{\partial s}(s,X_s) + b_s \frac{\partial f}{\partial x}(s,x_s) + \frac{\sigma_s^2}{2}\frac{\partial^2 f}{\partial x^2}(s,X_s) \right) ds. \end{aligned} \tag{2.24}$$

A connection between a second order partial differential equation and the stochastic process is suggested by the Itô formula. Then lets define the generators concept that gives this link.

Definition 2.2.4 (of generator of Itô diffusion)
Let X_t be a time-homogeneous process that is diffusion in $\mathbb{R}^n$. The limite,

$$Lf(x) = \lim_{t\downarrow 0} \frac{E^x[f(X_t)] - f(x)}{t}; \;\; x \in \mathbb{R}^n, \tag{2.25}$$

defines the infinitesimal generator L of the diffusion process X_t. $\mathcal{D}_L(x)$ represents the set of functions $f : \mathbb{R}^n \to \mathbb{R}$ such that the limit exists at x. In addition, the set of functions for which the limit holds for every $x \in \mathcal{R}^n$ is indicated by the symbol $\mathcal{D}_L$.

In Oksendal, 2000, the authors present the derivation of the generator formula L for an Itô diffusion process. The main concept, is to compute the expectation $E^x[f(X_t)]$ in (2.25) as follows,

$$\begin{aligned} E^x[f(X_t) &= f(x) + \sum_{ik} E^x[\sigma_{ik}\frac{\partial f}{\partial x_i}(X)dB_k] + \\ &\quad + E^x\left[\int_0^t \left(\sum_i b_i \frac{\partial f}{\partial x_i}(X) + \frac{1}{2}\sum_{ij}(\sigma\sigma^T)_{ij}\frac{\partial^2 f}{\partial x_i \partial x_j}(X) \right) ds \right] \end{aligned} \tag{2.26}$$

In addition, in order to vanish the limit of the second term in (2.26), it is assumed that the process f is a bounded Borel function. Consequently, any Itô diffusion process X_t in $\mathbb{R}^n$ will always be connected to the generator L provided by,

$$Lf = \sum_i b_i \frac{\partial f}{\partial x_i} + \frac{1}{2} \sum_{ij} (\sigma\sigma^T)_{ij} \frac{\partial^2 f}{\partial x_i \partial x_j}; \;\; f = f(x) \in \mathrm{C}_0^2(\mathbb{R}^n). \tag{2.27}$$

2.2.3 The Feynman-Kac formula

A generalization of Kolmogorov's backward equations is the Feynman-Kac theorem. It establishes a relationship between a partial differential equation and a stochastic process, if it has an associated infinitesimal operator. Insofar as L is the generator of the process X_t, the stochastic process X_t is related to a second order partial differential operator L. By using Itô's formula on the martingale term, the PDE and the Markov property of X_t are connected. Then, assume that the diffusion process X_t satisfies the following SDE

$$dX_t = b(X_t, t)dt + \sigma(X_t, t)dB_t \text{ and } X_s = x. \tag{2.28}$$

Theorem 2.2.2 (Feynman-Kac Formula)
Given a bounded functions $r(x,t)$ and $g(x)$, let

$$V(x,t) = E\left(e^{-\int_t^T r(X_u,u)du} g(X_T)|X_t = x\right). \tag{2.29}$$

We consider that the Cauchy problem

$$\frac{\partial f}{\partial t}(x,t) + L_t f(x,t) = r(x,t)f(x,t), \text{ with } f(x,T) = g(x) \tag{2.30}$$

has solution. Then the solution is unique and is given by $V(x,t)$.

The Feynman-Kac theorem can be proved by using the Itô formula associated with the solutions of the linear SDE. Initially, we solve (2.30) using the Itô formula, which leads to

$$df(X_t,t) = \left(\frac{\partial f}{\partial t}(X_t,t) + L_t f(X_t,t)\right)dt + \frac{\partial f}{\partial x}(X_t,t)\sigma(X_t,t)dB_t. \tag{2.31}$$

dM_t represents the last component in (2.31), which is a martingale term. The linear SDE,

$$df(X_t,t) = r(X_t,t)f(X_t,t)dt + dM_t, \tag{2.32}$$

is obtained by substituting the first equation of (2.30) into (2.31). After that, the SDE (2.32) is integrating between t and T. Assuming $T \geq t$ as the time variable and t as

the start we deduce

$$f(X_T, T) = f(X_t, t)e^{\int_t^T r(X_u,u)du} + e^{\int_t^T r(X_u,u)du} \int_t^T e^{\int_t^T r(X_u,u)du} dM_s. \tag{2.33}$$

Next, we change (2.33) to contain the terminal conditions $f(X_T, T) = g(X_T)$ of the Cauchy problem (2.30). After rearranging, we arrive at

$$g(X_T)e^{-\int_t^T r(X_u,u)du} = f(X_t, t) + \int_t^T e^{\int_t^T r(X_u,u)du} dM_s. \tag{2.34}$$

Therefore, applying the expectation to (2.34) given $X_t = x$, we get,

$$\begin{aligned} &E\left(g(X_T)e^{-\int_t^T r(X_u,u)du}|X_t = x\right) = \\ &= E\left[\left(f(X_t, t) + \int_t^T e^{\int_t^T r(X_u,u)du} dM_s\right)|X_t = x\right]. \end{aligned} \tag{2.35}$$

Then, using the linearity property of the expectation in (2.35) we obtain,

$$\begin{aligned} &E\left(g(X_T)e^{-\int_t^T r(X_u,u)du}|X_t = x\right) = \\ &= E\left(f(X_t, t)|X_t = x\right) + E\left(\int_t^T e^{\int_t^T r(X_u,u)du} dM_s|X_t = x\right). \end{aligned} \tag{2.36}$$

With regard to martingale, the final term (2.36) is an integral of a bounded function. It is then a zero mean martingale. Consequently,

$$E\left(g(X_T)e^{-\int_t^T r(X_u,u)du}|X_t = x\right) = E\left(f(X_t, t)|X_t = x\right) \tag{2.37}$$

We are unable to establish that $V(x, t) = f(x, t)$. On the other hand, the quantity $e^{-\int_t^T rdu}E\left(g(X_T)|X_t = x\right)$ is well-known in finance and represents the discounted expected payoff if r is constant.

2.2.4 Girsanv's theorem

The Girsanov's theorem, named after Igor Vladimirovich Girsanov, describes the dynamics of the stochastic process when the original measure is changed to an equivalent measure. This theorem is very important in stochastic analysis, particularly in financial mathematics, allowing us to convert the measure of the underlying asset from the real measure to the risk-neutral measure. The principal idea of the Girsanov theorem is that, if the drift coefficient of a given Itô process is changed by a non-degenerate diffusion coefficient, then the law of the process will not change dramatically. The law of the new process is absolutely continuous and written with respect to the law of the original process and the Radon-Nikodym derivative can be computed explicitly.

If the null sets of two measures P and Q in the probabilistic space $(\Omega, \mathcal{F}, P)$ are

the same, then they are equivalent. In the event that it occurs, a random variable M known as the Radon-Nikodym derivative will exist and is given by

$$M = \frac{dQ}{dP}$$

such that

$$Q(A) = \int_A M dP, \quad \forall A \in \mathcal{F}$$

gives the probabilities under Q. Then, the form of M can be found using the Girsanov's theorem.

Theorem 2.2.3 (Girsanov's theorem)
Consider a Brownian motion $B_t,\ t \in [0, T]$ with probability measure P. Let

$$W_t = B_t + \lambda t.$$

Using the stochastic process

$$M_t = \frac{dQ}{dP}(B_t) = e^{(\lambda B_t - \frac{1}{2}\lambda^2 t)},\ t \in [0, T], \tag{2.38}$$

we define the measure Q, which is equivalent to P,

$$\frac{dP}{dQ}(W_t) = e^{(\lambda W_t - \frac{1}{2}\lambda^2 t)},\ t \in [0, T]. \tag{2.39}$$

Here W_t is a $Q-$ Brownian motion.

The proof is founded on Levy's description of the Brownian motion as a continuous martingale with quadratic variation process t. By convergence in probability, quadratic variation is the same under P and Q (on the result of the general Bayes formula). Due to the smooth nature of λt, it does not contribute to the quadratic variation; hence,

$$[W_t, W_t] = [B_t + \lambda t, B_t + \lambda t] = [B_t, B_t] = t$$

We assume that $M_t = E^P(M|\mathcal{F}_t)$ in order to demonstrate that W_t is $Q-$martingale. Alternatively, we can use direct calculations to demonstrate that $M_t W_t$ is P - martingale, that is,

$$E^P(W_t M_t|\mathcal{F}_t) = E^P((B_t + \lambda t)e^{(-\lambda B_t - \frac{1}{2}\lambda^2 t)}|\mathcal{F}_t) = W_t M_t.$$

Chapter 3

Weather derivatives and the market

This section provide general considerations about the concept of weather derivatives, the history and evolution of the weather derivative market. The specification of weather derivative is outlined and the relevant formulae are provided, with principal focus on rain weather derivatives.

3.1 Overview of weather derivatives

Climate patterns have a significant impact on the operations of many companies', which can have a negative effect on their performance. Financial instruments, often known as financial weather contracts, can be used to mitigate weather risks. With weather derivatives, investors can protect themselves from the possibility that bad weather would damage their business.

The weather derivative market was started in the 1990's in the US, after the occurrence of an exceptional weather anomaly, El Niño, related to warm seas, which caused deregulation of the energy and utility industries in providing reliable services to consumers at reasonable prices. With the deregulation, the alternative supplier appeared in the market, which resulted in growing competition. As a result, the energy and utility companies were forced to study effective hedging tools to stabilize their earnings. Hence, they came to use the well-known mechanism of risk transfer, derivatives, to transfer weather risks. The first weather derivative deal came into existence in 1997 when Koch Energy and Enron (now a defunct company) entered into a contract using a swap on temperature index for Milwaukee, Wisconsin to hedge against warm days in the winter of 1997-1998 Alaton et al., 2002.

An structured electronic platform was launched two years later, by the Chicago Mercantile Exchange (CME) with the expansion of climatic contracts Kermiche and Vuillermet, 2016. The degree days in temperature contracts were basically the first

contracts negotiated. Then, in 2003 the CME established two subsidiaries, one in Japan and the other in Europe. Now the contract of weather derivatives are offered in 18 cities on three continents (North America, Europe and Asia) and only a few nations in Africa "Weather products", n.d. The proportion of all types of climatic contracts negotiated in 2005, as appointed in Kermiche and Vuillermet, 2016 indicates that 95% of the contracts are traded on the CME market, against 5% of OTC contracts. The demand for financial solutions that provide protection against unfavorable outcomes related to weather conditions is mostly driven by the growing awareness of hazards associated with climate change. As a result of the recommendations of the regulators institutions, more firms are becoming aware of climate-related risk. It has helped to drive up trading volumes of weather futures and options in CME Group. It also helped the addition of new players to the market of weather derivatives, such as asset managers and hedge funds. Until the year of 2020 has seen an increase of futures volumes in 60 percent, a notional value of $750 million, and a 143 percent increase in options volumes with a notional value of $480 million "Managing climate risk with cme", n.d.

A few African nations have begun to offer weather derivatives contracts, but their volume is still very low. Morocco and South Africa have launched a few OTC contracts. South Africa's first weather derivative was traded in 2002, by Gensec bank, a subsidiary of Sanlam, partnered with Aquila, a subsidiary of UtiliCorp United in Kansa USA. The demand for weather hedging products comes predominantly from the agricultural sector and underlying to temperature "Risk net. First south african weather derivatives contract", n.d.

Additional World Bank Group (WBG) projects in partnership with private businesses to reduce the risks associated with extreme weather in developing nations have proven to be highly significant, primarily requested by small farmers holders. For instance, the government of Malawi purchased the first weather derivative contract, offered by the WBG, structured as an option on a rainfall index in 2008.

The effect of the variation of the rainfall on maize production is catched trough the rainfall weather index. Then, if the quantity of rain is below a given threshold, the rainfall index will reflect the loss in maize production. For the transaction, the WBG served did intermediate the transactions between the government and investment banks or reinsurance companies "Malawi-WeatherHedge-FoodSecurity", n.d. In December of 2009, the WBG launched the Global Index Insurance Facility (GIIF) program with the objective of reducing natural extreme weather risks by promoting the creation in developing nations of efficient and long-lasting markets for extreme weather risk and indexed weather insurance. Seven grants have been awarded under the GIIF initiative since its official launch. Actually, this project has been expanded into other countries such as, Mozambique, Rwanda, and Kenya. The most offered weather contracts are based on the rainfall index. In developing

countries, the variability of weather may be considered as one of the most predominant risks to agriculture. The World Bank estimates that nearly 7 percent of the world's population will still be living with less than US $2.15 a day in 2030. Among these percentage, the majority are from Africa "World Bank. 2022. Poverty and Shared Prosperity 2022", n.d. Furthermore, the report "World Bank. Agriculture and ruraldevelopment", n.d. state that three-quarters of the world's poor live in rural areas and most earn their living from farming.

Following Dischel and Barrieu Dischel and Barrieu, 2002, the weather derivative is a weather contingent contract whose payoff is determined by a future weather event. The settlement value of future weather events is calculated based on a weather index, which is expressed as values of a weather variable measured at a specified location. Next, we list some underlying weather indexes that are common in the literature.

- temperature,
- rainfall,
- humidity,
- wind and
- snowfall.

The weather derivatives are like other financial derivative securities and can be traded as options, future, swaps and forward contracts. They are formulated by specifying the following parameters Nhangumbe et al., 2020; Zeng, 2000:

- contract type (contingent claims), which includes Future, Swap, and European or American options;
- contract period, typically one month or six months (six months indicates hedging for either the summer or winter);
- the starting point where the meteorological data is taken from;
- the contract underlying index for each commodity (temperature, precipitation, wind, etc.);
- the strike level or pre-negotiated threshold for the weather index (S);
- a tick or constant payment for a linear or binary payment scheme "τ" (convert the payoff to monetary values) and
- the premium.

However, there is another form of financial weather contract called weather insurance (WI) contracts. The key distinction between weather derivatives and weather insurance policies follow from a legal and regulatory standpoint and are

listed below Geyser, 2004; Nhangumbe et al., 2020; Stoppa and Hess, 2003:

- While WD also cover low risks with high probability of occurrence, WI only cover high risks with low probability of occurrence;
- the WD are less expensive and do not rely on losses, but rather on the observation of the weather indexes; the WI are typically more expensive and demand proof of losses;
- the payoff on WD contracts must be proportionate to the size of the phenomena, whereas on WI contracts, it can only be based on the total amount of losses.

Depending on the situation, the flexibility and efficiency of WD will make it more appealing than WI. On a WD contract, the payment is based on weather indexes and there is no need to prove that the investor has suffered a loss. The seller might track the underlying weather variable from a location. WD is one of the less conventional market, that is in the early stages of development. These markets are typically associated with risks, such as those related to weather, energy prices, and insurance.

Using WD primarily serves to cover weather events that are not catastrophic in their nature. Companies, for example, can use the rainfall derivatives to hedge against fluctuations in their revenues caused on by periods of frequent rain (floods) or dry weather (drought). For instance, in agriculture, the amount of rainfall can affect crop yield, since wheat yield and rainfall are strongly correlated Odening et al., 2007 and Stoppa and Hess, 2003. Furthermore, it is shown in Geyser, 2004 a significant correlation between rainfall and maize yield. The amount of rainfall that is expected, that is, the normal quantity of rainfall will then determine the crop yield. Farmers may experience crop yield losses or increases if the observed rainfall exceeds or falls short of the required amount. The risk to crop yield will significantly drop off if farmers can hedge their production against unfavorable rainfall patterns during the crucial growth stages. In Geyser, 2004, Geyser suggested a few potential rainfall weather contracts strategies for maize yield. The author recommended the *long strangle* options risk protection strategy, which combines a long call and a long put. The farmer will benefit from this combination because it offers a hedge that is typically associated with high volatility of the underlying risk exposure in financial markets.

The majority of traded weather contracts are currently being written on temperature variables. The bases indexes for temperature contracts are Heating Degree Day (HDD) and Cooling Degree Day (CDD). A degree day is defined as the temperature deviation measured at from 65"F, or 18"C. The theory is that more energy will be required for heating and cooling as the temperature falls below 65"F. Thus, these types of contracts provide a way for companies to protect themselves from periods

that are unpredictably warm or cold. In actuality, CDDs are utilized during the summer and HDDs during the winter. In addition to monthly and annual cumulative temperatures, other variables could be the average daily or monthly temperature. However, there has been increasing demand for weather contracts underlying other weather variables, such as rainfall, particularly in developing countries. We will constrain our studies on rainfall derivatives.

3.2 Rainfall index

Generally, the risks of drought or flooding are evaluated based on commonly used indicators. The most popular index is the Standardized Precipitation Index (SPI). The SPI index measures the catchment's precipitation deficits and the severity of the drought over various time periods, generally on monthly basis and is determined using the following formula,

$$SPI = \frac{P_{ik} - \bar{P}_i}{Std_i}. \tag{3.1}$$

Here, P_{ik} represent the precipitation for the ith station and kth observation. The variable $\bar{P}_i$ represent the mean precipitation for the ith station, and Std_i is the standard deviation of precipitation for the ith station.

However, other rainfall indices have been proposed in the literature for assessing the severity of droughts and floods. The aridity index, which measures the degree of dryness, is commonly calculated as the yearly precipitation divided by the evapotranspiration.

$$AI = \frac{P}{PET}, \tag{3.2}$$

with the variable PET representing the potential evapotranspiration and the variable P representing the precipitation per year. This index was used, for example, in the UNESCO report "Maps of the world distribution of arid regions" "Unesco report: World distribution of arid regions", n.d., to quantify the degree of bioclimatic aridity. In Tsakiris et al., 2007, the AI was also presented as an indicator of drought intensity.

Furthermore, Odening et al., 2007 proposed the cumulative index Y_t, which is a measure of rainfall over time and is computed using rainfall deficit. The methodology that is used in this research for computing the rainfall index is based on deficit or excess rain days. It appears to be more appropriate to define and evaluate rainfall variability using indexes quantified as a standard metric Odening et al., 2007. Next we present the definitions of the rainfall indexes as in Nhangumbe et al., 2020.

Definition 3.2.1 (of rainfall deficit)
The *rainfall deficit*, denoted by RD and used to quantify the precipitation deficits

(drought severity) on different time scales, is the number of millimeters by which the average rainfall X_t is below the base rainfall X_{ref}, that is,

$$f(X_t) = (X_{ref} - X_t)^+. \tag{3.3}$$

Definition 3.2.2 (of rainfall excess)
The *rainfall excess*, denoted by RE and used to quantify the excesses (flooding severity) on different time scales, is the number of millimeters by which the average rainfall X_t is above the base rainfall X_{ref}, that is,

$$f(X_t) = (X_t - X_{ref})^+. \tag{3.4}$$

The definition3.2.1 of RD can be taken in the point of view of the necessity of water in non-rain periods. And, the definition 3.2.2 is taken in the view point of the existence of more water than required in rain periods. As a result, an company can buy RD contracts to hedge against lower rain quantities, and the contracts will pay out in accordance with the equation (3.3). In contrast, if the company need protection against higher quantities of rain, can buy the RE contracts. It will pay out in accordance with the equation (3.4).In Geyser, 2004 the strategy suggests that investors should position themselves on both RD and RE contracts. For example, taking into account the annual base rain of 200mm for RD contracts and the annual base rain of 800mm for RE contracts if the expected annual rainfall is given between 200mm and 800mm.

The following equation describes the cumulative index, Y_t, of the rainfall underlying weather variable. It gives the total amount of rainfall deficit or excess over all periods $[0, t]$ Li, 2018,

$$Y_t = \int_0^t f(X_s)ds, \tag{3.5}$$

that is,

$$dY_t = f(X_t)dt. \tag{3.6}$$

Chapter 4

Rain weather derivatives models and pricing

This chapter focus on modeling the dynamics of rainfall process and on discussing how these models can be used to develop a rainfall pricing model based on partial differential approach.

4.1 Rain weather derivatives model

In this section we describe the proposed model. We start doing the literature review about existing approaches to model the dynamics of rainfall process. We provide a data visualization of the rainfall process and we discuss the features of the rainfall dynamics and we propose our rainfall model. We also present the methodology which will be used to estimate the parameter of the rainfall model.

4.1.1 Overview of rainfall modelling

The rainfall structure consists of two components; the discrete component, indicating the occurrence of rainfall, and a continuous component, determining the magnitude of rainfall. The modeling procedure is typically divided into two stages: the intensity modeling and the occurrence modeling (Coe and Stern, 1982; Katz, 1977). There are several types of the rainfall models. For instance, the Meteorological models, with aim to represent the dynamics of the large-scale atmospheric processes governing precipitation Little et al., 2009. The stochastic process-based models, which describe the rainfall behavior by a small set of physically meaningful parameters driving a stochastic process Carmona and Diko, 2005. The Statistical models which use the statistical techniques to fit the rainfall data to well-known distribution types Coles et al., 2003. And, the artificial neural networks, which use a set of meteorological variables, such as temperature, humidity, and wind, to forecast possible precipitation amounts Feng and Kitzmiller, 2006; Ramirez et al., 2005; Williams, 1997.

To model rainfall as a continuous process, we can use parametric models or non-parametric models. Their approaches vary on the way is modeled the amount of precipitation.The traditional parametric models are based on point process and cluster models. Point process, is the approach where the number of storm arriving at a location in a time interval is assumed to be Poisson distributed and the rainfall amount associated with a storm arrival is assumed independent to a number of storms and being white noise, such as gamma distributed. Then, the rainfall amounts generating process corresponding to storms occurrence is called Poisson white noise. Under this formulation, the cumulative rainfall in the successive overlapping time intervals is a compound Poisson process. However, using these assertions to investigate the statistical properties of the cumulative rainfall for non-overlapping successive time intervals can lead to contradictions when small time intervals are considered. The auto-correlation function is equal to zero for all lags greater than zero, but it can be contradictory if it is considered hourly precipitation for a rainy month. However, the Poisson white noise model has proven helpful in forecasting yearly and extremely rare precipitation events. The Poisson rectangular pulse model result on changing the Poisson white noise model by treat rainfall as an event with random length and intensity Rajagopalan et al., 1996.

Neyman and Scott proposed the two-level Clusters process to model the spatial distribution of galaxies and then used it to model continuous time rainfall in Foufoula-Georgiou and Guttorp, 1986; Kavvas and Delleur, 1981; Rodriguez-Iturbe et al., 1987. Initially, the storms arrival are modeled by Poisson distribution with a given parameter. Then, each storm is associated with a quantity of precipitation bursts. It usually assumed to be Poisson or geometric distributed. Furthermore, is assumed that the time of burst occurrence in relation to the storm follows an exponential distribution. Neyman-Scott white noise is the term for the precipitation process that results if the precipitation burst is described by instantaneous random precipitation depth. On the other hand, if the precipitation burst is a rectangular pulse, the precipitation process is known as Neyman-Scott rectangular pulse.

Although the traditional frameworks for modeling rainfall as a continuous process are point process and cluster process based on over-lapping time intervals, models for aggregate rainfall may also be formulated directly at a desired time scale (hour, day, week, month, year). First, the occurrence process is modeled using Markov chain models or alternating renewal models and then the amount of rain is modeled using parametric statistical non-Gaussian distributions, typically, a parsimonious member of the exponential family (Gamma, Lognormal, Weibull, pareto) that best fits the data Rajagopalan et al., 1996.

In Cox and Isham, 1988; Rodriguez-Iturbe et al., 1987, the jump Markov model was applied, and it was assumed that the rainfall process took the form of storms, which are made up of individual cells. The rainfall process jumps up randomly

at a cell arrival time and jumps down randomly at an extinction time. Jerson Kelman Kelman, 1977, present an alternative approach suggesting to assuming that the same transformed latent Gaussian process can be used to model the occurrence and intensity of daily rainfall. The rainfall is then represented as a censored process, with zero rainfall corresponding to censored values under a threshold. The concept of modeling rainfall as a diffusion process was firstly developed by Pavlopoulos Kedem et al., 1994; Pavlopoulos, 1991; Pavlopoulos and Kedem, 1992. The occurrence process and several other facts related to the rain process such as, positivity, the growth and decay properties, were taken into account to generate some meaningful family of distribution by assuming that the rain rate is a temporally homogeneous diffusion process with appropriate boundary conditions, drift and diffusion coefficients. By assuming those conditions, they were able to derive the propriety truncated family of probability distribution.

In Unami et al., 2010, the mean reverting Ornstein Uhlenberg process was proposed. The stochastic differential equation was used to simulate the evolution of point rainfall over a cumulative rainfall depth with principal proposal of assessing the risk of both droughts and floods. Both events lie at the extremes of rainfall intensity when it is considered long time interval scale.

In Glasbey and Nevison, 1997; Hannachi, 2014; Zeger and Brookmeyer, 1986, a latent variable approach based on censored data was used to model the frequency and intensity of rainfall, which was assumed to follow a discrete-time intermittent process. However, the idea of modelling daily precipitation as censoring process was applied previously by Kelman Kelman, 1977. The author used the techniques of continuous time series with censoring to model daily precipitation time series. Then, the precipitation process was considered a realization of the truncated first order auto regressive model AR(1), with censored vales under level zero. We refer to the most recent work Tong and Liu Tong and Liu, 2021, where, following the same ideas, they modeled the rainfall intensity using a continuous time model with censored distribution rather than the discrete-time process. They proposed a censored power-transformation Ornstein Uhlenbeck process to model the daily rainfall, instead of fitting non-Gaussian distribution, as an alternative to reduce the non-normality of daily precipitation. More recent studies on modelling the dynamics of the rainfall variable by continuous stochastic models can be found in Chidzalo et al., 2023.

4.1.2 Rainfall dynamics

Our approach will be based on stochastic models. First, let us have a look at some rainfall data visualization. The public rainfall data was obtained from the German weather service "The Deutscher Wetterdienst", n.d., and refer to the weather station in Tempelhot, between the years 1948 and 2021.

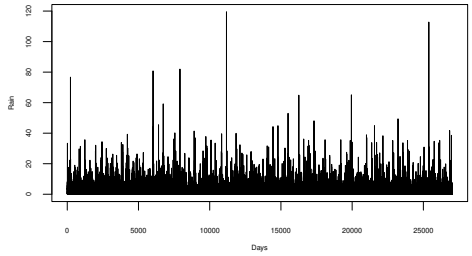

FIGURE 4.1: Daily rain at Tempelhot, 1948-2021.

In Figure (4.1), we plot the time series of the daily rainfall data. It looks like the daily data is a binary event with plenty of data, more than half taking the value of zero. The daily rainfall data typically have a distribution with a singularity at zero and a long upper tail when a short time scale, such as a day, is considered. Then, it is modeled as a intermittent process with discontinuities, with zero representing intermittent dry periods Zeger and Brookmeyer, 1986. These processes are most studied in climate and hydrology sciences and are generally modeled using binary generators, based on two-state Markov chains are typically used to determine whether the process is zero or not and simulate in the latter case Smith and Schreiber, 1973; Todorovic and Woolhiser, 1975. The authors also used also used higher order Markov models and more than two states in later investigations Coe and Stern, 1982; Haan et al., 1976; Hess et al., 1989. Alternatively, a Poisson point process is also used to generate the daily rainfall occurrence. These models are far more difficult than Gaussian ones to study analytically. Then alternative models based on monotonic power transformations to achieve marginal normality have been developed. In Hannachi, 2014; Tong and Liu, 2021; Zeger and Brookmeyer, 1986 an approach based on censored data is presented. In other words, the intermittent process is thought to arise from truncating a continuous process by observing $max(P, 0)$, which is referred to as a censoring model, and taking into consideration only values greater than zero.

Truncation and censoring are two quite similar processes, but they differ from each other. Lets consider two random variables, X and Y, and let W be 1 if $X \leq Y$ and, otherwise 0. Random censoring is obtained when either $min(X, Y)$ or $max(X, Y)$ is observed along with W and is called respectively by right and left censoring. The random truncation model is obtained when both $min(X, Y)$ and $max(X, Y)$ are observed, when $W = 1$ or $W = 0$, getting respectively a random right or a random left truncation model. The censoring model is basically a problem of missing observation, whereas truncation is a selection bias problem Mandel, 2007; Vardi, 1985. For daily rainfall time series, the truncation and censoring are used interchangeably. The censoring problem is precisely when one observes $max(P, 0)$ by taking into account only positive values. On the other hand, it is incapable of taking negative

values. It could be argued that the process of taking positive values into account is just a truncation, that is, selection bias problem. However, this assumptions does not affect the results, as stated in Hannachi, 2014; Park et al., 2007; Zeger and Brookmeyer, 1986. Tong and Liu Tong and Liu, 2021, modeled the daily rainfall intensity, assuming that the rainfall process follows a censored power-transformation Ornstein Uhlenbeck process. However, in Odening et al., 2007 it is mentioned that daily precipitation models should be used with some caution in the context of derivative pricing because they tend to underestimate rainfall variability.

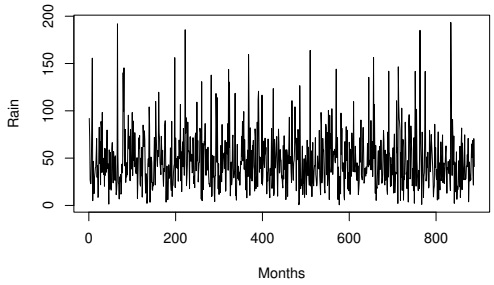

FIGURE 4.2: Monthly rain at Tempelhot, 1948-2021.

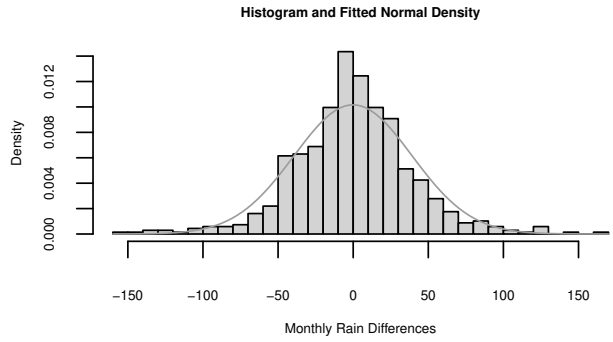

FIGURE 4.3: The density of the monthly rain differences at Tempelhot, 1948-2021

Next, we have a look at monthly rain. In Figure (4.2), we illustrate the graphic of monthly rainfall data. The general impression is that the dynamics of rainfall show seasonal patterns, randomness, and frequent reversion to a mean whose value varies with the season. Furthermore, it is noted that rainfall values do not indefinitely increase or decrease. In general, Gaussian-based processes can be used to model the total rainfall over a long periods of time, such as a months, seasonality, and annually. This mathematical model is predicated on the idea that the dynamics of precipitation are stochastic, highly volatile, fluctuate around a mean, and have seasonal effects. Current research in various contexts suggests using a mean reverting process-based model to explain the evolution of the monthly precipitation. Allen, 2007; Emmerich et al., 2005; Nhangumbe et al., 2020; Unami et al., 2010. The

choice of the Wiener process for noise is also justified by the good fit to the normal distribution of monthly rainfall differences, as shown in Figure 4.3.

Assume that the random variable X_t represents the monthly total amount of rainfall at time t. The deterministic mean reverting process, can then be used to model potential changes in the total rainfall over time,

$$dX_t = [k(\theta(t) - X_t) + \theta'(t)]dt + \sigma X_t^p dW_t. \tag{4.1}$$

W_t denotes the Wiener process, σ is the constant volatility of the rainfall, $\theta(t)$ is the long-term mean of the process, and k is the rate of mean reversion. The values of k and the mean amount of rain, $\theta(t)$, should be calculated taking into account the actual data.

The stochastic process X_t fluctuates around θ, where θ is a mean factor. The mean factor θ is surrounded by fluctuations of the stochastic process X_t. Then, the mean function θ can be obtained by fitting an annual periodic truncated Fourier series to the empirical mean of each month. In particular, we can use the partial sum $\theta_n(t)$, which is defined as following, to approximate the function $\theta(t)$,

$$\theta_n(t) = \alpha_0 + \sum_{i=1}^{n} \alpha_k \sin\left(\frac{2k\pi}{12}(t-\nu)\right) + \sum_{i=1}^{n} \beta_k \cos\left(\frac{2k\pi}{12}(t-\nu)\right), \tag{4.2}$$

where t represents the time of a monthly scale, α_k, β_k, ν are parameters to be fitted, α_0 is the sine curve's mean, α_k the oscillation, and ν is denote the shift of the by $X - axis$ (which we divide by 12 to scale up to months). The number of sine terms can be determined by examining the data from the weather station, which will be utilized to estimate the parameters.

In this study we assume that the monthly rainfall dynamics are driven by the mean reverting Ornstein-Uhlenbeck process. Hence, we let $p = 0$ in (4.1) and we get the equation,

$$dX_t = [k(\theta(t) - X_t) + \theta'(t)]dt + \sigma_t dW_t, \tag{4.3}$$

called mean reverting Ornstein-Uhlenbeck process.

We can derive the unconditional mean and variance of the Ornstein-Uhlenbeck process, X_t, by using the integrating factor and Itô product rule on (4.3) to deduce

$$d(\exp(kt)X_t) = \exp(kt)[(k\theta(t) + \theta'(t))dt + \sigma_t dW_t]. \tag{4.4}$$

From which, integrating the equation (4.4) from 0 to t, gives,

$$X_t = \exp(-kt)X_0 + \exp(-kt)\int_0^t \exp(ks)(k\theta(s) + \theta'(s))ds +$$

$$+\exp(-kt)\int_0^t \exp(ks)\sigma_s dW_s. \tag{4.5}$$

Then, the unconditional mean derived taking expectations of both sides of equation (4.5) yields,

$$E(X_t) = \exp(-kt)X_0 + \exp(-kt)\int_0^t \exp(ks)(k\theta(s) + \theta'(s))ds, \tag{4.6}$$

since $E\left[\int_0^t \exp(ks)\sigma_s dW_s\right] = 0$.

The variance is derived as $E[(X_t - E(X_t))^2]$ and, after applying the Itô isometric property $E\left[\left(\int_0^t \exp(ks)dW_s\right)^2\right] = E\left[\int_0^t (\exp(ks))^2 ds\right]$, we have

$$\begin{aligned} Var[X_t] &= E\left[\sigma^2 \exp(-2kt)\left(\int_0^t \exp(ks)dW_s\right)^2\right] \\ &= \sigma^2 \exp(-2kt)E\left[\int_0^t (\exp(ks))^2 ds\right] \\ &= \sigma^2 \exp(-2kt)\int_0^t E\left[(\exp(ks))^2\right] ds \\ &= \sigma^2 \exp(-2kt)\int_0^t \exp(2ks)ds \\ &= \sigma^2 \frac{1-\exp(-2kt)}{2k}. \end{aligned} \tag{4.7}$$

Then, the distribution of X_t can be written as,

$$X_t \sim N\left(\exp(-kt)X_{t_0} + \exp(-kt)\int_0^s \exp(ks)(k\theta(s) + \theta'(s))ds\,,\, \sigma^2 \frac{1-\exp(-2kt)}{2k}\right), \tag{4.8}$$

and the transition density from X_0 to X_t is given by

$$P(X_t|X_0) = \sqrt{\frac{2k}{2\pi\sigma^2(1-\exp(-2k(t-t_0)))}}\exp\left\{-\frac{2k(X_t - X_{t_0}\exp(-kt))^2}{\sigma^2(1-\exp(-2k(t-t_0)))}\right\}. \tag{4.9}$$

The Ornstein-Uhlenbeck stochastic paths can thus be simulated using

$$X_t = \exp(-kt)X_t + \exp(-kt)\int_0^t \exp(ks)(k\theta(s) + \theta'(s))ds + \sigma\sqrt{\frac{1-\exp(-2kt)}{2k}}dW. \tag{4.10}$$

From (4.9), we write

$$E(X_{t+\Delta t}|X_t) = X_t \exp(-k\Delta t) + \exp(-k\Delta t)\int_0^{\Delta t} \exp(ks)(k\theta(s) + \theta'(s))ds, \tag{4.11}$$

$$Var(X_{t+\Delta t}|X_t) = \sigma^2 \frac{1 - \exp(-2k\Delta t)}{2k}. \tag{4.12}$$

4.1.3 Parameter estimation

Several authors have examined the issue of parameter estimation for diffusion processes using discrete observed data. Different approaches were suggested, depending on the features of the data that was observed. The following succinctly describes the primary features of the data Iacus, 2009; Nhangumbe et al., 2020:

- large sample scheme: the most natural, when the time lag between consecutive observations is fixed and the number of observations increases with the path (window) of observations $[0, n * lag = T]$. The continuous model that is underlying it is predicated on the assumptions of stationarity and/or ergodicity. The ergodicity process is an recurrent positive recurrent with a stationary distribution. It suggests that after leaving start point $x \in \mathbb{R}^n$, the expected time that the process hits a ball about any point $y \in \mathbb{R}^n$ is finite.
- High-frequency scheme: as n increases, the lag decreases to zero and the path (window) of observation remains fixed.
- Rapidly increasing design: as n increase, the lag between observations decreases to zero, and the path of observations also increases. Furthermore, the requirement for stationarity or ergodicity must be met. $n * lag_n^k \to 0,\ k \geq 2$ defines the rapid convergence rate for lag. In contrast, the slow convergence of the lag between observations is thought to occur for high values of k.

As a matter of course, each model will need to be adjusted to the unique circumstance of at least one of the following components: high dimension of parameter space, non-ergodic case, non-stationary case, drift parameters, diffusion parameters, etc. Applications of the combinations of the estimating functions are made for high dimension of the parameter space. The schemes to estimate the parameter of the mean-reverting process include the least squares approach, maximum likelihood estimation and adaptive Bayes estimation.

Next, we employ the estimating schemes methodology, which was introduced in Alaton et al., 2002, to determine the temperature model parameter described by the Ornstein-Uhlenbeck process. The model's parameters were estimated using three different methods. The volatility is estimated using quadratic variation. The mean reverting parameter is estimated using the martingale estimation functions. Additionally, the least squares method is used to estimate the parameter of the mean function. The estimator for the mean reverting parameter case is derived as a modification of the estimator obtained on the continuous time likelihood functions by replacing the Lebesgue and the Itô integral by the Riemann-Itô sums,

when the time interval between observations is bounded away from zero. Since the estimators are based only on the Riemann-Itô approach, it performs best when the observation time is is closely spaced Bibby and Sørensen, 1995.They also proposed and proved the usefulness of the modified estimators, which are improved by constructing a martingale estimating function from the Riemann-Ito approximation of the likelihood function. The estimation can be carried out using the software *R*.

The seasonal component

The parameters of the θ-function α_k, β_k, ν, can be estimated using the least squares method. Then, the numerical schemes, like the Gauss-Newton algorithm is used. The approximated values of parameters are obtained by minimising

$$\min_{\cdot,\alpha_0,\alpha_k,\beta_k\nu} \|\Theta(\cdot,\alpha_0,\alpha_k,\beta_k,\nu) - M(\cdot)\|, \tag{4.13}$$

where $M(j)$, $j = 1,\ldots,12$ is the monthly empirical mean, and it is given by

$$M(j) = \frac{1}{N}\sum_{i=1}^{N} R(j,i). \tag{4.14}$$

$R(j,i)$ is the amount of rainfall in month j of year i, and N is the number of periods (years) to be taken into consideration.

The volatility

We employ the method in Alaton et al., 2002 in order to estimate the volatility σ. In this work, the authors analysed two estimators: the first was a quadratic variation proposed in Basawa and Rao, 1980 and the second was derived by discretizing the process proposed in Brockwell et al., 1991, and. The authors discovered that applying the second estimator may result in an error in the derivative's price since it undervalues the mean-reversion parameter k. Then, the formula,

$$\hat{\sigma}_\mu^2 = \frac{1}{N_\mu}\sum_{j=0}^{N_\mu-1}(X_{j+1} - X_j)^2, \tag{4.15}$$

provides the estimator based on quadratic variation of X_t. Here, N_μ, denotes the data points to be used, that is, for monthly data $N_\mu = 12 \times N$.

The mean-reversion parameter

Alaton et al., 2002 used the martingale estimation functions method to estimate k for the mean-reversion parameter. Justified by the fact that there is a delay of more than one day (observations) between them. The efficient estimator $\hat{k}_n$ for k is

obtained as a root of the equation

$$G_n(\hat{k}_n) = 0, \tag{4.16}$$

for collated data over n days. Here,

$$G_n(\hat{k}_n) = \sum_{i=1}^{n} \frac{\dot{b}(X_{i-1}, k)}{\sigma_{i-1}^2} \{X_i - E[X_i|X_{i-1}]\} \tag{4.17}$$

and the derivative drift term $\dot{b}(X_i, k)$ of the process (4.3), written on k is calculated as

$$\dot{b}(X_i, k) = \theta(t) - X_t. \tag{4.18}$$

$\theta(t)$ is the mean function represented by (4.2). After the equation (4.16) is solved, the unique estimator, then, the unique zero of the equation is,

$$\hat{k}_n = -log \left[\frac{\sum_{i=1}^{n} Y_{i-1}(X_i - \theta(i))}{\sum_{i=1}^{n} Z_{i-1}(X_{i-1} - \theta(i-1))} \right], \tag{4.19}$$

where,

$$Z_{i-1} \equiv \frac{\theta(i-1) - X_{i-1}}{\sigma_{i-1}^2}, \ i = 1, 2, \ldots, n \tag{4.20}$$

as well as n being the number of observations, or the number of months multiplied by the number of years in question.

4.2 From the Ornstein-Uhlenbeck process to the PDE model

In this section, we develop a PDE model governing the price of the European option based on the assumption that the rainfall dynamics are described by the Ornstein-Uhlenbeck process. We conclude the section with a crucial discussion on the selection of the suitable boundary conditions for our problem, given that it is a terminal value problem.

4.2.1 The PDE model

First, we modify the measure using Girsanov's theorem. With respect to the risk neutral measure Q, which is represented by the risk market price λ. Then, we define

$$W_t^Q = W_t + \lambda t. \tag{4.21}$$

Differentiating both sides we get $dW_t^Q = dW_t + \lambda dt$. Then isolating dW_t we get, $dW_t = dW_t^Q - \lambda dt$ and replacing it into stochastic differential equation (4.3) we deduce

$$dX_t = [k(\theta(t) - X_t) + \theta'(t) - \lambda\sigma_t]dt + \sigma_t dW_t^Q, \tag{4.22}$$

where dW_t^Q is the Brownian increment under risk neutral measure Q, see for example Pirrong and Jermakyan, 2001, Pirrong and Jermakyan, 2008, Li, 2018. By the Girsanov's theorem, Theorem 2.2.3, and under the equivalent probability measure Q, W_t^Q represents a standard Brownian motion, and the solution to (4.22) is martingale. We also take into account the initial condition $X_0 = x_0$, $t \geq 0$, and $k \geq 0$.

The weather derivative incomes are determined by the evolution of an underlying meteorological index Alaton et al., 2002, Hamisultane, 2008. The majority of the time, rainfall is represented as an average monthly or daily total Emmerich et al., 2005. Then, we will consider the underlying meteorological index defined in (3.5-3.6), with the payoff functions $f(x_t)$ defined depending on the contract is a rainfall defice (3.3), or if is for rainfall excess(3.4). That is, $dY_t = f(X_t)dt$. In this specific case, the total rainfall for all of period $t \in [0, T]$ is represented by the index Y_t. The index is the total RDD or RED for the entire time period under consideration.

One way to manage the risk of rain is to purchase RDD or RED (American, Asian, or European) options and take either short or long positions.

The weather models in the weather derivatives market do not follow Geometric Brownian motion, and the underlying is not a tradable asset Alaton et al., 2002. As a result, direct application of the Black-Scholes methodology is not possible. Alternative approaches have been proposed, including an actuarial approach Brix et al., 2002, equilibrium models Cao and Wei, 2004, and arbitrage-free pricing methods Pirrong and Jermakyan, 2008. The modelling of temperature derivatives has been proposed using partial differential equations in Pirrong and Jermakyan, 2008, and subsequently adopted by other researchers in Alaton et al., 2002; Balter and Pelsser, 2018; Li, 2018. The underlying is a non-tradable asset. Then the price is determined on the theory of incomplete markets. Therefore it does not always guarantee that the risk neutral equivalent probability is unique, unlike the Black Scholes framework theory. The self-financing portfolio principle is unable to hedge the claims. Hence, the discounted conditional expectation is used to determine the weather option price Alaton et al., 2002; Björk, 1998; Pirrong and Jermakyan, 2008

$$V(x, y, t) = \mathbb{E}\left[e^{-r(T-t)}V(T, X_T, Y_T)|X_t = x, Y_t = y\right], \tag{4.23}$$

r denoted the risk-free interest rate. In order to ensure that movements in the derivative are balanced by changes in a multiple of the underlying, option valuation typically depends on the underlying quantity being used to hedge the position of the option. This allows the portfolio to be assumed to be risk-free. In these cases, a variant of Black and Scholes analysis can be used to derive unique prices. The primary assumptions of their methodology are that the underlying is tradeable and that the portfolio can be continuously delta-hedged. An alternative method is

to establish a connection between partial differential equations and stochastic differential equations in order to utilise the Feynman-Kac formula Oksendal, 2003, pag. 145. Here, we employ this strategy.

In view of (4.23) and because X_t and Y_t satisfy (3.6) and (4.22) respectively, the Feynman-Kac theorem Oksendal, 2003, p 145 allows to derive a partial differential equation that governs the price of the weather derivative under a risk neutral probability Q given by

$$\frac{\partial V}{\partial t} = rV - f(x,t)\frac{\partial V}{\partial y} - \gamma(x,t)\frac{\partial V}{\partial x} - \frac{1}{2}\sigma^2\frac{\partial^2 V}{\partial x^2}, \tag{4.24}$$

where t is time, x is the average rainfall, y is the cumulative index of the underlying weather variable, $f(x)$ is defined as in (3.3) for *rainfall deficit* or as in (3.4) for *rainfall excess*, that is, respectively by

$$f(x) = (x - x_{ref})^+ \qquad \text{or} \qquad f(x) = (x_{ref} - x)^+,$$

where the function $\gamma(x,t)$ is defined by,

$$\gamma(x,t) = k(\theta(t) - x) + \theta'(t) - \lambda\sigma, \tag{4.25}$$

with k as the rate of the mean reversion, $\theta(t)$ is the long term mean of the process, λ is the market price of risk and σ is the volatility.

To solve the partial differential equation (4.24) a terminal condition is necessary together with some boundary conditions. The terminal condition for $t = T$ is of the form

$$V(x,y,T) = \psi(y),$$

where y is the cumulative index of the underlying weather variable.

In particular, the terminal conditions, for a European put and a call, are respectively given by

$$V_P(x,y,T) = tick \times (K - y_T)^+, \qquad V_C(x,y,T) = tick \times (y_T - K)^+. \tag{4.26}$$

where K is the strike level (defined at time t), y_T is the value of the RDD or RED index at maturity, and "*tick*" is used to translate the quantity $(y_T - K)^+$ into monetary terms.

The equation (4.24) is an element of the class of backward Kolmogorov equations. Compared to convection effects, diffusion effects are substantially smaller. A technique based on PDEs was proposed by Pirrong and Jermakyan Pirrong and Jermakyan, 2001 for pricing weather derivatives. By generating market prices of risk from weather futures quotations and taking the weather options market's liquidity

into account, they were able to derive the weather options' arbitrage-free prices.

The weather option contract lacks a negotiable underlying index in reality, and the model is still very abstract. For instance, improvements of weather derivatives pricing by PDEs are found in Broni-Mensah, 2012 for practical applications. The authors in Broni-Mensah, 2012 derived a PDE introducing a hedging instrument that is imperfectly correlated with the underlying index, assuming a mean-self financing portfolio and partial hedging. By taking into account the stochastic volatility, (4.24) can be further improved, allowing to compute market prices of risk rather than extracting them from quotations. However, as stated in Hamisultane, 2008, in order to extract a risk-neutral distribution, we must have access to quotations of the weather contracts. The quoted weather contracts must be liquid in order to support both risk-neutral distribution and market prices of risk.

Boundary conditions must be added in order to have a clearly defined problem. In the following section, we address boundary condition selection.

4.2.2 Boundary conditions

Generally speaking, there are no universal a priori rules for calculating the best truncated far field or figuring out what the right boundary conditions are. Chen Chen, 2017 suggests the following boundary conditions in the case of a spread option:

- Boundary condition based on analytical solution: (for an exchange option, we could apply the Margrabe formula Haug, 2007; Margrabe, 1978. Naturally, this strategy is effective in the case we know the analytical solution or how to be located;
- Pay-off boundary conditions: The far-field values in the pay-off function are used in this instance and will subsequently serve as the boundary condition. Although issues may occur when both state variables are close to the far-field boundary, this is a reasonable solution;
- On the near-field and far-field boundaries, let the PDE be satisfied. If we are lucky, we might be able to define Dirichlet boundary conditions in certain special cases. A put option, for instance, has zero boundary condition in the far field, and the pay-off function can be used to determine its value in the near field. This strategy employed in Topper Topper, 2005;
- Linearity boundary condition.

Our suggested boundary conditions have never been published in the literature before. First of all, the boundary conditions should not be extremely artificial, as they are inspired by the financial interpretation. They should also be compatible conditions with the terminal condition from a mathematical perspective.

Several works (Broni-Mensah, 2012; Tang and Chang, 2016) have proposed boundary conditions in the context of temperature weather derivatives. Let's talk about what they did and what we propose in this case. We begin by talking about the put option and remembering that the terminal condition is

$$V_P(x, y, T) = tick \times (K - y)^+.$$

Without losing generality, we take into consideration the deficit index,

$$f(x) = (x_{ref} - x)^+.$$

In the case of a European put options, the put option loses value due to a large RD index in the absence of precipitation. Consequently,

$$V_P(x^{min}, y, t) = 0$$

is a potential boundary condition at x^{min}, as proposed in the temperature weather derivatives context Broni-Mensah, 2012; Tang and Chang, 2016. As acknowledged in Broni-Mensah, 2012, page 118, when the index y is small, this condition is too severe and poorly adjusted to the financial argument. As a result, an alternative is suggested in Broni-Mensah, 2012, page 118, to evaluate the partial differential equation at x^{min} without using the second order derivative. Nevertheless, this condition was not applied in the following references (Li, 2018, 2021; Li et al., 2020; Tang and Chang, 2016), possibly due to its difficulty in application and potential impact on the overall accuracy of the numerical method.

Then, we propose the following boundary condition,

$$V_P(x^{min}, y, t) = tick \times (K - (y + f(x^{min})(T - t)))^+. \tag{4.27}$$

There are three reasons for this decision. First, we have a condition that is consistent with the terminal condition when $t = T$. Second, we obtain zero when y is large, indicating that the put becomes worthless for a large index, according to the financial interpretation. Third, according to the equation (3.6), which represents a transport equation with drift $f(x)$, the put is not zero for a small index and evolves from the terminal condition to the initial time. This is $f(x^{min})$ at x^{min}. Since we update the rainfall index as we evolve over time for a fixed minimum rainfall precipitation, x^{min}, this also makes financial sense. Alternatively, the partial differential equation (4.24) indicates that the dynamics are dominated by the first two terms, since $f(x)$ reaches its maximum value at x^{min}.

On the other side of the x domain, at x^{max}, an excessive amount of precipitation results in a small accumulated RD index, since there is enough water. Given that

we have lower index values under raining conditions, we can infer from the payoff condition (4.26) that, if the domain is large enough, the payoff is almost guaranteed. The Neumann boundary condition, which appears in the literature, is suggested also here,

$$\frac{\partial V_P}{\partial x}(x^{max}, y, t) = 0. \tag{4.28}$$

It is also widely agreed upon that the boundary condition for the accumulated weather index when y approaches infinity is

$$\lim_{y\to\infty} V_P(x, y, t) = 0. \tag{4.29}$$

This is easily understood by observing that $K - y < 0$ is implied when y approaches infinity.

For a European call option, a similar discussion can be had, and we also propose alternative boundary conditions to those found in the literature. We agree with the literature's suggested conditions at x^{min} and at the point where the index y reaches infinity, that is,

$$\frac{\partial V_C}{\partial x}(x^{min}, y, t) = 0, \quad \lim_{y\to\infty} V_C(x, y, t) = \infty. \tag{4.30}$$

We can observe that at $x = x^{max}$, it is suggested in Li, 2018, 2021; Li et al., 2020 that

$$V_C(x^{max}, y, t) = 0.$$

This relates to temperature, but the issue with this condition is also present in the rain context. Although it is in accordance with the initial condition, that is, when $y = 0$ becomes zero, this condition is incompatible with the fact that we have infinity when y goes to infinity. Our numerical experiments also demonstrate that, for large values of y, this condition is not a good choice. Consequently, we propose the boundary condition.

$$V_C(x^{max}, y, t) = tick \times (y - Ke^{-r(T-t)})^+. \tag{4.31}$$

This is zero for a small index, as it should logically be. However, the likelihood of the call option being exercised increases with y. As a result, the call option's value increases with each passing maturity date, until it equals the index value minus the exercise price, we must pay to exchange the index.

Using a similar explanation, we must have a real value rather than the value infinity in (4.30) when determining the numerical solutions. We substitute the boundary,

$$\lim_{y\to\infty} V_C(x, y, t) = \infty$$

by

$$\lim_{y\to\infty}(y - V_C(x,y,t)) = Ke^{-r(T-t)}.$$

Naturally, the put call parity served as the model for this. Given that the boundary condition,

$$V_P(x, y^{max}, t) = 0$$

has been proposed, the parity put call results in the call option's prior condition.

At last, our problem formulation is achieved through the manipulation of the variable $\tau - \tau_0 = T - t$ in equation (4.24). In this sense, rather than having the data as a terminal condition, we have it as an initial condition. The formula turns into,

$$\frac{\partial V}{\partial \tau} - f(x)\frac{\partial V}{\partial y} - \gamma(x,\tau)\frac{\partial V}{\partial x} - \frac{1}{2}\sigma^2\frac{\partial^2 V}{\partial x^2} + rV = 0, \tag{4.32}$$

now, the function $\gamma(x,\tau)$ is defined as follows

$$\gamma(x,\tau) = k(\theta(T + \tau_0 - \tau) - x) - \theta'(T + \tau_0 - \tau) - \lambda\sigma.$$

We denote this as $\tau_f := \tau_0 + T$. The differential problem is usually solved on the time interval $[\tau_0, \tau_f]$, where $T = \tau_f - \tau_0$ is the maturity. The initial condition for the European put option a is as follows.

$$V_P(x, y, \tau_0) = tick \times (K - y)^+ \tag{4.33}$$

and for an European call option we have the initial condition

$$V_C(x, y, \tau_0) = tick \times (y - K)^+. \tag{4.34}$$

Given that the computational domain for the problem is defined by,

$$[x^{min}, x^{max}] \times [y^{min}, y^{max}],$$

the following are the boundary conditions for the European put option are:

$$V_P(x^{min}, y, t) = tick \times (K - (y + f(x^{min})(\tau - \tau_0)))^+, \tag{4.35}$$

$$\frac{\partial V_P}{\partial x}(x^{max}, y, \tau) = 0, \tag{4.36}$$

$$V_P(x, y^{max}, \tau) = 0. \tag{4.37}$$

For a European call option are defined by

$$\frac{\partial V_C}{\partial x}(x^{min}, y, \tau) = 0, \tag{4.38}$$

$$V_C(x^{max}, y, \tau) = tick \times (y - Ke^{-r(\tau-\tau_0)})^+, \tag{4.39}$$

$$V_C(x, y^{max}, \tau) = tick \times (y^{max} - Ke^{-r(\tau-\tau_0)}). \tag{4.40}$$

Chapter 5

An explicit numerical method for the PDE model

This chapter involves the numerical evaluation of weather derivatives. We first provide a review on finite difference methods and we define some relevant concepts. To effectively handle the various coefficient choices in the equation that depend on the amount of precipitation (amount of rain) and the deficit or excess of rainfall, we propose an explicit numerical method. Since it is an explicit numerical method, it will be conditionally stable, and we will address the problem of its order of convergence and stability region. Finally, we look at two test scenarios in which precipitation data is used to estimate the model's parameters. The research results were partially published in Nhangumbe and Sousa, 2024.

5.1 The generalities of finite difference methods

The finite difference method is numerical procedure used to approximate the partial differential equations. This consist of the discretization of the continuous physical domain into a discrete finite difference grid, the individual exact partial derivatives in the partial differential equations are approximated by algebraic finite difference approximations (FDA). Then, the approximated derivatives are substituted into the partial differential equations to obtain an algebraic finite difference equation (FDE). Therefore, the resulting algebraic finite difference equations for the dependent variable are solved to get the approximated solutions of the PDE.

In order to find the approximated solution of the PDE using finite differences, the functions and the derivative that appear in the equation are approximated at the mesh points. The multiple possibilities that can be used include:

- one-sided differences,
- centred differences.

The number of steps required at each time level to calculate the solution of the PDE can be selected as:

- One-step: is a method for computing finite differences that uses the solution at time-level n to calculate the solution at time-level $n+1$. To calculate the solution at level $n+1$;, no information from levels $n-1$, $n-2$, or earlier levels is required;
- Multi-step methods: is a difference scheme in which values at levels n, $n-1$, and possibly earlier time levels determine the solution at level $n+1$.

In general, the multi-step methods are complex to handle, and the common methods are based on the one-step methods:

- Explicit: is one in which the data at level n can be used directly to calculate the solution at time $n+1$. No additional arithmetic is required, such as when dividing or inverting a matrix;
- Implicit schemes: is one where the solution at this level can only be found by grouping the terms involving the approximate solution at level $n+1$. We must find a solution to this system of equations at each time step.

There are a variety of explicit and implicit schemes. However, the most common and useful difference schemes that approximate the solution of the PDE are,

- explicit Euler,
- implicit Euler,
- Crank–Nicolson (or Box scheme): is seen as an average of explicit and implicit Euler schemes,
- the trapezoidal method: is comparable to Crank-Nicolson; however, the averaging mechanism is slightly different.

However, the PDE in question needs to be investigated in order to better understand its qualitative characteristics, before deciding which scheme to employ. The qualitative characteristics, which must be represented in the difference scheme, enable the description of the behaviour of the PDE solutions. Examples of these characteristics include positivity or monotonicity, and how the solutions grow or decrease with time.

When we choose which numerical method to use, we have to consider some general concerns related to how the discrete solution of the approximated problem $P2$ is a good approximation to the exact solution of the original problem, $P1$. These concerns include D. Duffy, 2022:

- Is it the case that $P2$ maintains the positivity, monotonicity, and energy conservation of $P1$? Does it adhere to the principle of discrete maximum?

- How accurate is the problem *P*2 as an approximation to the problem P1 as a function of mesh sizes? Is a first-order accurate, is a second-order accurate, or even higher order schemes of particular interest to us?
- Is *P*2 well-posed in the sense that minor modifications to the input data (such as initial or boundary conditions) result in minor modifications to the approximate solution?
- Computational efficiency: Is it possible to solve P2 with a reasonable amount of memory and time? To put it another way, how well-performing is the P2 algorithm at runtime?

These issues are related to the ideas of how the solution of a finite difference equation converge to the solution of a partial differential equation that it approximate and it involves the study of consistency, accuracy, stability and convergence. These conditions are related to each other and the precise relation described in the Lax Equivalence Theorem. This theorem allows to prove the convergence of a well-posed problem scheme by proving the consistency and stability. The definition of stability depends on the context. In numerical linear algebra, the principal concern is instabilities caused by proximity to singularities of various kinds, such as very small or nearly colliding eigenvalues. In numerical algorithms for differential equations the concern is the growth of round-off errors and/or small fluctuations in initial data which might cause a large deviation of final answer from the exact solution. There are various concepts of numerical stability, for instance, A-stability. They are related to some concept of stability in the dynamical systems sense, often the Lyapunov stability. On partial differential equations, an algorithm for solving a linear evolutionary partial differential equation is stable if the total variation of the numerical solution at a fixed time remains bounded as the step size goes to zero.Then, the notion of stability is addressed in the sense of Lax-Richtmyer stability, that is, a necessary and sufficient condition for a consistent scheme to give a convergent approximation to the solution of a well-posed linear problem, as the mesh is refined in a given way, Morton, 1996, p 16

The explicit Euler methods, that our studies will be based on, are associated with two forms of instabilities Roache, 1998:

- Dynamic instability: the large time step sizes cause oscillatory errors in the scheme;
- Static instability: the convection (advection) term in the convection diffusion PDE is what causes this type of instability, particularly when it is large in comparison to the volatility term;

The dynamic stability of a time-dependent convection-diffusion equation can be managed through either explicit or implicit methods that establish the relationship

between the mesh sizes in the space and time dimensions. Following D. Duffy, 2022, in order to control the static stability, one of the following methods can be used:

- Exponential fitting, a type of exact scheme, which is stable and convergent for any value of the diffusion and convection functions as well as any mesh size in space;
- Lax-Wendroff schemes, which add an artificial diffusion to a first-order PDE and the stability condition is independent of the sign of the convection term;
- Upwinding, which is one-sided difference scheme for the convection term and takes in account that the coefficient of the convection term can be positive or negative and the correct kind of upwinding must be used in each case.

The following definitions are extracted from Sod, 1985, p 13. Let us consider the the finite difference method $P2 : u^{n+1} = Qu^n$ of the initial value problem $P1 : \frac{\partial v}{\partial t} = Lv + F,\ v(x, t_0) = v_0, x \in \mathcal{R}, t \geq 0$ and L is a differential operator.

Definition 5.1.1 (of consistency)
A finite difference method, $P2$, is consistent up to time τ_f in a norm $\| - \|$ with equation $(P1)$ if the solution to the initial value problem $P1$ "almost" satisfies the finite difference method $P2$, that is,

$$v^{n+1} = Qv^n + k\tau^n,$$

where $\|\tau^n\| < \tau(h)$, $nk < T$ and $t(h) \to 0$ as $k \to 0$. Further is assumed that h is defined in terms of k and goes to zero with k. τ^n is the local truncation error at time nk.

Definition 5.1.2 (of accuracy)
The finite difference method, $P2$, is accurate of order (p, q) if

$$\|V^{n+1} - QV^n\| = k(O(h^p) + O(k^q)).$$

In this case, $O(h^p) + O(k^q)$ is called the local truncation error associated with the finite difference method.

Definition 5.1.3 (of stability)
A finite difference method is called stable if there exist constants K and β and some norm $\| - \|$ such that,

$$\|u^{n+1}\| \leq Ke^n\|u^0\| = Ke^{\beta\tau}\|u^0\|,$$

where $\tau = nk$, and K and β are independent of h and k.

Definition 5.1.4 (of unconditionally stability)

A finite difference method is called unconditionally stable if it is stable for any time step k and grid spacing h.

Definition 5.1.5 (of convergence)
The finite difference method, $P2$, is convergent in a norm $\| - \|$, if

$$\|v(x,t) - u_i^n\| \to 0 \text{ as } h \to 0 \ \wedge \ k \to 0.$$

It is convergent of order (p,q) in a norm $\| - \|$, if

$$\|v(x,t) - u_i^n\| = O(h^p) + O(k^q).$$

Roughly speaking, these concepts mean:

- Consistency: When space and time mesh sizes approach zero, do the values of $P2$ look similar to the values of P1?
- Stability: Are the norms of the initial solution limiting the norm of the P2 solution at every time step?
- Convergence: The norm of the difference between the solutions of $P2$ and $P1$ at each time level is limited by the truncation error (polynomial power of the mesh sizes)?

Theorem 5.1.1 (Lax)
If a consistent finite difference method of a linear well posed problem is stable, and accurate of order (p,q), then it is convergent of order (p,q), Sod, 1985, pp.14-15.

The Discrete Maximum Principle, von Neumann stability criterion, and matrix theory are the usual methods for demonstrating stability D. Duffy, 2022; Richtmyer, 1967; Sod, 1985. Generally, all of them are restricted to linear problems. Nevertheless, the investigation of stability for initial, boundary value problems can be extremely complicated, particularly in the presence of boundary conditions and their numerical representation Hirsch, 2007, p 292. The Von Neumann stability analysis, based on a Fourier analysis in space of the errors of the numerical solution is most popular. It is strictly designed for smooth initial values problems with constant coefficients in an infinite domain and with periodic boundary condition. For the problems with variable coefficients it is applied locally and only provide necessary conditions for stability D. Duffy, 2004; Morton, 1996. On the other hand, for the problems with many types of boundaries, it can provide the stability conditions that are very close to the necessary and sufficient condition for practical stability Sousa, 2009, p 10 . The von Neumann stability analysis gives useful results even in cases where its application is not fully justified.

The von Neumann stability analysis, applies the Fourier decomposition of numerical error and the approximate solution is represented as follows:

$$v_j^n = \rho^n e^{ij\alpha\Delta x},\ i = \sqrt{-1},\ (\alpha \text{ is a number}). \tag{5.1}$$

The symbol ρ denotes the amplification factor of the difference scheme under consideration. The formula (5.1) is applied into the difference method. Then, it is solved for ρ. The criterion for stability is $\|\rho\| \leq 1$ for strong stability D. Duffy, 2022, p 235 or in terms of Lax-Richtmyer stability $\|\rho\| \leq 1 + O(\Delta t)$. LeVeque, 2007, p 190

When the Von Neumann analysis is applied for linear problems with non-constant coefficients, a local von Neumann analysis will typically provide the necessary condition for stability. To achieve sufficient conditions for stability, more restrictions on the amplification factor must be implemented Richtmyer, 1967. These conditions are connected to the non-linear behavior's production of high-frequency harmonics and the need to dampen these frequencies to preserve stability. This is particularly significant because non-linear hyperbolic problems describe essentially propagating waves without physical damping. Where such physical damping exists, even with parabolic problems, an additional condition on the amplification factor might be necessary. This problem is given in the definition of dissipative schemes given below Hirsch, 1988, p 323.

Definition 5.1.6 (of dissipative scheme)
A finite difference method, $P2$, is called dissipative if for all ξ, $\|\rho(\xi)\| \leq 1$ and $\|\rho(\xi)\| < 1$ for some ξ, where $\rho(\xi)$ is the symbol of Q.

Definition 5.1.7 (of dissipative scheme of order 2)
A finite difference method $P2$ is called dissipative of order $2s$ where s is a positive integer, if there exists a constant $\delta > 0$ (independent of h, k and ξ) such that

$$\|\rho(\xi)\| < 1 - \delta\|\xi\|^{2s}$$

for $0 \leq \xi \leq \pi$.

5.2 Computational domain

In order to use a finite difference method to approximate the differential equation, we must take into account a computational domain. We take into consideration the truncated computational domain

$$[x^{min}, x^{max}] \times [y^{min}, y^{max}] \times [\tau_0, \tau_f]$$

for the partial differential equation (4.32). The discrete domain's grid points are distributed equally across time and space, with the time and space steps provided,

respectively, by

$$\Delta\tau = \frac{\tau_f - \tau_0}{N_\tau}, \qquad \Delta x = \frac{x^{max} - x^{min}}{N_x}, \qquad \Delta y = \frac{y^{max} - y^{min}}{N_y}.$$

Therefore, the computational domain is

$$\{(x_j, y_k, \tau_n), j = 0, \ldots, N_x; k = 0, \ldots, N_y; n = 0, \ldots, N_\tau\}$$

with

$$x_j = x^{min} + j\Delta x; \;\; y_k = y^{min} + k\Delta y; \;\; \tau_n = \tau_0 + n\Delta\tau. \tag{5.2}$$

The approximated solution of $V(x, y, \tau)$ is represented by $V_{j,k}^n \approx V(x_j, y_k, \tau_n)$. The values of the functions $f(x)$ and $\gamma(x, \tau)$ are represented, respectively, by $f_j = f(x_j)$ and $\gamma_j^n = \gamma(x_j, \tau_n)$.

5.3 Numerical method I

In selecting a suitable numerical technique for the studied equation, the following factors should be considered:

- the advection component may be dominant, and the coefficients not constant;
- when boundaries exist, the method's accuracy must be implemented appropriately to maintain the accuracy of the scheme;
- the discontinuity in the initial conditions could be a factor in the rate of convergence being reduced.

In the hyperbolic direction, y, we have a one-sided boundary condition. In this direction, we can choose to use a first order approximation to approximate the first order derivative if we do not want to take into account numerical (artificial) boundaries. In the parabolic direction, where the diffusive term associated with volatility is present, we require a numerical technique capable of handling a potential dominant addictive term.

To avoid the numerical (artificial) boundaries, we use the first order upwind approximation to approximate the first order derivative in the y direction, the hyperbolic direction. We consider a Lax-Wendroff type scheme in the parabolic direction, which provides us with a spatial second order approximation and stable scheme if the volatility is low in relation to the coefficient of the advective term, $\gamma(x, \tau)$.

The signs of the functions f and γ must be considered. In the y direction, a

downwind difference approximation is taken into consideration because the function f is always non-negative. However, since the Lax-Wendroff scheme is employed and $\gamma(x,\tau)$ is a positive or negative variable, we do not need to worry about the sign of γ.

We can derive the Lax–Wendroff scheme by applying the Taylor series expansions on the expression

$$\frac{\partial V}{\partial \tau} - \gamma(x,\tau)\frac{\partial V}{\partial x}$$

of equation (4.32), to obtain

$$V(x,y,\tau+\Delta\tau) = V(x,y,\tau) + \Delta\tau V_\tau(x,y,\tau) + \frac{1}{2}\Delta\tau^2 V_{\tau\tau}(x,y,\tau) + \dots. \tag{5.3}$$

Then replacing V_τ by $\gamma(x,\tau)\frac{\partial V}{\partial x}$ and $V_{\tau\tau}$ by $\gamma(x,\tau)^2\frac{\partial^2 V}{\partial x^2}$ in (5.3) gives

$$V(x,y,\tau+\Delta\tau) = V(x,y,\tau) + \Delta\tau\gamma(x,\tau)\frac{\partial V}{\partial x} + \frac{1}{2}\Delta\tau^2\gamma(x,\tau)^2\frac{\partial^2 V}{\partial x^2} + \dots. \tag{5.4}$$

Therefore, by using the standard centered approximations for the first order and second order derivatives in x direction of PDE (4.32) we end up with the Lax-Wendroff scheme.

We define the following difference operators,

$$\Delta_y^+ V_{j,k}^n = V_{j,k+1}^n - V_{j,k}^n; \quad \Delta_{0x} V_{j,k}^n = V_{j+1,k}^n - V_{j-1,k}^n; \quad \delta_x^2 V_{j,k}^n = V_{j+1,k}^n - 2V_{j,k}^n + V_{j-1,k}^n.$$

Next, we introduce the explicit difference scheme that takes into account the Lax-Wendroff scheme in x and in y a first order downwind. For $j = 1,\cdots,N_x$; $k = 0,\cdots,N_y-1$, we have

$$\begin{aligned} V_{j,k}^{n+1} &= V_{j,k}^n - r\Delta\tau V_{j,k}^n + \frac{\Delta\tau}{\Delta y} f_j \Delta_y^+ V_{j,k}^n + \frac{\gamma_j^n \Delta\tau}{2\Delta x}\Delta_{0x} V_{j,k}^n + \\ &\quad + \left(\frac{(\gamma_j^n)^2\Delta\tau^2}{2\Delta x^2} + \frac{\sigma^2\Delta\tau}{2\Delta x^2}\right)\delta_x^2 V_{j,k}^n. \end{aligned} \tag{5.5}$$

Without getting too technical, let's talk about boundary conditions for the put option. There is only a boundary condition at $y = y^{max}$ in the y direction, since the convection coefficient in this direction is always positive. Boundary conditions are needed on both sides in the x direction.

The Dirichlet boundary conditions are present at the nodes $\{(0,k) : k = 0,\cdots,N_y\}$ and $\{(j,N_y), j = 0,\cdots,N_x\}$. We have a Neumann boundary condition at the nodes $\{(N_x,k) : k = 0,\cdots,N_y-1\}$. The implementation of Dirichlet boundary conditions is straightforward (see Figure 5.1). Regarding the Neumann boundary conditions, the solution at the boundary must be obtained. At each time step, we obtain

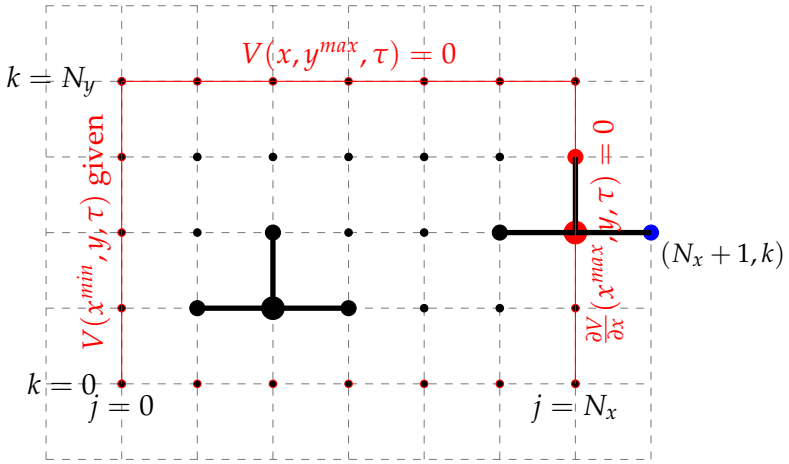

FIGURE 5.1: Explicit scheme that is Lax-Wendroff in x and downwind in y for a put option. Black dots are internal nodes; Blue dots are ghost nodes; Red dots are boundary nodes.

$V^n_{N_x+1,k} = V^n_{N_x-1,k}$, taking into account the Neumann boundary condition and using a centred difference approximation for the first order derivative. We compute the function at the boundary values $V^{n+1}_{N_x,k}$, $k = 0, \cdots, N_y - 1$, using this equality and (5.5).

Remark 1

Figure 5.1, provides the explanation of put option. However, the methodology is the same for the call option, the variations stem from the different boundary selections. We now have a Dirichlet boundary condition at node $\{(N_x, k) : k = 0, \cdots, N_y - 1\}$ and a Neumann boundary condition at node $\{(0, k) : k = 0, \cdots, N_y\}$. Since the ghost points are therefore close to $j = 0$, we proceed in the same manner as we did for $j = N_x$ in the put option scenario. Using the centred difference approximation, we can calculate the first order derivative for the call option at $j = 0$ by obtaining $V^n_{1,k} = V^n_{-1,k}$ at each time step. We can then use this equality along with (5.5) to compute the function at the boundary values $V^{n+1}_{0,k}$, $k = 0, \cdots, N_y - 1$.

The application of explicit schemes result on discrete systems of equations that can be solved without the use of matrix solvers . That explicit numerical method is conditionally consistent with only one particular PDE. It suggests that the step sizes in space and time must be related to each other in order for the scheme to converge to the PDE.

5.3.1 Convergence analysis

In this section, the theoretical characteristics of the finite difference method, such as consistency and stability, are addressed. Deriving the stability conditions is important because the numerical method is explicit. The stability region provides guidance on the selection of time and space steps for a convergent numerical method.

We provide a test problem as well to validate the theoretical findings.

Consistency

The truncation error can be used to determine the numerical method's order of accuracy. Roughly speaking, the truncation error can be understood as the difference between the two sides of the equation when the approximation $V_{j,k}^n$, is substituted by the exact solution of the differential equation, $V(x_j, y_k, \tau_n)$.

The exact solution at the discrete points (x_j, y_k, τ_n) and $\Omega = (x^{min}, x^{max}) \times (y^{min}, y^{max}) \times (\tau_0, \tau_f)$ is represented by the notation $v_{j,k}^n$. The set of functions with continuous derivatives up to the exponent's order in x, y and t, respectively, is represented by the set $C^{(4,2,2)}(\Omega)$.

As we know, if $v \in C^{(4,2,2)}(\Omega)$, then we have

$$\begin{aligned} \frac{v_{j,k}^{n+1} - v_{j,k}^n}{\Delta\tau} &= \frac{\partial v_{j,k}^n}{\partial\tau} + O(\Delta\tau), \qquad \frac{\Delta_y^+ v_{j,k}^n}{\Delta y} = \frac{\partial v_{j,k}^n}{\partial y} + O(\Delta y), \\ \frac{\Delta_{0x} v_{j,k}^n}{2\Delta x} &= \frac{\partial v_{j,k}^n}{\partial x} + O((\Delta x)^2), \qquad \frac{\delta_x^2 v_{j,k}^n}{\Delta x^2} = \frac{\partial^2 v_{j,k}^n}{\partial x^2} + O((\Delta x)^2). \end{aligned} \tag{5.6}$$

As a result of the numerical approach used, we have

$$\begin{aligned} T_{j,k}^n &= \frac{v_{j,k}^{n+1} - v_{j,k}^n}{\Delta\tau} + r v_{j,k}^n - \frac{1}{\Delta y} f_j \Delta_y^+ v_{j,k}^n - \frac{\gamma_j^n}{2\Delta x} \Delta_{0x} v_{j,k}^n + \\ &\quad - \left(\frac{(\gamma_j^n)^2 \Delta\tau}{2\Delta x^2} + \frac{\sigma^2}{2\Delta x^2} \right) \delta_x^2 v_{j,k}^n. \end{aligned} \tag{5.7}$$

Therefore, we obtain

$$\begin{aligned} T_{j,k}^n &= \frac{\partial v_{j,k}^n}{\partial\tau} + O(\Delta\tau) + r v_{j,k}^n - f_j \left(\frac{\partial v_{j,k}^n}{\partial y} + O(\Delta y) \right) - \gamma_j^n \left(\frac{\partial v_{j,k}^n}{\partial x} + O((\Delta x)^2) \right) \\ &\quad - \left(\frac{(\gamma_j^n)^2 \Delta\tau}{2} + \frac{\sigma^2}{2} \right) \left(\frac{\partial^2 v_{j,k}^n}{\partial x^2} + O((\Delta x)^2) \right). \end{aligned}$$

After all, we can conclude that the method is of order $O((\Delta x)^2, \Delta y, \Delta\tau)$ accuracy.

Stability

We will now discuss about the numerical method's stability. The following result can be used to examine the stability of the interior scheme Richtmyer, 1967; Sod, 1985. Let us consider the finite difference scheme of the following form

$$V_{j,k}^{n+1} = Q V_{j,k}^n, \tag{5.8}$$

with

$$Q = \sum_{l=-l_1}^{l_2} \sum_{m=-m_1}^{m_2} c_{l,m}(x,y) S^{l+m}.$$

The coefficients $c_{l,m}(x,y)$ are functions of x and y and S^{l+m} represents the forward and backward shift operators, that is,

$$S^{l+m} V_{j,k}^n = V_{j-l,k-m}^n.$$

A consistent method is stable if the function

$$\rho(x,y,\xi) = \sum_{l=-l_1}^{l_2} \sum_{m=-m_1}^{m_2} c_{l,m}(x,y) \mathrm{e}^{-il\xi_x} \mathrm{e}^{-im\xi_y}, \quad \xi = (\xi_x, \xi_y), \tag{5.9}$$

satisfies the following assumptions:

(a) It is Lipschitz continuous in (x,y).

(b) For $\xi \neq 0$ and $\max\{|\xi_x|, |\xi_y|\} \leq \pi$, we have $|\rho(x,y,\xi)| < 1 + O(\Delta\tau)$ for all (x,y).

(c) The scheme is dissipative of order $2q$, where q is a positive integer, that is, for $\max\{|\xi_x|, |\xi_y|\} \leq \pi$, $\Delta\tau$ less than some $\tau_f > 0$ and $\delta(x,y) > 0$, for all (x,y), we have $|\rho(x,y,\xi)| \leq 1 + O(\Delta\tau) - \delta(x,y)|\xi|^{2q}$, with $|\xi|^2 = \xi_x^2 + \xi_y^2$.

The proof for the following result, which pertains to the numerical method's stability, is based on some concepts discussed in Araújo et al., 2014; Sod, 1985. If the boundaries are periodic, the von Neumann method can be used for Cauchy problems or bounded domains. Nonetheless, the application of von Neumann conditions enables us to get the necessary stability conditions for more general boundary conditions, which results in helpful limitations on the selection of Δt. The stability conditions derived from the von Neumann analysis are generally very close to the necessary and sufficient conditions for practical stability for linear problems with boundaries.

Theorem 5.3.1

Let f be a non-negative function and denote

$$\|f\|_\infty = \max_x(f(x)), \qquad \|\gamma\|_\infty = \max_{x,\tau} |\gamma(x,\tau)|.$$

Define

$$\nu_x = \frac{\Delta\tau}{\Delta x}, \qquad \nu_y = \frac{\Delta\tau}{\Delta y}, \qquad \mu = \frac{\sigma^2 \Delta\tau}{(\Delta x)^2}.$$

If

$$\|f\|_\infty \nu_y + \|\gamma\|_\infty^2 \nu_x^2 + \mu \leq 1, \qquad \|f\|_\infty \nu_y + \frac{\|\gamma\|_\infty^2 \nu_x^2}{\|\gamma\|_\infty^2 \nu_x^2 + \mu} < 1 \tag{5.10}$$

then the amplification factor for the numerical method (5.5) satisfies the conditions (a), (b) and (c) stated previously.

Proof. (a) The Lipschitz condition of $\rho(x, y, \xi)$ is trivially satisfied if we assume that the functions f, γ are Lipschitz continuous in x.

(b) The behaviour of the amplification factor can be found by incorporating the Fourier mode

$$U_{j,k}^n = \rho^n(x_j, y_k, \xi)\mathrm{e}^{ij\xi_x + ik\xi_y}, \text{ for } \xi_x, \xi_y \in [-\pi, \pi], \ (\xi_x, \xi_y) \neq (0, 0)$$

into the scheme. The amplification factor for the numerical method (5.5), for f_j and γ_j^n non-negative is given by

$$\begin{aligned} \rho(x_j, y_k, \xi) &= 1 - r\Delta\tau + f_j\nu_y(e^{i\xi_y} - 1) + \frac{\gamma_j^n \nu_x}{2}(e^{i\xi_x} - e^{-i\xi_x}) + \\ &\quad + \frac{\gamma_j^2 \nu_x^2 + \mu}{2}(e^{-i\xi_x} - 2 + e^{i\xi_x}). \end{aligned} \tag{5.11}$$

For the sake of clarity, we denote

$$\nu_{x,j} = \frac{\Delta\tau}{\Delta x}\gamma_j^n, \quad \nu_{y,j} = \frac{\Delta\tau}{\Delta y}f_j, \quad \mu = \sigma^2\frac{\Delta\tau}{(\Delta x)^2}$$

and substituting into (5.11), we deduce

$$\begin{aligned} \rho(x_j, y_k, \xi) &= 1 - r\Delta\tau + \nu_{y,j}(\cos\xi_y - 1) + \frac{\nu_{x,j}^2 + \mu}{2}(2\cos(\xi_x) - 2) + \\ &\quad + i(\nu_{y,j}\sin(\xi_y) + \nu_{x,j}\sin(\xi_x)). \end{aligned}$$

Now, denoting $s_x = 1 - \cos(\xi_x),\ s_y = 1 - \cos(\xi_y)$, we can rewrite the above equation as

$$\rho(x_j, y_k, \xi) = 1 - r\Delta\tau - \nu_y s_{y,j} - (\nu_{x,j}^2 + \mu)s_x + i(\nu_{y,j}\sin(\xi_y) + \nu_{x,j}\sin(\xi_x)),$$

from where we deduce

$$|\rho(x_j, y_k, \xi)|^2 = (1 - r\Delta\tau - \nu_{y,j}s_y - (\nu_{x,j}^2 + \mu)s_x)^2 + (\nu_{y,j}\sin(\xi_y) + \nu_{x,j}\sin(\xi_x))^2.$$

or equivalently

$$\begin{aligned} |\rho(x_j, y_k, \xi)|^2 &= (1 - r\Delta\tau)^2 - 2(\nu_{y,j}s_y + (\nu_{x,j}^2 + \mu)s_x) + 2r\Delta\tau(\nu_{y,j}s_y + (\nu_{x,j}^2 + \mu)s_x) \\ &\quad + (\nu_{y,j}s_y + (\nu_{x,j}^2 + \mu)s_x)^2 + (\nu_{y,j}\sin(\xi_y) + \nu_{x,j}\sin(\xi_x))^2. \end{aligned}$$

Since $0 < s_x, s_y \leq 2$ and by hypothesis $\nu_{y,j} + (\nu_{x,j}^2 + \mu) \leq 1$, then $\nu_{y,j}s_y + (\nu_{x,j}^2 + \mu)s_x \leq 2$. Therefore,

$$\begin{aligned} |\rho(x_j, y_k, \xi)|^2 &\leq (1 + r\Delta\tau)^2 - 2(\nu_{y,j}s_y + (\nu_{x,j}^2 + \mu)s_x) + (\nu_{y,j}s_y + (\nu_{x,j}^2 + \mu)s_x)^2 \\ &\quad + (\nu_{y,j}\sin(\xi_y) + \nu_{x,j}\sin(\xi_x))^2. \end{aligned} \tag{5.12}$$

Applying the Cauchy-Schwartz inequality we obtain

$$(\nu_{y,j}\sin(\xi_y) + \nu_{x,j}\sin(\xi_x))^2 \leq \left(\frac{\nu_{y,j}^2}{\nu_{y,j}} + \frac{\nu_{x,j}^2}{\nu_{x,j}^2 + \mu}\right)\left(\nu_{y,j}\sin(\xi_y)^2 + (\nu_{x,j}^2 + \mu)\sin(\xi_x)^2\right).$$

Since $\sin^2(\xi_x) = s_x(2 - s_x)$, $\sin^2(\xi_y) = s_y(2 - s_y)$ and by hypothesis $\nu_{y,j} + \nu_{x,j}^2/(\nu_{x,j}^2 + \mu) < 1$, we deduce

$$(\nu_{y,j}\sin(\xi_y) + \nu_{x,j}\sin(\xi_x))^2 < \nu_{y,j}s_y(2 - s_y) + (\nu_{x,j}^2 + \mu)s_x(2 - s_x).$$

Substituting this last inequality into (5.12), we obtain

$$\begin{aligned} |\rho(x_j, y_k, \xi)|^2 &< (1 + r\Delta\tau)^2 - 2(\nu_y s_y + (\nu_x^2 + \mu)s_x) + (\nu_y s_y + (\nu_x^2 + \mu)s_x)^2 \\ &\quad + \nu_{y,j}s_y(2 - s_y) + (\nu_{x,j}^2 + \mu)s_x(2 - s_x). \end{aligned} \tag{5.13}$$

Using the Cauchy-Schwarz inequality again, and the hypotheses $\nu_{y,j} + \nu_{x,j}^2 + \mu \leq 1$, we have

$$(\nu_{y,j}s_y + (\nu_{x,j}^2 + \mu)s_x)^2 \leq (\nu_{y,j} + \nu_{x,j}^2 + \mu)(\nu_{y,j}s_y^2 + (\nu_{x,j}^2 + \mu)s_x^2) \leq \nu_{y,j}s_y^2 + (\nu_{x,j}^2 + \mu)s_x^2.$$

Hence, we deduce from (5.13), the following

$$\begin{aligned} |\rho(x_j, y_k, \xi)|^2 &< (1 + r\Delta\tau)^2 - 2(\nu_{y,j}s_y + (\nu_{x,j}^2 + \mu)s_x) + 2(\nu_{y,j}s_y + (\nu_{x,j}^2 + \mu)s_x) \\ &\quad + \nu_{y,j}s_y^2 + (\nu_{x,j}^2 + \mu)s_x^2 - \nu_{y,j}s_y^2 - (\nu_{x,j}^2 + \mu)s_x^2. \end{aligned}$$

Finally we arrive at $|\rho(x_j, y_k, \xi)|^2 < (1 + r\Delta\tau)^2$, that is, $|\rho(x_j, y_k, \xi)| < 1 + r\Delta\tau$.

(c) One method to demonstrate the dissipative property is to look for the amplification factor's behaviour following a Taylor expansion of the sine and cosine functions up to a higher order (see Hirsch, 1988, pages 321-323 and Richtmyer, 1967, page 102). In other words, we want to demonstrate that,

$$|\rho(x_j, y_k, \xi)|^2 \leq 1 + r\Delta\tau - A|\xi|^p + O(|\xi|^{p+1}).$$

Next, we use this inequality along with what we have demonstrated in (b) to support our assertion. That is, $|\rho(x_j, y_k, \xi)| < 1 + r\Delta\tau$ in the period $(-\pi, \pi)$, except at $\xi_x = \xi_y = 0$. Then, it follows that $|\rho(x_j, y_k, \xi)| \leq 1 + r\Delta\tau - \delta|\xi|^2$ for all $|\xi| \leq \pi$, for

some $\delta > 0$. We have

$$|\rho(x_j, y_k, \xi)|^2 = (1 - r\Delta\tau - \nu_{y,j}s_y - (\nu_{x,j}^2 + \mu)s_x)^2 + (\nu_{y,j}\sin(\xi_y) + \nu_{x,j}\sin(\xi_x))^2.$$

Performing Taylor expansions, we deduce

$$\begin{aligned} |\rho(x_j, y_k, \xi)|^2 &= (1 - r\Delta\tau - \nu_{y,j}\frac{\xi_y^2}{2} - (\nu_{x,j}^2 + \mu)\frac{\xi_x^2}{2} + O(|\xi^4|))^2 + \\ &\quad +(\nu_{y,j}\xi_y + \nu_{x,j}\xi_x + O(|\xi|^3))^2. \end{aligned}$$

Therefore,

$$\begin{aligned} |\rho(x_j, y_k, \xi)|^2 &= (1 - r\Delta\tau)^2 - (1 - r\Delta\tau)(\nu_{y,j}\xi_y^2 + (\nu_{x,j}^2 + \mu)\xi_x^2) + \\ &\quad +\nu_{y,j}^2\xi_y^2 + \nu_{x,j}^2\xi_x^2 + O(|\xi|^4). \end{aligned}$$

Since $\Delta\tau \leq \tau_f$ and $\nu_{y,j} + \nu_{x,j}^2 + \mu \leq 1$ considering the stability requirement, following a Cauchy-Shwartz inequality, we get

$$\begin{aligned} r\Delta\tau(\nu_{y,j}\xi_y^2 + (\nu_{x,j}^2 + \mu)\xi_x^2) &\leq r\tau_f(\nu_{y,j} + \nu_{x,j}^2 + \mu)(\nu_{y,j}\xi_y^4 + (\nu_{x,j}^2 + \mu)\xi_x^4) \\ &\leq r\tau_f(\nu_{y,j}\xi_y^4 + (\nu_{x,j}^2 + \mu)\xi_x^4). \end{aligned}$$

Hence,

$$|\rho(x_j, y_k, \xi)|^2 \leq (1 - r\Delta\tau)^2 - (\nu_{y,j}\xi_y^2 + (\nu_{x,j}^2 + \mu)\xi_x^2) + \nu_{y,j}^2\xi_y^2 + \nu_{x,j}^2\xi_x^2 + O(|\xi|^4),$$

or equivalently,

$$|\rho(x_j, y_k, \xi)|^2 \leq (1 - r\Delta\tau)^2 - \nu_{y,j}\xi_y^2(1 - \nu_{y,j}) - \nu_{x,j}\xi_x^2(1 - \nu_{x,j}) - \mu\xi_x^2 + O(|\xi|^4).$$

Since by the stability conditions $\nu_{x,j} \leq 1, \nu_{y,j} \leq 1$, we write

$$|\rho(x_j, y_k, \xi)|^2 \leq (1 - r\Delta\tau)^2 - \lambda_{\min}(\xi_x^2 + \xi_y^2) + O(|\xi|^4),$$

where $\lambda_{\min} = \min\{\nu_{y,j}(1 - \nu_{y,j}), \nu_{x,j}(1 - \nu_{x,j}) + \mu\}$.

For a small ξ, there exists λ such that $|\rho(x_j, y_k, \xi)| \leq \sqrt{(1 - r\Delta\tau)^2 - \lambda|\xi|^2}$.

Consequently

$$|\rho(x_j, y_k, \xi)| \leq |1 - r\Delta\tau|\sqrt{1 - \frac{\lambda|\xi|^2}{(1 - r\Delta\tau)^2}} \leq |1 - r\Delta\tau|\left(1 - \frac{\lambda|\xi|^2}{(1 - r\Delta\tau)^2}\right).$$

Hence,

$$|\rho(x_j, y_k, \xi)| \leq |1 - r\Delta\tau| - \frac{\lambda|\xi|^2}{|1 - r\Delta\tau|}.$$

Since $|1 - r\Delta\tau| \leq 1 + r\tau_f$, then there exists a $\delta > 0$ such that

$$|\rho(x_j, y_k, \xi)| \leq |1 - r\Delta\tau| - \delta|\xi|^2 \leq 1 + r\Delta\tau - \delta|\xi|^2.$$

□

It is possible to verify numerically that the conditions obtained define distinct stability regions with regard to the stability of the numerical method in the presence of boundaries. We demonstrate that using a test problem in the following section.

5.3.2 Test problem: stability and convergence rate

In this section, we present the numerical method's performance for a specific case. We discuss how strict the stability requirements are and also check if the rate of convergence matches the earlier discussion. We select a test problem, that is, a problem for which we are aware of the analytical solution, in order to accomplish that. We provide this test problem by adding a source term to the equation of interest, that is,

$$\frac{\partial V}{\partial \tau} + rV - f(x,\tau)\frac{\partial V}{\partial y} - \gamma(x,\tau)\frac{\partial V}{\partial x} - \frac{1}{2}\sigma_\tau^2\frac{\partial^2 V}{\partial x^2} = S(x,y,\tau). \tag{5.14}$$

The computational domain is defined in $0 \leq x \leq 1/2$, $0 \leq y \leq 1$ and $0 \leq \tau \leq 1/2$. The initial condition is similar to the initial condition of a European put option, that is,

$$V(x,y,0) = [(K-y)^3]^+. \tag{5.15}$$

The boundary conditions are also similar to the expected boundaries for a European put option, that is,

$$V(x^{min},y,\tau) = [(K-y)^3]^+ e^{-\pi^2\tau}\cos\frac{\pi\tau}{2}, \tag{5.16}$$

$$\frac{\partial V}{\partial x}(x^{max},y,\tau) = 0, \tag{5.17}$$

$$V(x,y^{max},\tau) = [(K-y^{max})^3]^+ e^{-\pi^2\tau}\cos[\pi(\frac{1}{2}-x)\tau]. \tag{5.18}$$

The source term $S(x,y,\tau)$ in (5.14) is a function such that the equation has the following analytical solution

$$V(x,y,\tau) = [(K-y)^3]^+ e^{-\pi^2\tau}\cos\left[\pi(\frac{1}{2}-x)\tau\right]. \tag{5.19}$$

In this test example we consider the functions

$$f(x) = (x - x_{ref})^+, \quad \gamma(x,\tau) = k(\theta(\tau) - x) + \theta'(\tau) - \lambda\sigma,$$

with

$$\theta(\tau) = \frac{74}{50} + \frac{19}{50}\sin\left(\frac{\pi(\tau-6)}{6}\right)$$

and the respective test values

$$K = \frac{1}{2}, \quad x_{ref} = \frac{1}{4}, \quad r = 0.02, \quad \sigma = \frac{55}{50}, \quad \lambda = 0.8, \quad k = 3.$$

TABLE 5.1: Behaviour of the numerical method when different discretization steps are considered in order to obtain different values for the stability conditions (5.10) denoted respectively by $C_1 : \|f\|_\infty \nu_y + \|\gamma\|_\infty^2 \nu_x^2 + \mu \leq 1$ and $C_2 : \|f\|_\infty \nu_y + \|\gamma\|_\infty^2 \nu_x^2 / (\|\gamma\|_\infty^2 \nu_x^2 + \mu) < 1$.

C_1	C_2	State of Convergence
1.1545	0.0464	Diverge
0.0727	1.0142	Diverge
0.9673	0.0392	Converge
0.0043	0.9936	Converge

We show the test results for the numerical method's stability (5.5) in Table 5.1. The numerical method's behaviour is contingent upon the values of the conditions (5.10), which vary based on the discretization steps both spatially and temporally. We refer to the conditions (5.10) as C1 and C2, respectively.

$$C_1 : \|f\|_\infty \nu_y + \|\gamma\|_\infty^2 \nu_x^2 + \mu \leq 1, \qquad C_2 : \|f\|_\infty \nu_y + \frac{\|\gamma\|_\infty^2 \nu_x^2}{\|\gamma\|_\infty^2 \nu_x^2 + \mu} < 1.$$

Table 5.1 illustrates how the method blows up, or fails to converge, when either of the conditions C1 or C2 is broken. This demonstrates how precise the stability conditions found using the von Neumann analysis are.

TABLE 5.2: Convergence rate of the numerical method with $\Delta x = 1/1024$, $\Delta\tau = (\Delta x)^2$, $\tau_n = 0.1$.

Δy	E_∞	E_2	R_∞	R_2
1/8	3.3019e-04	5.3757e-05		
1/16	1.7289e-04	2.6169e-05	0.93	1.03
1/32	8.8397e-05	1.2893e-05	0.96	1.02
1/64	4.4683e-05	6.3971e-06	0.98	1.01
1/128	2.2461e-05	3.1857e-06	0.99	1.00

Regarding the rate of convergence, the numerical errors are measured by the discrete norms

$$E_\infty(\tau_n) = \max_{1\le j\le N_x, 1\le k\le N_y} (V(x_j, y_k, \tau_n) - V^n_{j,k}),$$

$$E_2(\tau_n) = \left(\Delta x \Delta y \sum_{j=1}^{N_x} \sum_{k=1}^{N_y} \left(V(x_j, y_k, \tau_n) - V^n_{j,k} \right)^2 \right)^{1/2}.$$

The Tables 5.2-5.4 shows the results of the method I, that is, downwind in y and Lax-Wendroff in x. The final time $\tau_n = 0.1$ was selected to allow for very small time steps in the experiments.

TABLE 5.3: Convergence rate of the numerical method with $\Delta\tau = 1/128$, $\Delta y = \Delta x$, $\tau_n = 0.1$.

Δx	E_∞	E_2	R_∞	R_2
1/8	3.3128e-04	5.6959e-05		
1/16	1.7304e-04	2.6964e-05	0.93	1.07
1/32	8.8415e-05	1.3089e-05	0.96	1.04
1/64	4.4686e-05	6.4445e-06	0.98	1.02
1/128	2.2462e-05	3.1968e-06	0.99	1.01

TABLE 5.4: Convergence rate of the numerical method with $\Delta\tau = 1/128$, $\Delta y = (\Delta x)^2$, $\tau_n = 0.1$.

Δx	E_∞	E_2	R_∞	R_2
1/8	2.2537e-05	3.3753e-06		
1/16	5.6399e-06	8.1785e-07	1.99	2.04
1/32	1.4074e-06	2.0098e-07	2.00	2.02
1/64	3.4880e-07	4.9543e-08	2.01	2.02
1/128	8.4111e-08	1.2030e-08	2.05	2.04

As expected, the convergence in the direction y is first order, as shown in Table 5.2. As a result of our hyperbolic equation and our decision to avoid artificial boundary conditions, we have opted for a lower degree of accuracy in this direction. Table 5.3 illustrates how the first order convergence of y can dominate, when both step sizes are assumed to be the same. Table 5.4 shows that second order convergence is achieved if the step size in direction y is equal to the square of the step size in direction x.

5.4 Case studies with weather data

In this section, we estimate the parameters of rainfall model using historical precipitation data. Two distinct locations are considered as test case. Then, we take

this two locations as test cases, in which we use numerical solutions to the partial differential equation to determine the option's price. The first case, which is based on data from Tempelhot, Germany, is taken from Odening et al., 2007 to provide a test problem that already exists in the literature. We offer a second example, based on data from Tofo-Inhambane, Mozambique, to further solidify the application of our methodology.

5.4.1 Case study with Tempelhot (Germany) data

We begin with an empirical study that examines an application to the rainfall options valuation for grain producers in northeastern Germany, as reported in Odening et al., 2007. While a month is the unit of time used in our study, the authors of this study use a day unit. We employ the publicly available data from the German weather service "The Deutscher Wetterdienst", n.d. to estimate the parameters involved in the Ornstein-Uhlenbeck process. The rainfall information from the Tempelhot, Germany, weather station extends over the years 1948 through 2005, Figure 5.2.

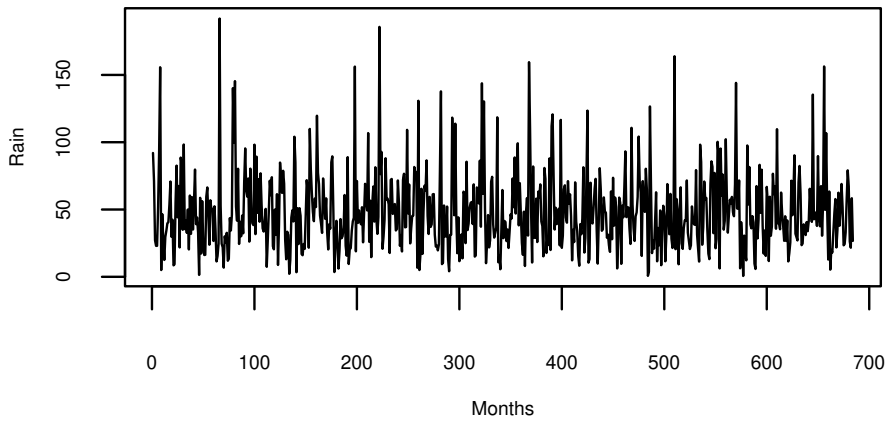

FIGURE 5.2: Monthly rain at Tempelhot-Germany 1948-2005.

The price of the put option on deficit rainfall is performed using this data, and results are obtained for several contracts with different durations.

The parameters for the Ornstein-Uhlenbeck process that describe the dynamics of real precipitation data, were estimated using the methodology described in section 4.1.3. It is also necessary to calculate λ, the market price of risk. Our presumption is that this amount is constant. We should look at market prices for a few contracts to determine which values of λ yield prices from the model that fit the market price, in order to arrive at an accurate estimate of λ. Unfortunately, there is not yet a completely established market for contract weather derivatives. In light

of what we have seen in the literature, we thus present results for λ between 0 and 2.

TABLE 5.5: Model parameters: monthly rain model, Tempelhot, 1948-2005.

r	λ	$tick$	K	k	σ	x_{ref}	x_{min}	x_{max}	y_{min}	y_{max}
0.05	0	8.1	33	3.7	39	48	0	150	0	$T(x_{ref} + x_{min})$

Without lost the generalities, this test case is performed using the rainfall deficit indexes, that is, the function f defined as $f(x) = (0, x_{ref} - x)^+$. The estimated parameters, based on the data between January 1 and December 31 using the monthly rain unit are displayed in Table 5.5. Based on the study case in Odening et al., 2007, we define a risk-free discount interest rate r of 5% and a market price of risk λ of 0, which means that $r = 0.05$ and $\lambda = 0$, respectively. The tick size value of 8.1 euros index point is taken. It was also selected based on one of the test cases in Odening et al., 2007. The volatility σ and k are calculated using the monthly unit data for a year and the methodology described in the preceding sections. In each case, x_{ref} is the average monthly precipitation divided by the total number of months in the accumulation period. The minimum and maximum values of the precipitations are denoted by $x_{min} = 0$ and x_{max}, respectively; however, in certain displayed figures, we extend the x_{max} to 300. The rainfall deficit interval is also calculated, with $y_{min} = 0$ and $y_{max} = T(x_{ref} + x_{min})$. The same technique to determine the y_{max} value is also used in Broni-Mensah, 2012; Li, 2018. The rainfall option's strike price K was established by averaging the rainfall index that was calculated for each month of the contract.

Based on the Templhot data, we now determine an approximation of $\theta(t)$ defined by (4.2). We observe that the most appropriate fit only takes into account the odd harmonics, that is, we have $\beta_k = 0$ in (4.2), see Figure 5.3. We have,

$$\theta_n(t) = \alpha_0 + \sum_{k=1}^{n} \beta_k \cos\left(\frac{2\pi k}{12}(t - \nu)\right). \tag{5.20}$$

In Figure 5.3, we also show how the partial sum (5.20) for $n = 2$, $\theta_2(t)$, fits the data and we plot also the best option, that is, for $n = 5$, $\theta_5(t)$. Then, the parameters of the mean function used are:$\alpha_0 = 2.3$, $\beta_1 = 0.35178$, $\beta_2 = -0.31198$, $\beta_3 = -0.08059$, $\beta_4 = -0.25732$, $\beta_5 = -0.23084$ and $\nu = -0.45334$.

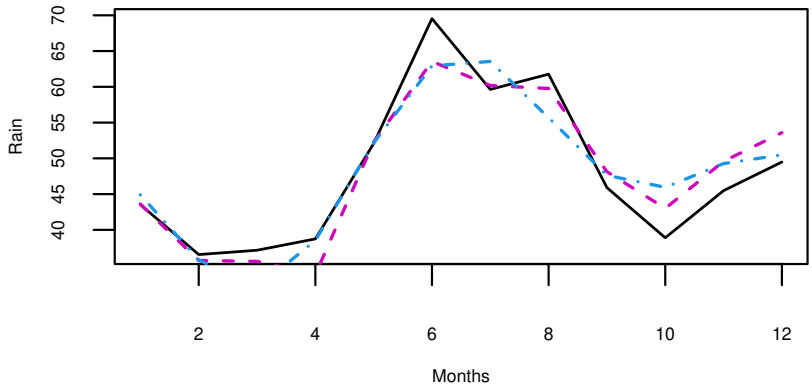

FIGURE 5.3: Monthly average (-) versus $\theta(t)$ with Tempelhot data (1948-2005): Approximation of $\theta(t)$ with $\theta_2(t)$ $(- \cdot -)$ and $\theta_5(t)$ $(-- -)$ defined in (5.20).

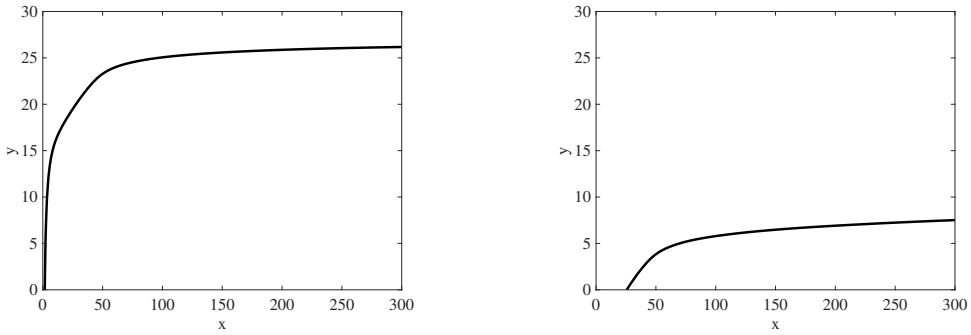

FIGURE 5.4: Two different contract periods in Tempelhot. An illustration of the different values of rain (x) and rain index (y), for which the European RD put option price reaches 50, that is, $V(x, y, \tau_f) = 50$. Left: Contract June, that is, $\tau_0 = 5$ (initial time) and $\tau_f = 6$; Right: Contract between April and June, that is, $\tau_0 = 3$ (initial time) and $\tau_f = 6$;

Two experiments are conducted, with varying contract duration: the first contract is for one month, ending in June with $\tau_0 = 5$ and a final time of $T + \tau_0 = 6$. The second contract is for two months, ending in April with $\tau_0 = 3$ and a final time of $T + \tau_0 = 6$.

The values of x and y, for which we derive the option value 50 for the two periods, June and April-June, are plotted in Figure 5.4. Rainfall amounts must be not less than approximately 1.7 for the contract in June and at less than approximately 34.5 for the contract in April-June. Nevertheless, it is challenging to draw this conclusion from a visual examination of Figure 5.4. Furthermore, for the contract June, the quantity of the rain index must not exceed approximately 25.3, and for the contract April-June, it cannot exceed approximately 5.7.

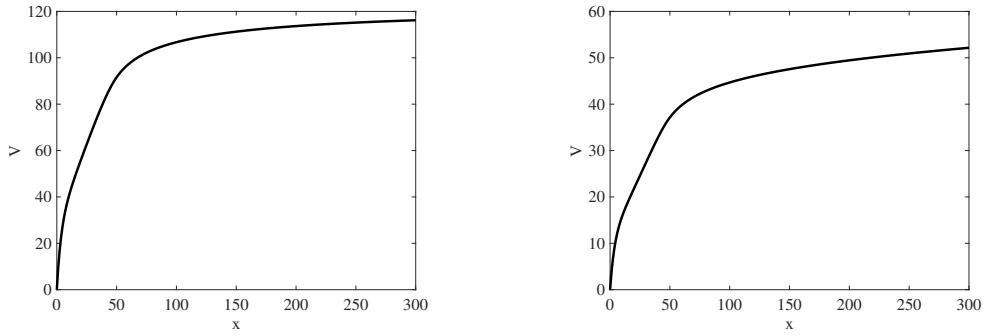

FIGURE 5.5: Two different contracts periods in Tempelhot. Profile of European RD put option for a fixed value of rain weather index y. Left: Contract June for the rain weather index $y = 17$; Right: Contract between April and June for the rain weather index $y = 7$.

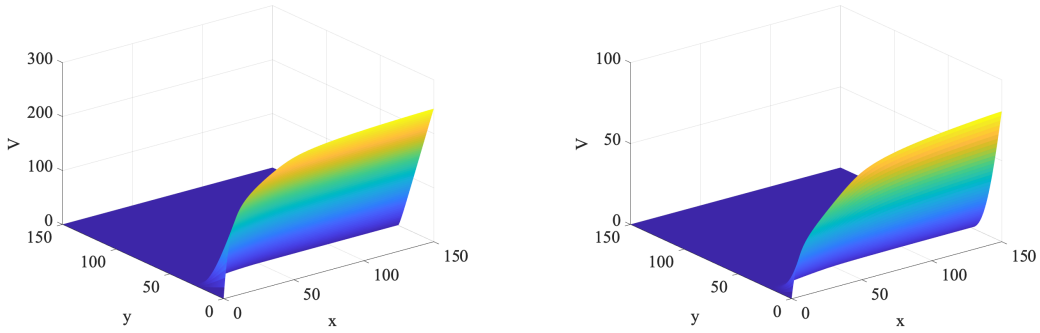

FIGURE 5.6: Two different contracts periods in Tempelhot. European RD put option profile. Left: Contract June. Right: Contract April-June.

The value of the put option for a fixed index value for both contracts, that are June and April-June, is plotted in Figure 5.5. The value for the contract of June is shown in Figure 5.5 on the left. We plot the put option's value for a fixed index value of 17, and we can observe that the put option's value is approximately 50. It is evident that the put option's 50 threshold is reached for precipitation values of approximately 16. The value of the contract April-June is shown in Figure 5.5 on the right, where the value of the put option is plotted for a fixed index value of 7. In this case, the put option's value is likewise approximately 50. In this instance, the put option's 50 threshold is met for precipitation values greater than 215.

The corresponding precipitation values of 50 for the April-June contract are reduced in half, when compared to the corresponding precipitation values of the June contract.

The put option of June reaches the value 50 for fixed index values higher than in the case of the contract April-June. Since the June contract involves hedging drought risks or the deficit of rainfall given by $y = \sum_j \max(x_{ref} - x_j, 0)$, the higher values of the fixed index value in the June contract may be justified by the fact that

we have lower values of precipitation when compared with the values of precipitation during the April-June contract.

Figure 5.6 illustrates the rain put option's global behaviour. The outcome for the contract period of June is plotted on the left figure, and the put option price for the contract period of April-June is plotted on the right figure. The put option reaches a value of 250 in the figure on the left, and a value of approximately 81 in the figure on the right, which is related to the contract period of April to June.

In both contracts, the value of the rainfall put option increases as the amount of rain x increases and decreases as the rain index values y increase. In the case where the weather index values fall below the strike price $K = 33$, the rain put option values for the April-June contract are less than those for the June contract. This indicates that the option value decreases as the contract life time increases.

At last, based on our model, we find that the put options values for the April–June contract, which has a 39 volatility, can go as high as 100 euros. This value is comparable to those found in Odening et al., 2007 for volatility of 17.3. Prices obtained through models based on different unit of times may be different since they can be affected by factors, such as, the different levels of expected weather outcomes and the associated volatility.

5.4.2 Case study with Tofo (Mozambique) data

In this second scenario, we present a simulation that uses precipitation data from the "Nasa Power Data Access Viewer", n.d. site Nasa Power Data Access Viewer corresponding to the weather station Tofo in the Mozambican province of Inhambane between the years 1981 and 2021. We take into account the month as the unit of time. The dynamics of rain at Tofo-Inhambane are displayed in Figure 5.7.

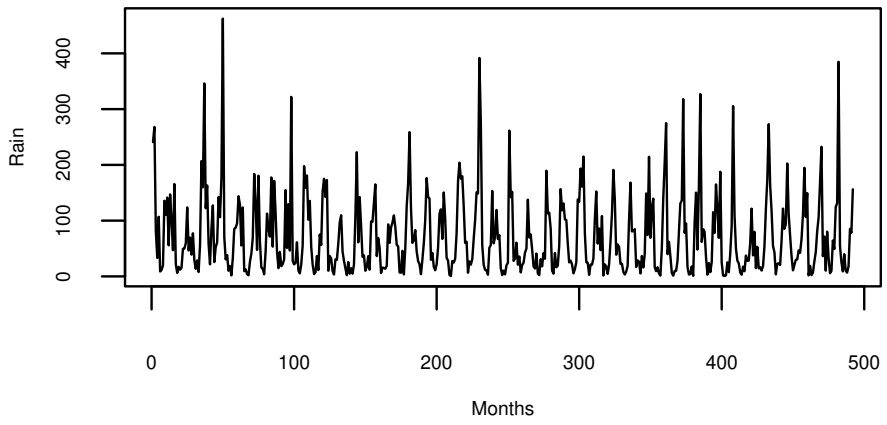

FIGURE 5.7: Monthly rain at Tofo-Inhambane 1981-2021.

TABLE 5.6: Model parameters: monthly rain model, Tofo-Inhambane, 1981–2021.

r	λ	$tick$	K	k	σ	x_{ref}	x_{min}	x_{max}	y_{min}	y_{max}
0.05	0	1	31	2.8	72.6	71	0	300	0	$T(x_{ref} + x_{min})$

The methods outlined in the preceding sections are used to estimate the Ornstein-Uhlenbeck process parameters for monthly rainfall dynamics. The Table 5.6 displays them. The value of $r = 0.05$ for the risk-free interest rate is retained from the previous example, and the market price of risk is generally $\lambda = 0$, unless a different value is specified. 1 is the value of the tick size. The volatility and mean reversion parameters are $\sigma = 72.6$ and $k = 2.8$, respectively, and the strike prize is $K = 31$. They were acquired by following the earlier sections' description. The precipitation has an average value of $x_{ref} = 71$ and a maximum value of $x_{max} = 300$.

As in the previous example, we first observe the monthly average in Figure 5.8 and then fit this to a series of cosines to compute an approximation to the mean $\theta(t)$. A suitable approximation is

$$\theta_n(t) = \alpha_0 + \sum_{k=1}^{n} \beta_k \cos\left(\frac{2\pi k}{12}(t - \nu)\right). \tag{5.21}$$

We found that $\theta_4(t)$ is a good fit, see Figure 5.8. The parameters of the $\theta_4(t)$ used are: $\alpha_0 = 71.0$, $\beta_1 = 68.93715$, $\beta_2 = 13.77723$, $\beta_3 = 0.66969$, $\beta_4 = 2.11359$ and $\nu = 0.93973$.

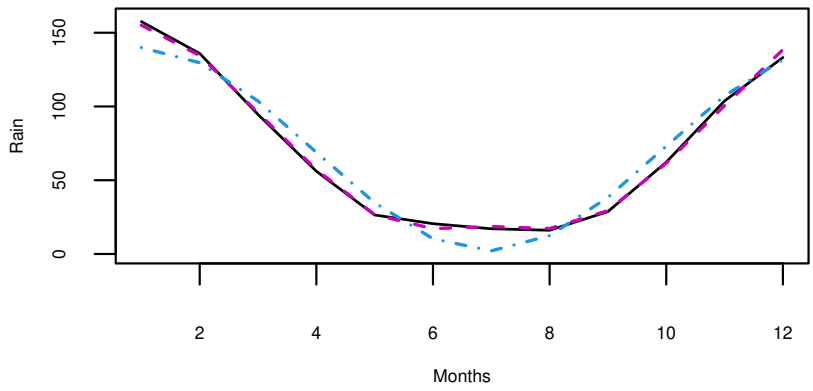

FIGURE 5.8: Monthly average (-) versus $\theta(t)$ with Tofo data (1981-2021): Approximation of $\theta(t)$ with $\theta_1(t)$ $(- \cdot -)$ and $\theta_4(t)$ $(--)$ defined in (5.21).

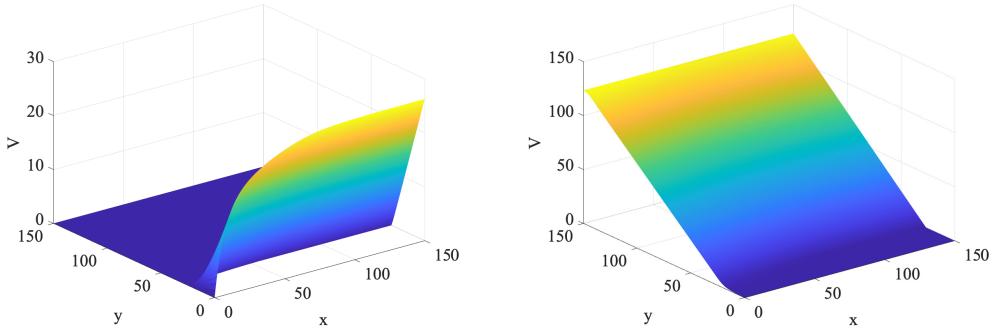

FIGURE 5.9: Contract period January-March in the city of Tofo. Plot of the overal function $V(x, y, T)$, for $\tau_0 = 0$ and maturity $T = 3$. Left: Put option; Right: Call option.

The global behaviour of the rain put option for the contract period of January–March in the city of Tofo in Inhambane, Province of Mozambique, is illustrated on the left in Figure 5.9. It is evident that the value of the rain put option increases as the amount of rain x increases and decreases as the amount of rain index values y increases. The global behavior of the rain call option is displayed for the same contract period in Figure 5.9, on the right. As expected, the rainfall call option value increases with an increase in rain index values y and decreases slightly with an increase in rain quantities x.

We go over the put and call behaviour in the following figures. For a better understanding, we show the contours of the function $V(x, y, t)$ for fixed values of x and y in Figure 5.10. These outcomes cover the January–March contract period in Tofo. We plot the put option behaviour at the top of Figure 5.10, and show the call option prices at the bottom. The price of the put option decreases as the RD index y values increase, and it increases as the amount of rain x increases. Conversely, the price of the call option rises in tandem with the RD index y and decreases with the increasing of the rain quantity x.

The behaviour of the weather option prices as the contract period is changed is displayed in Figure 5.11. It shows the results for the contracts periods of January, January-March, and January-April. Figure 5.11 displays the put option pricing behaviour at the top and the call option price behaviour at the bottom. We can see from these figures that the rain call option rises with a longer contract life and the rain put option decreases with a longer contract life. Specifically, we can see in the bottom left figure that the call option only increases as the contract life time increases and only in the cases where the weather index values are less than the strike price $K = 31$. We have also seen an analogous behaviour for the put option in the previous Tempelhot test case, namely that the put option declines as the contract life increases if the weather index values are less than the strike price $K = 33$.

The impact of altering the market price of risk, $\lambda = 0, 0.5, 1, 2$, for the contract

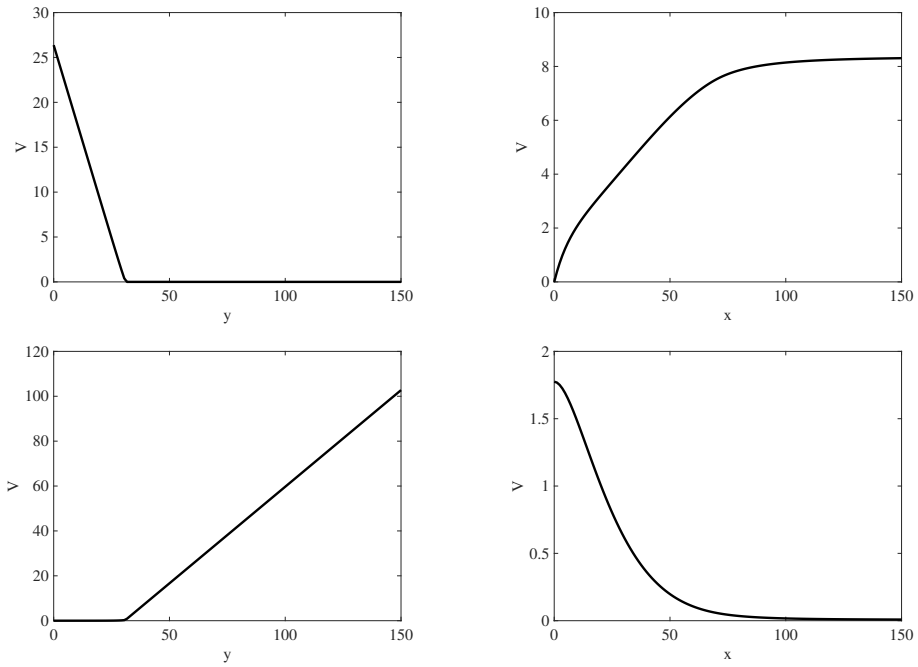

FIGURE 5.10: Contract period January-March in the city of Tofo. Two dimensional profiles of the function $V(x, y, T)$, $\tau_0 = 0$ and $T = 3$. Top Left: Put option when $x = 116$; Top Right: Put option when $y = 21$; Bottom Left: Call option when $x = 116$; Bottom Right: Call option when $y = 21$.

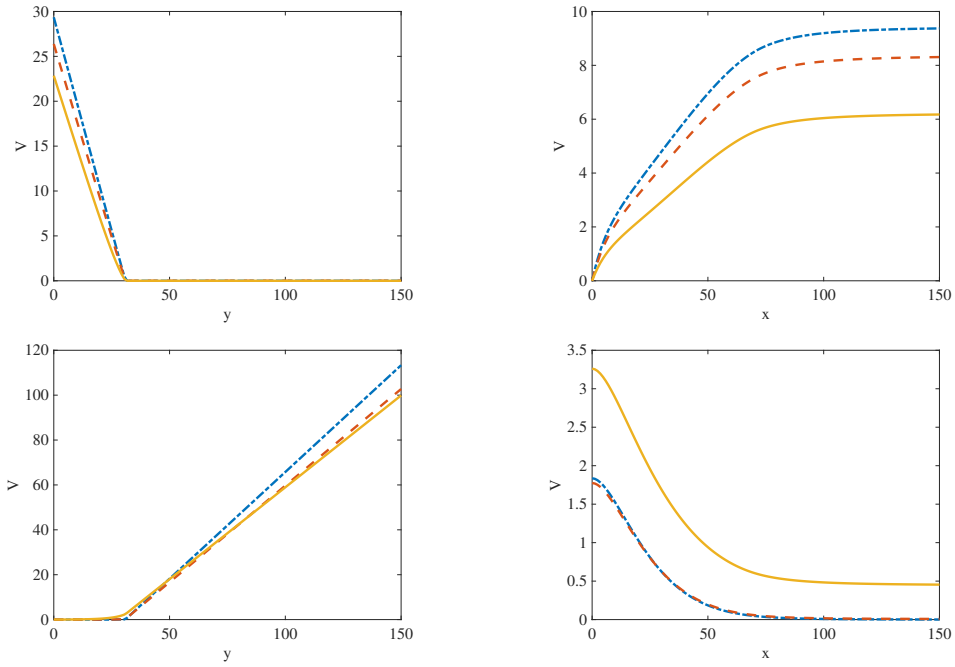

FIGURE 5.11: Effect of changing the maturity of the contracts in the city of Tofo, namely for $T = 1(- \cdot -)$, $T = 3(--)$ $T = 4(-)$. Top Left: Put option when $x = 116$; Top Right: Put option when $y = 21$; Bottom Left: Call option when $x = 116$; Bottom Right: Call option when $y = 21$.

period of January-March in the city of Tofo is shown in Figure 5.12. The put option is shown at the top of Figure 5.12, while the call option is shown at the bottom. Rain call options increase as the values of the market prices of risk increase, while rain put options decrease as the values of the market prices of risk increase. However, these price changes only become noteworthy when we alter the rain values for a fixed value of y; they do not occur when we alter the values of the weather rain index and fix the value of x.

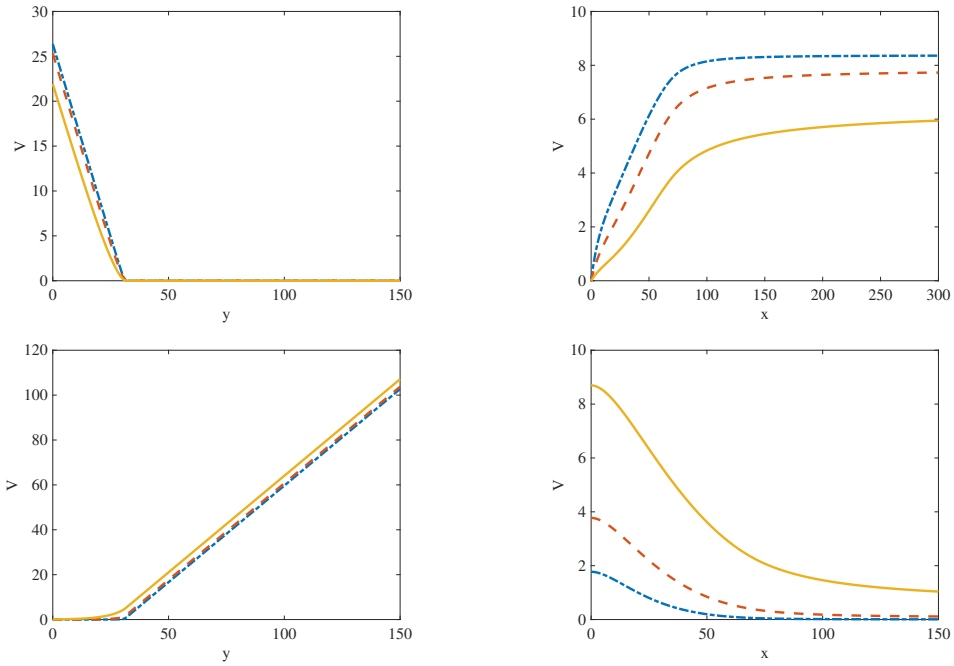

FIGURE 5.12: Effect of changing the market price of risk, $\lambda = 0(- \cdot\cdot -)$, $\lambda = 0.75(--)$ and $\lambda = 1.5(-)$, for the contract period January-March, in the city of Tofo. Top Left: Put option when $x = 116$; Top Right: Put option when $y = 21$; Bottom Left: Call option when $x = 116$. Bottom Right: Call option when $y = 21$.

5.5 Numerical method II

Another possibility would be to have a first order upwind in y and second order upwind in x, but in this case we would need to deal with the fact that the convection coefficient in x change the signal, so the derivatives will be discretized by second order upwind approximation according to the sign of the convection coefficient. Therefore we have the explicit difference scheme given by,

$$\begin{aligned} V_{j,k}^{n+1} &= V_{j,k}^n - r\Delta\tau V_{j,k}^n + \frac{\Delta\tau}{\Delta y} f_j \frac{1+sign(f_j)}{2}\Delta_y^+ V_{j,k}^n \\ &\quad \frac{\Delta\tau}{2\Delta x}\gamma_j^n \left(\frac{1+sign(\gamma_j^n)}{2}\delta_x^+ + \frac{1-sign(\gamma_j^n)}{2}\delta_x^- \right) V_{j,k}^n + \frac{\sigma^2\Delta\tau}{2\Delta x^2}\delta_x^2 V_{j,k}^n \end{aligned} \quad (5.22)$$

According to the sign of γ the equation (5.22) arise two equations, first equation when $\gamma \geq 0$,

$$\begin{aligned} V_{j,k}^{n+1} &= V_{j,k}^n - r\Delta\tau V_{j,k}^n + \frac{\Delta\tau}{\Delta y} f_j \frac{1+sign(f_j)}{2}\Delta_y^+ V_{j,k}^n \\ &\quad \frac{\Delta\tau}{2\Delta x}\gamma_j^n \frac{1+sign(\gamma_j^n)}{2}\delta_x^+ V_{j,k}^n + \frac{\sigma^2\Delta\tau}{2\Delta x^2}\delta_x^2 V_{j,k}^n, \end{aligned} \quad (5.23)$$

for for $j = 1, \cdots, N_x - 1$; $k = 0, \cdots, N_y - 1$. At $j = 0$; $k = 0, \cdots, N_y$ and $j = 0, \cdots, N_x$; $k = N_y$ we have a Direchlet boundary condition. At $j = N_x$; $k = 0, \cdots, N_y - 1$ we have a Neumann boundary condition.

At $j = N_x - 1$ we use a centered difference approximation for the Neumann boundary $V_{N_x+1,k}^n = V_{N_x-1,k}^n$ to eliminte the ghost points produced by the scheme and obtaining the values of $V_{N_x-2,k}^{n+1}$. In other hand, at $j = N_x$ the scheme (5.23) has the ghost points $V_{N_x+1,k}^n$ and $V_{N_x+2,k}^n$ then, the combination of Neumann boundary condition and the the scheme (5.23) can not eliminate all the ghost points. As alternative we had modified the scheme (5.23) at boundary $j = N_x$; $k = 0, \cdots, N_y - 1$ using a second order centered in x, getting the explicit difference,

$$\begin{aligned} V_{j,k}^{n+1} &= V_{j,k}^n - r\Delta\tau V_{j,k}^n + \frac{\Delta\tau}{\Delta y} f_j \frac{1+sign(f_j)}{2}\Delta_y^+ V_{j,k}^n + \frac{\Delta\tau}{2\Delta x}\gamma_j^n \Delta_{0x} V_{j,k}^n + \\ &\quad + \frac{\sigma^2\Delta\tau}{2\Delta x^2}\delta_x^2 V_{j,k}^n. \end{aligned} \quad (5.24)$$

The scheme (5.23)-(5.23) is $5-$point stencil for internal points and $4-$point stencil for boundary points to be obtained, as we can see in the following diagram,

Remark 2

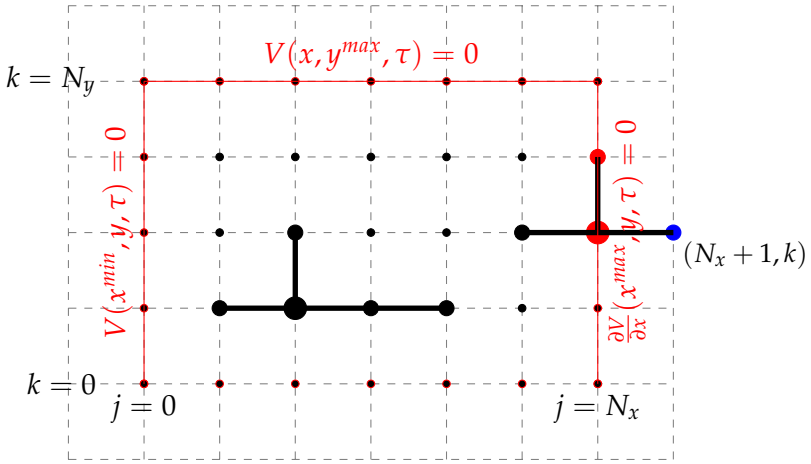

FIGURE 5.13: Explicit scheme that is second order downwind in x and downwind in y for a put option. Black dots are internal nodes; Blue dots are ghost nodes; Red dots are boundary nodes.

The description above is regarding to the put option. In the case of call option we have to adequate the discretization near and at the call boundary conditions (4.38), in order to avoid the ghost point. At $j = N_0; k = 0, \cdots, N_y$ we have a Neumann boundary condition, we use the principal scheme (5.23) for $j = 0, \cdots, N_{x-2}; k = 0, \cdots, N_y$. At $j = N_{Nx-1}; k = 0, \cdots, N_y - 1$, the scheme (5.23) produce ghost point and the Direchlet boundary condition at $j = N_{Nx}; k = 0, \cdots, N_y$ can not eliminate it, so we propose the centered difference approximation (5.24).

The second equation we get when $\gamma < 0$,

$$\begin{aligned} V_{j,k}^{n+1} &= V_{j,k}^n - r\Delta\tau V_{j,k}^n + \frac{\Delta\tau}{\Delta y} f_j \frac{1 + sign(f_j)}{2} \Delta_y^+ V_{j,k}^n \\ &\quad \frac{\Delta\tau}{2\Delta x} \gamma_j^n \frac{1 - sign(\gamma_j^n)}{2} \delta_x^- V_{j,k}^n + \frac{\sigma^2 \Delta\tau}{2\Delta x^2} \delta_x^2 V_{j,k}^n, \end{aligned} \tag{5.25}$$

for $j = 2, \cdots, N_x; k = 0, \cdots, N_y - 1$. At $j = 1$ we have used a centered difference approximation in $x-$direction, scheme (5.24), in order to avoid the ghost points produced by scheme (5.25) and, at $j = 0; k = 0, \cdots, N_y$ and $j = 0, \cdots, N_x; k = N_y$ we have a Direchlet boundary condition. At $j = N_x; k = 0, \cdots, N_y - 1$ we have a Neumann boundary condition, that is used to eliminate the ghost points produced by the scheme (5.25) at $j = N_x$. Below we have the illustration of the points stencil.

Remark 3

In the case of call option we also have to adequate the discretization near and at

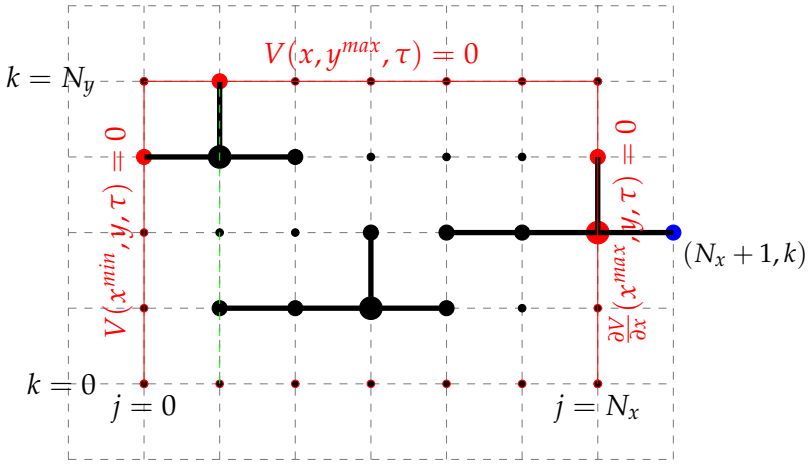

FIGURE 5.14: Explicit scheme that is second order upwind in x and downwind in y for a put option. Black dots are internal nodes; Blue dots are ghost nodes; Red dots are boundary nodes.

the call boundary conditions (4.38), in order to avoid the ghost point. At $j = N_0$; $k = 0, \cdots, N_y$ we have a Neumann boundary condition, and the principal approximation (5.25) use two points left, so we propose the centered difference scheme (5.24). At $j = 1, \cdots, N_{x-1}$; $k = 0, \cdots, N_y - 1$ we use the principal scheme (5.25). At $j = N_{Nx}$; $k = 0, \cdots, N_y$.

The consistency is straightforward using the truncation error as in the preview section. In this case, the method II is also $O(\Delta y) + O(\Delta x^2)$ accuracy. Regarding to the stability, we had difficulties on determine the analytical region of stability. However, we have noticed the existence of good similarity between the results performed through this numerical method when compared with method I. Then, we present this results in the following subsection.

5.5.1 Comparative results

In this subsection, we present the perfomance of the method II, (5.22), that is, the first order upwind in Y direction and second order upwind in X direction. In order to do that, first check if the rate of convergence is according to the what is expected, using the test problem given in section 5.3.2.

As we can see on the Tables 5.7-5.9, the convergence of the numerical method II is in accordance to what was expected. That is, in the y directions, the hyperbolic direction, it is first order accuracy. Since we have chosen a lower order of accuracy to avoid to deal with artificial boundary conditions. If we assume that both step sizes are equal, the first order convergence of y is dominant, Table 5.8. If the step size in the y direction is the square of the step size in the x direction, the parabolic direction, we obtain second order convergence, Table 5.9.

TABLE 5.7: Convergence rate of the numerical method with $\Delta x = 1/1024$, $\Delta\tau = (\Delta x)^2$, $\tau_n = 0.1$.

Δy	E_∞	E_2	R_∞	R_2
1/8	3.3020e-04	5.3757e-05		
1/16	1.7290e-04	2.6170e-05	0.93	1.04
1/32	8.8397e-05	1.2894e-05	0.97	1.02
1/64	4.4684e-05	6.3971e-06	0.98	1.01
1/128	2.2461e-05	3.1857e-06	0.99	1.01

TABLE 5.8: Convergence rate of the numerical method with $\Delta\tau = 1/128$, $\Delta y = \Delta x$, $\tau_n = 0.1$.

Δx	E_∞	E_2	R_∞	R_2
1/8	3.3804e-04	5.8231e-05		
1/16	1.7401e-04	2.7121e-05	0.96	1.10
1/32	8.8545e-05	1.3109e-05	0.98	1.05
1/64	4.4703e-05	6.4469e-06	0.99	1.02
1/128	2.2465e-05	3.1971e-06	0.99	1.01

Next we present some results of options pricing, considering respectively the case study with Tempelhot (Germany) rainfall data, (cite) and Tofo (Mozambique) rainfall data.

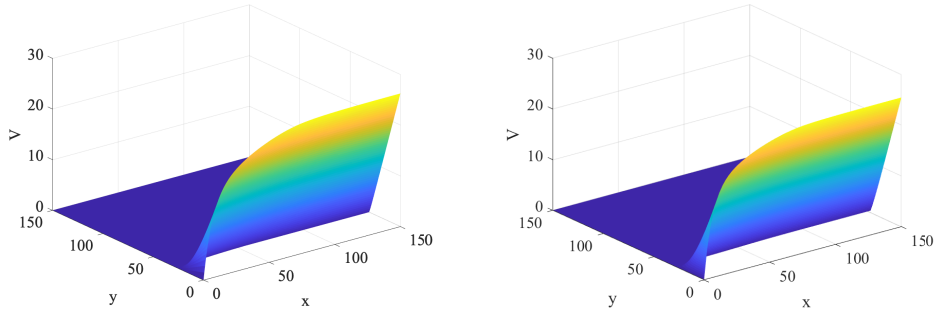

FIGURE 5.15: Contract period January-March in the city of Tofo. Plot of the overal function $V(x, y, T)$, for $\tau_0 = 0$ and maturity $T = 3$. Left: Put option (Method I); Right: Put option (Method II).

The Figures 5.15-5.16, shows the global behaviour of the respectively rainfall put option and call option performed by the method I (on the left) and method II (on the right), for the contract period January-March in the city of Tofo in Inhambane, Province of Mozambique. We can observe that the values of the rainfall put option given by the methods I and method II, are very close, Figure 5.15. We can conclude the same for the values of rainfall call option given by the methods I and method II, Figure 5.15.

TABLE 5.9: Convergence rate of the numerical method with $\Delta\tau = 1/128$, $\Delta y = (\Delta x)^2$, $\tau_n = 0.1$.

Δx	E_∞	E_2	R_∞	R_2
1/8	2.2999e-05	3.4505e-06		
1/16	5.6718e-06	8.2261e-07	2.02	2.07
1/32	1.4096e-06	2.0129e-07	2.01	2.03
1/64	3.4895e-07	4.9564e-08	2.01	2.02
1/128	8.4127e-08	1.2032e-08	2.05	2.04

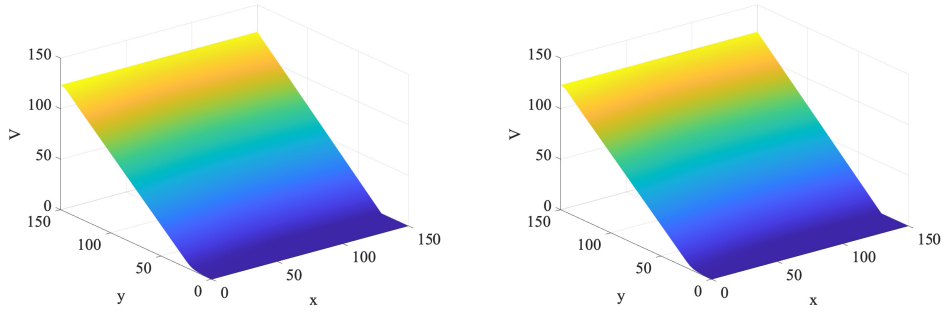

FIGURE 5.16: Contract period January-March in the city of Tofo. Plot of the overal function $V(x, y, T)$, for $\tau_0 = 0$ and maturity $T = 3$. Left: Call option (Method I); Right: Call option (Method II).

Lets have a closer perspective of the values of the put option and call option given by the method I and method II on the Figures 5.17-5.18. In these figures we display contours of the function $V(x, y, t)$ for fixed values of x and y, for the contract period January-March in Tofo. In the top of Figure 5.17, we plot the results of the put option performed by the method I and in the bottom we display the results of the put option performed by the method II. In the top of Figure 5.18, we plot the results of the call option performed by the method I and in the bottom we display the results of the call option performed by the method II. We can observe that in both figures the values of the rainfall option given by the methods I and method II, are very close.

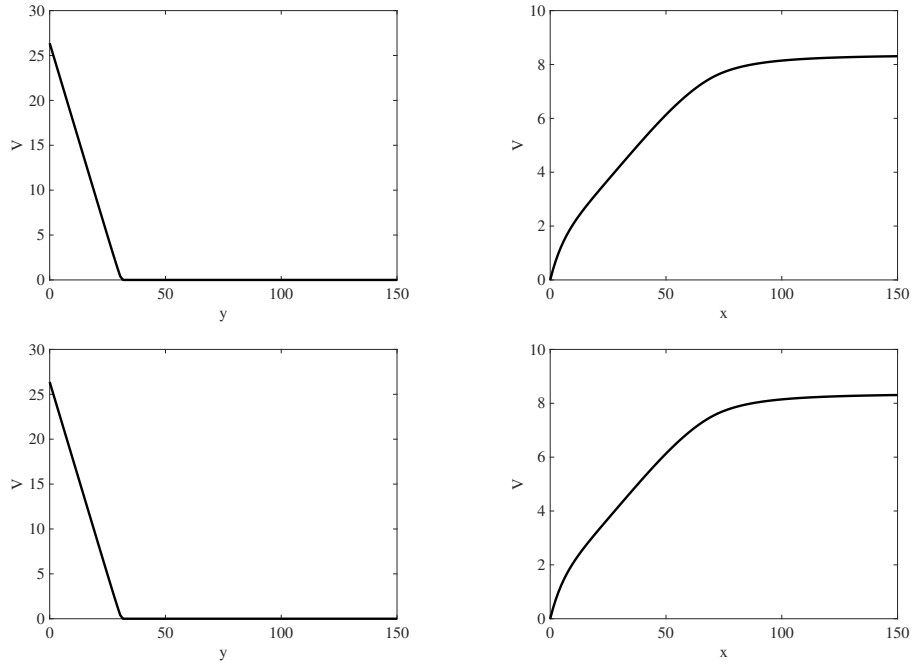

FIGURE 5.17: Contract period January-March in the city of Tofo. Two dimensional profiles of the function $V(x, y, T)$, $\tau_0 = 0$ and $T = 3$. Top Left: Put option when $x = 116$(Method I); Top Right: Put option when $y = 21$(Method I); Bottom Left: Put option when $x = 116$ (Method II); Bottom Right: Put option when $y = 21$ (Method II).

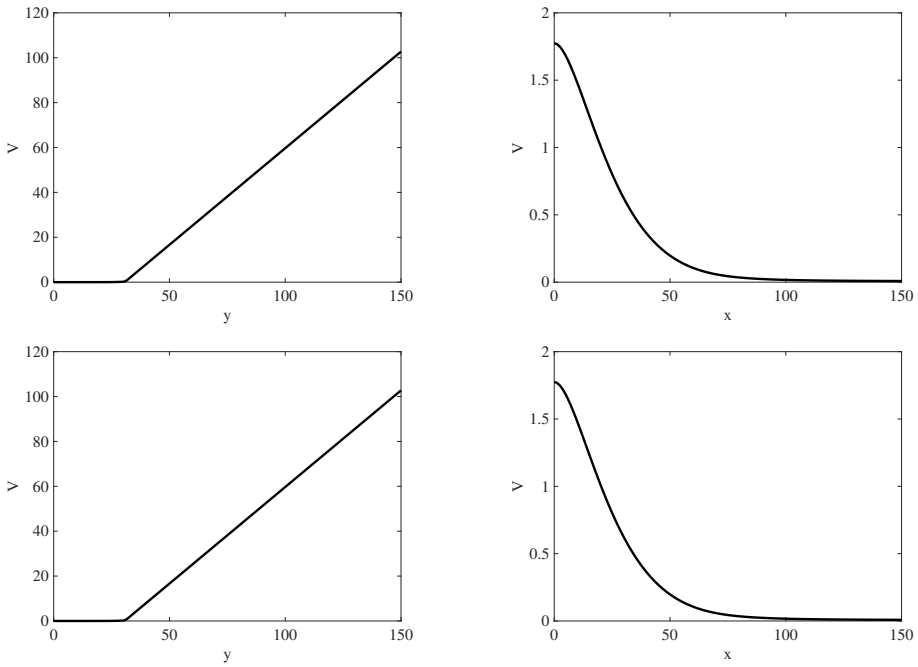

FIGURE 5.18: Contract period January-March in the city of Tofo. Two dimensional profiles of the function $V(x, y, T)$, $\tau_0 = 0$ and $T = 3$. Top Left: Call option when $x = 116$(Method I); Top Right: Call option when $y = 21$(Method I); Bottom Left: Call option when $x = 116$ (Method II); Bottom Right: Call option when $y = 21$ (Method II).

Chapter 6

A splitting finite difference method for the PDE model

Multidimensional partial differential equations are difficult to discretize. Since we solve a large system of equations at each time level, there is an additional cost associated with the direct extensions of finite difference methods used for one dimensional PDEs. An alternate numerical technique for the rainfall pricing model, based on the splitting approach, is developed in this chapter. The two-dimensional problem is decomposed into a sequence of simpler two one-dimensional problems. Then, the numerical schemes are applied to one dimensional equations, including the analysis of stability and accuracy. Then, are implemented in such a way to produce the solution of the original equation.

6.1 The generalities of splitting methods

A universal concept, the splitting process is used extensively in exponential splitting schemes and computational fluid dynamics Geiser, 2015. There are numerous ways to divide a PDE or matrix into more manageable sub-problems, and there are a number of factors to consider when selecting an appropriate splitting strategy. Examples of splitting strategies taken from D. Duffy, 2022 are:

- split an evolution operator into its components related to convection and diffusion;
- dimensional splitting: split an evolution operator into operators according to spatial dimensions;
- using the finite difference method, we can discretize a PDE and then perform matrix splitting on the resulting discrete system.This is a typical method for time-independent problems,Varga, 1962, Hageman and Young Hageman and Young, 2012;

- separate the Schrödinger evolution operator into alternating increments of kinetic and potential operators;
- splitting for multiscale problems: decompose behaviors into its smallest and largest components;
- Stochastic splitting schemes: in an SDE model, separate the deterministic and stochastic terms.

In the literature of finance, the most widespread strategy is the second one, based on dimensional splitting. The multidimensional partial differential equation is decomposed into a sequence of simpler one-dimensional problems. In finance, ADI methods tend to be the most used. However, the application of the splitting method was introduced in Duffy D. J. Duffy, 2006. Since then, many researchers have been applying the splitting methods to solve problems in finance and the results are found to be more robust. For instance, Sheppard Sheppard, 2007 used the split methods to price options in the Heston stochastic volatility model and for which ADI did not perform as expected. Davidson and Levin Davidson and Levin, 2014, used the Marchuk two-cycle modification of the Crank–Nicolson splitting method on evaluation of mortgage-backed securities.

The splitting method consists in decomposing an original problem into sequence of other simpler problems. In general, there is discrepancy between the two problems which leads to so-called local splitting error. Let us consider the finite-dimensional vector initial problem:

$$\begin{cases} \frac{du}{dt} = (A_1 + A_2)u, & 0 < t \leq T \\ u(0) = u_0 \end{cases} \tag{6.1}$$

with solution

$$u(t) = e^{(A_1+A_2)t}u_0, \quad A_1, A_2 \in \mathbb{R}^{n,n}. \tag{6.2}$$

The naive approach of the problem (6.1) consists on breaking into a sequence of two simpler initial value problems:

$$\begin{cases} \frac{dv}{dt} = A_1 v & 0 < t \leq \tau \\ v(0) = u_0 & \\ \frac{dw}{dt} = A_2 w & 0 < t \leq \tau \\ w(0) = v(\tau) & \end{cases} \tag{6.3}$$

The solution of this last problem can be determined using the semi-group property and is

$$w(\tau) = e^{A_2\tau}v(\tau) = e^{A_2\tau}e^{A_1\tau}u_0, \tag{6.4}$$

while the analytical solution is given by

$$u(\tau) = e^{\tau(A_1+A_2)}u_0. \tag{6.5}$$

Then, there is discrepancy between (6.4) and (6.5), that is,

$$Error(\tau) = (\exp \tau(A_1 + A_2) - \exp(A_2\tau) \exp(A_1\tau))u_0 \tag{6.6}$$

Expanding these exponential terms by Taylor series, we can see that

$$\exp \tau(A_1 + A_2) - \exp(\tau A_2) \exp \tau A_1 = (A_1A_2 - A_2A_1)t^2 + O(\tau^3). \tag{6.7}$$

The second-order term in τ is zero only if the matrices A_1 and A_2 commute. In general, a splitting scheme is order p accurate if the following error holds for the local splitting error:

$$\|Error(\tau)\| = O(p^{p+1}).$$

The other common splitting methods are:

- basic two-leg scheme: first-order accurate;
- predictor-corrector scheme: second-order accurate;
- marchuk Two-Cycle method: second-order accurate;
- Lie–Trotter scheme: first-order accurate;
- Strang operator splitting scheme: second-order accurate.

The splitting method, as a discretization method, the interval $[0, T]$ is subdivided into N equal sub-intervals $[(n-1)\Delta t, n\Delta t]$, $n = 1, \ldots, N$. The splitting solution is defined at the mesh points $n\Delta t$, $n = 0, \ldots N$. The entire splitting procedure can be expressed as:

$$u^{n+1} = C(\Delta t)u^n, \quad u^0 = u_0 \tag{6.8}$$

where the matrix operator $C(\Delta t)$ represents an operator matrix that corresponds to the applied discretization.

Definition 6.1.1 (consistent splitting scheme)
A splitting process that approximates (6.1) is said to be consistent if for its solution $C(\Delta t)$ the relation:

$$\lim_{\Delta t \to 0} \|(\frac{C(\Delta t) - I}{\Delta t} - (A_1 + A_2))u(t)\| = 0, \ \ \forall t \in [0, T)],$$

holds and where $\|\cdot\|$ is the matrix norm.

Definition 6.1.2 (stable splitting scheme)

A splitting scheme with operator $C(\Delta t)$ is stable if there exists a constant $K > 0$ such that:

$$\|C(t)^n\| \leq K,$$

where $\|\cdot\|$ is a matrix norm.

A sufficient condition for the stability is $\|C(\Delta t)\| \leq 1 + M\Delta t$, where $M > 0$ is a constant. Once proved the consistency and stability, the Lax equivalence theorem allows to conclude the convergence. Some applications of these schemes in the financial literature can be found, for instance, in Davidson and Levin Davidson and Levin, 2014, Sheppard, 2007), and D. Duffy, 2022. Applying the splitting approach for convection-diffusion PDEs, we obtain, in one direction, a parabolic equation and, in the other direction, a first-order hyperbolic equation. Then we have to be careful and not applying the centred difference schemes, since are not suitable in hyperbolic direction. They tend to be weakly stable or even unstable. The one-sided (upwind) schemes are most appropriate since they take the characteristic direction of the first-order equations into account D. Duffy, 2022.

6.2 Strang splitting with upwind and Lax-Wendroff

Rather than discretizing the complete two-dimensional convection-diffusion equation to obtain a finite-difference formula based on a two-dimensional computational stencil, the two-dimensional problem can be splitted into a sequence of two one-dimensional problems. The natural way to split the two-dimensional equation (4.32) is, in terms of spatial coordinates, into two sub-problems. For y direction with fixed x we have the following problem

$$\frac{\partial V}{\partial \tau} - f(x)\frac{\partial V}{\partial y} = 0, \tag{6.9}$$

with initial conditions (4.33) and (4.34), for respectively put and call. The boundary condition are given by (4.37) and (4.40), for respectively put and call. In x direction with fixed y, the problem is given by,

$$\frac{\partial V}{\partial \tau} - \gamma(x,\tau)\frac{\partial V}{\partial x} - \frac{1}{2}\sigma^2\frac{\partial^2 V}{\partial x^2} = -rV, \tag{6.10}$$

with the initial conditions (4.33) and (4.34), for respectively put and call, and the boundary conditions (4.36) and (4.39), for respectively put and call. Then, the numerical methods for the sub-problems (6.9) and (6.10) are developed separately and implemented in such an alternating manner. From the properties of the operator Strang splitting, the solutions of the problem (6.9) is V^* when $t = t_{\frac{n}{2}}$, which can be used as the initial condition of the problem (6.10). Furthermore, V^{**} is the solution of the problem (6.10) at $t = t_n$, which can be used as the initial condition for

the problem (6.9) at second half time step $t = t_n$. Hence, $V_{j,k}^n$ is the solution of the problem (6.9) at $t = t_n$.

The full operator strang splitting scheme solves the problem (6.9) and (6.10) by carrying on the joint iterative calculations:

$$V^0 \to V^{*1} \to V^{**1} \to V^1 \to \ldots \to V^{k-1} \to V^{*k} \to V^{**k} \to V^k \to \ldots \to V^N.$$

Theoretically, it does not matter in which order the algorithm is implemented. However, since the hyperbolic equation tends to create discontinuities, it should be implemented before the parabolic equations D. Duffy, 2022.

To implement the strang splitting method, we consider the computational domain defined as in section 5.3. The first problem is solved over a half-time step. Then, the result is used to solve the second problem for a full time-step, and, again, the first problem is solved over a half step:

Leg 1 we take a time step of length $\frac{1}{2}n$ in y direction, starting with initial data V_{jk}^n to obtain the intermediate value V^*;

Leg 2 we solve at x direction by taking a time step of length n for the leg 2 starting with the data V^* obtained from the first leg;

Leg 3 Then we take, again, a time-step of length $\frac{1}{2}n$ for leg 3, we solve at y direction, starting with the data V^{**} obtained from the second leg.

We had split the equation 4.32 into two separate one-dimensional PDEs (6.9) and (6.10). The choice of the finite difference method to approximate the subproblems (6.9) and (6.10) is based on the character convection dominance of the PDE in x direction and hyperbole type in y direction.

Then, we have respectively the upwind scheme and Lax-wendroff schemes developed in section 5.3. Hence, the boundary conditions will have the same treatments. For instance, when the value V_{jk}^n is known, the first half step is applied to calculate the value V^* for each fixed x_j and based on V_{jk}^n by the following equation

$$V_{j,k}^{n+1} = V_{j,k}^n + \frac{\Delta\tau}{\Delta y} f_j \Delta_y^+ V_{j,k}^n, \tag{6.11}$$

and the value of V^{**} is obtained for each fixed y_k based on V^* by the following equation,

$$V_{j,k}^{n+1} = V_{j,k}^n - r\Delta\tau V_{j,k}^n + \frac{\gamma_j^n \Delta\tau}{2\Delta x}\Delta_{0x} V_{j,k}^n + \left(\frac{(\gamma_j^n)^2\Delta\tau^2}{2\Delta x^2} + \frac{\sigma^2\Delta\tau}{2\Delta x^2}\right)\delta_x^2 V_{j,k}^n. \tag{6.12}$$

Finally, the half step is applied again to calculate the value V_{jk}^{n+1} by (6.11), based on V^{**}.

6.2.1 Convergence analysis

To study the theoretical properties of upwind numerical method (6.11) and Lax-Wendroff numerical method (6.12), we recall again the Lax-equivalent theorem, which state that the convergence of a consistent scheme is synonymous with stability. Then we derive the truncation errors and the stability region in each direction. To analyze the convergence of the combined numerical methods, let us introduce a splitting time step $\frac{\Delta\tau}{2}$, the solution of the equation (4.32) is resolved from τ to $\tau + \frac{\Delta\tau}{2}$ via the Strang splitting method consisting of three sub-steps:

$$V(x, y, \tau + \frac{\Delta\tau}{2}) = \mathcal{S}_1(\frac{\Delta\tau}{2})\mathcal{S}_2(\tau)\mathcal{S}_1(\frac{\Delta\tau}{2}), \tag{6.13}$$

where $\mathcal{S}_1$ and $\mathcal{S}_2$ are solutions of the Lax-Wendroff numerical method (6.12) and upwind numerical method (6.11), respectively.

The theory state that, if all the solutions involved in the three-step splitting scheme (6.13) are smooth, the Strang operator splitting method is second-order accurate D. Duffy, 2022.

Stability

To analyze the stability of the forward Euler scheme, we use the "frozen coefficient" approach and the Fourier analysis method. Then, the symbol of the amplification factor for upwind numerical method (6.11), is

$$\rho(x_j, y_k, \xi) \quad = \quad 1 + f_j \nu_y (e^{i\xi_y} - 1),$$

where

$$\nu_y = \frac{\Delta\tau}{\Delta y}.$$

Applying the equivalent polar form of a complex number, we get

$$\rho(x_j, y_k, \xi) = 1 + \nu_{y,j}(\cos(\xi_y) - 1) + i\nu_{y,j}\sin(\xi_y) = .$$

Hence,

$$|\rho(x_j, y_k, \xi)|^2 = [1 + \nu_{y,j}(\cos(\xi_y) - 1)]^2 + \nu_{y,j}^2 \sin^2(\xi_y).$$

Using the identity

$$\sin^2(\xi_y) = 1 - \cos^2(\xi_y) = (1 - \cos^{(}\xi_y))(1 + \cos(\xi_y))$$

and $(a+b)^2 = a^2 + 2ab + b^2$ we get,

$$\begin{aligned} |\rho(x_j, y_k, \xi)|^2 &= 1 + 2\nu_{y,j}(\cos(\xi_y) - 1) + \nu_{y,j}^2(\cos(\xi_y) - 1)^2 + \\ &\quad + \nu_{y,j}^2(1 - \cos^(\xi_y))(1 + \cos(\xi_y)). \end{aligned}$$

Therefore,

$$|\rho(x_j, y_k, \xi)|^2 = 1 - 2\nu_{y,j}(1 - \cos(\xi_y))(1 - \nu_{y,j}).$$

$0 < 1 - \cos(\xi_y) \leq 2$.

If we choose $\nu_{y,j}$ such the

$$\nu_{y,j} > 0 \text{ and } 1 - \nu_{y,j} > 0$$

we deduce

$$|\rho(x_j, y_k, \xi)|^2 < 1.$$

Then, the condition for stability in y direction is

$$0 < \nu_{y,j} < 1, \tag{6.14}$$

For the Lax-Wendroff numerical method (6.12), the symbol of the amplification factor is given by,

$$\rho(x_j, y_k, \xi) = 1 - r\Delta\tau + \frac{\nu_{x,j}}{2}(e^{i\xi_x} - e^{-i\xi_x}) + \frac{(\nu_{x,j}^2 + \mu}{2}(e^{-i\xi_x} - 2 + e^{i\xi_x}), \tag{6.15}$$

where

$$\nu_{x,j} = \frac{\Delta\tau}{\Delta x}\gamma_j^n, \quad \mu = \sigma^2\frac{\Delta\tau}{(\Delta x)^2}.$$

After transforming the exponential form of the complex number to polar form, that is, $e^{i\alpha} = \cos(\alpha) + i\sin(\alpha)$ in (6.15) we get,

$$\rho(x_j, y_k, \xi) = 1 - r\Delta\tau + \frac{\nu_{x,j}}{2}(2i\sin(\xi_x)) + \frac{\nu_{x,j}^2 + \mu}{2}(2i\cos\xi_x - 2), \tag{6.16}$$

Then, applying the equivalent polar form of a complex number and, using the designations $s_x = 1 - \cos(\xi_x)$, we obtain

$$\rho(x_j, y_k, \xi) = 1 - r\Delta\tau - (\nu_{x,j}^2 + \mu)s_x + i\nu_{x,j}\sin(\xi_x).$$

Hence,

$$\rho(x_j, y_k, \xi)^2 = [1 - r\Delta\tau - (\nu_{x,j}^2 + \mu)s_x]^2 + \nu_{x,j}^2\sin^2(\xi_x).$$

Applying the identities $(a+b)^2 = a^2 + 2ab + b^2$ and $\sin^2(\xi_x) = S_x(2 - S_x)$, we get,

$$\rho(x_j, y_k, \xi)^2 = (1 - r\Delta\tau)^2 - 2(1 - r\Delta\tau)(\nu_{x,j}^2 + \mu)s_x + (\nu_{x,j}^2 + \mu)^2 s_x^2 + \nu_{x,j}^2 S_x(2 - S_x).$$

Since $0 \leq S_x \leq 2$, we have $2 - S_x \geq 0$. In addition, $\mu > 0$ then,

$$\begin{aligned}\rho(x_j, y_k, \xi)^2 \quad &< \quad (1 - r\Delta\tau)^2 + 4r\Delta\tau(\nu_{x,j}^2 + \mu) - 2(\nu_{x,j}^2 + \mu)s_x + (\nu_{x,j}^2 + \mu)^2 s_x^2 + \\ &\quad + (\nu_{x,j}^2 + \mu)S_x(2 - S_x).\end{aligned}$$

In addition, if we assume $v_{x,j}^2 + \mu < 1$, then

$$\rho(x_j, y_k, \xi)^2 < (1 + r\Delta\tau)^2 - 2(\nu_{x,j}^2 + \mu)s_x + (\nu_{x,j}^2 + \mu)s_x^2 + 2(\nu_{x,j}^2 + \mu)S_x - (\nu_{x,j}^2 + \mu)S_x^2.$$

Therefore,

$$\rho(x_j, y_k, \xi)^2 < (1 + r\Delta\tau)^2 < 1 + r\Delta\tau.$$

Then, the condition for stability $v_{x,j}^2 + \mu < 1$.

Now, recalling the strategies Hirsch, 1988, pp 321-323 and Richtmyer, 1967, p 102 to prove the dissipative property, by looking for the behaviour of the amplification factor, we have,

$$\rho(x_j, y_k, \xi)^2 = [1 - r\Delta\tau - (\nu_{x,j}^2 + \mu)s_x]^2 + \nu_{x,j}^2 \sin^2(\xi_x).$$

By using the identities $s_x = 2\sin^2(\frac{\xi}{2})$ and $\sin^2(\xi) = 4\sin^2(\frac{\xi}{2})(1 - \sin^2(\frac{\xi}{2}))$, we deduce

$$\rho(x_j, y_k, \xi)^2 = [1 - r\Delta\tau - 2(\nu_{x,j}^2 + \mu)\sin^2(\frac{\xi}{2})]^2 + 4\nu_{x,j}^2 \sin^2(\frac{\xi}{2})(1 - \sin^2(\frac{\xi}{2})).$$

Since $\nu_{x,j}^2 \sin^2(\frac{\xi}{2})(1 - \sin^2(\frac{\xi}{2})) \leq$ and $\mu > 0$, we can put

$$\rho(x_j, y_k, \xi)^2 < [1 - r\Delta\tau - 2(\nu_{x,j}^2 + \mu)\sin^2(\frac{\xi}{2})]^2 + 4(\nu_{x,j}^2 + \mu)\sin^2(\frac{\xi}{2})(1 - \sin^2(\frac{\xi}{2})).$$

From $0 \leq \sin^2(\frac{\xi}{2}) \leq 1$ and the stability condition, $\nu_{x,j}^2 + \mu \leq 1$, we deduce $4r\Delta\tau(\nu_{x,j}^2 + \mu)\sin^2(\frac{\xi}{2}) < 4r\Delta\tau$, then

$$|\rho(x_j, y_k, \xi)|^2 < (1 + r\Delta\tau)^2 + 4(\nu_{x,j}^2 + \mu)^2 \sin^4(\frac{\xi}{2}) - 4(\nu_{x,j}^2 + \mu)\sin^4(\frac{\xi}{2})).$$

Therefore,

$$|\rho(x_j, y_k, \xi)|^2 < (1 + r\Delta\tau)^2 - 4(\nu_{x,j}^2 + \mu)(1 - (\nu_{x,j}^2 + \mu))\sin^4(\frac{\xi}{2}).$$

Consistence

As in the previous sections, the accuracy of the numerical method in each direction is determined based on the truncation error, which is the difference between the two sides of the equation when the approximation $V_{j,k}^n$ is replaced by the exact solution of the differential equation, $V(x_j, y_k, \tau_n)$.

The exact solution at the discrete points (x_j, y_k, τ_n) and $\Omega = (x^{min}, x^{max}) \times (y^{min}, y^{max}) \times (\tau_0, \tau_f)$ is denoted $v_{j,k}^n$. In addition, $V \in C^{(4,2,2)}(\Omega)$, is the set of functions that have continuous derivatives until the order of the exponent in x, y and t respectively. Then, we recall the approximation of the derivatives (5.6).

For the numerical method (6.11) in y with a fixed x direction, the truncation error is

$$T_{j,k}^n = \frac{v_{j,k}^{n+1} - v_{j,k}^n}{\Delta\tau} - \frac{1}{\Delta y} f_j \Delta_y^+ v_{j,k}^n = \frac{\partial v_{j,k}^n}{\partial \tau} + O(\Delta\tau) - f_j \left(\frac{\partial v_{j,k}^n}{\partial y} + O(\Delta y) \right).$$

Then, in y direction the order of accuracy is $O(\Delta y, \Delta\tau)$.

And for the numerical method (6.12) in x direction with a fixed y,

$$\begin{aligned} T_{j,k}^n &= \frac{v_{j,k}^{n+1} - v_{j,k}^n}{\Delta\tau} + r v_{j,k}^n - \frac{\gamma_j^n}{2\Delta x} \Delta_{0x} v_{j,k}^n - \left(\frac{(\gamma_j^n)^2 \Delta\tau}{2\Delta x^2} + \frac{\sigma^2}{2\Delta x^2} \right) \delta_x^2 v_{j,k}^n. \\ &= \frac{\partial v_{j,k}^n}{\partial \tau} + O(\Delta\tau) + r v_{j,k}^n - \gamma_j^n \left(\frac{\partial v_{j,k}^n}{\partial x} + O((\Delta x)^2) \right) \\ &\quad - \left(\frac{(\gamma_j^n)^2 \Delta\tau}{2} + \frac{\sigma^2}{2} \right) \left(\frac{\partial^2 v_{j,k}^n}{\partial x^2} + O((\Delta x)^2) \right). \end{aligned} \tag{6.17}$$

Then, in x direction the order of accuracy is $O((\Delta x)^2, \Delta\tau)$.

6.2.2 Test problem: stability and convergence rate

In this section, we take the examples from Section 5.3.2, page 58 , to analyze the performance of the strang splitting numerical method. The test problem can be obtained by adding a source term in one of the equations. In this case, we add the source term in x direction with fixed y,

$$\frac{\partial V}{\partial \tau} + rV - \gamma(x, \tau) \frac{\partial V}{\partial x} - \frac{1}{2}\sigma^2 \frac{\partial^2 V}{\partial x^2} = S(x, y, \tau), \tag{6.18}$$

where the source term $S(x, y, \tau)$ is taken as a function such that the equation has the following analytical solution (5.19). The computational domain is defined in $0 \leq x \leq 1/2$, $0 \leq y \leq 1$ and $0 \leq \tau \leq 1/2$. The initial condition for a European put option is (5.15)

The coefficients on the equations functions (6.9) and (6.10) are given by,

$$f(x) = (x - x_{ref})^+, \quad \gamma(x,\tau) = k(\theta(\tau) - x) + \theta'(\tau) - \lambda\sigma,$$

with

$$\theta(\tau) = \frac{74}{50} + \frac{19}{50}\sin\left(\frac{\pi(\tau - 6)}{6}\right)$$

and the respective test values

$$K = \frac{1}{2}, \quad x_{ref} = \frac{1}{4}, \quad r = 0.02, \quad \sigma = \frac{55}{50}, \quad \lambda = 0.8, \quad k = 3.$$

The numerical errors are measured by the discrete norms

$$E_\infty(\tau_n) = \max_{1\le j\le N_x, 1\le k\le N_y} (V(x_j, y_k, \tau_n) - V_{j,k}^n),$$

$$E_2(\tau_n) = \left(\Delta x \Delta y \sum_{j=1}^{N_x}\sum_{k=1}^{N_y}\left(V(x_j, y_k, \tau_n) - V_{j,k}^n\right)^2\right)^{1/2}.$$

Next, we present the results for the numerical method based on operator splitting approach. It is downwind in y direction and Lax-Wendroff in x direction. We run the experiments for very small time steps as in preview section, then we take the final time $\tau_n = 0.1$.

TABLE 6.1: Convergence rate of the numerical method with $\Delta x = 1/1024$, $\Delta\tau = (\Delta x)^2$, $\tau_n = 0.1$.

Δy	E_∞	E_2	R_∞	R_2
1/8	3.4268e-04	5.6675e-05		
1/16	1.7944e-04	2.7589e-05	0.97	1.02
1/32	9.1738e-05	1.3592e-05	0.98	1.01
1/64	4.6369e-05	6.7430e-06	0.99	1.01
1/128	2.3304e-05	3.3574e-06	1.0	1.0

TABLE 6.2: Convergence rate of the numerical method with $\Delta\tau = 1/128$, $\Delta y = \Delta x$, $\tau_n = 0.1$.

Δx	E_∞	E_2	R_∞	R_2
1/8	3.4342e-04	5.9881e-05		
1/16	1.7954e-04	2.8385e-05	0.97	1.04
1/32	9.1761e-05	1.3787e-05	0.98	1.02
1/64	4.6381e-05	6.7895e-06	0.99	1.01
1/128	2.3315e-05	3.3684e-06	1.0	1.01

TABLE 6.3: Convergence rate of the numerical method with $\Delta\tau = 1/128$, $\Delta y = (\Delta x)^2$, $\tau_n = 0.1$.

Δx	E_∞	E_2	R_∞	R_2
1/8	2.3365e-05	3.5483e-06		
1/16	5.8534e-06	8.6098e-07	1.99	2.04
1/32	1.4621e-06	2.1177e-07	2.00	2.02
1/64	3.6337e-07	5.2276e-08	2.01	2.02
1/128	8.4127e-08	1.2032e-08	2.11	2.12

Looking for the Tables 6.1-6.3, we can see that the convergence of the numerical method based on operator splitting approach is in accordance to the theoretical results in both directions. It is first order accuracy in y direction and second order accuracy in x direction. Then the method can be used as an alternative to calculate the approximated values of the European rainfall options. The results are expected to be approximately the same as those obtained in chapter 5.

Chapter 7

Nonstandard finite differences for the PDE model

The concept of stability is a concern in the development of numerical method. In the explicit schemes, for example, the time steps have to be much smaller than required by the structure of the approximated solution, since otherwise it causes instability of the numerical scheme. On the other hand, the implicit schemes for which are allowed the large time step without instability, require much more computational effort per time step than explicit methods. In addition, it can lead to the problem of super stability, where the numerical method delivers a decaying solution even though the underlying physical problem has an exponentially growing one. In this chapter, we develop numerical method for the European rainfall options based on nonstandard methodology. The numerical solutions are evaluated based on the concept of exact schemes and nonstandard modeling rules which tend to preserve all the underlying physical properties for the corresponding underlying problem. The nonstandard modeling rules also include the use of more complicated denominator functions, allowing us to take large time steps without sacrificing the solution's accuracy of the nonstandard method.

7.1 The generalities of nonstandard numerical methods

In this section, we focus on the foundations of nonstandard numerical methods and their methodology. In the traditional theory of numerical methods, both the differential equations and difference equations are not treated in the environment of dynamic consistence concepts, and it can lead to unstable solutions, especially when we deal with problems with open time intervals and long step time integration that are often difficult to guarantee small global errors R. Mickens, 2000, pp. 181-219.

7.1.1 Foundations

The classical criteria of nonstandard is based on the concept of exact schemes. The numerical method are developed and evaluated in the context of dynamical consistence theory. The concept of dynamic consistency is very important, since it allow to incorporate into numerical methods the physics proprieties of the underlying problem. Then, it allows us to develop schemes which preserve particular properties such as fixed points and their stability, closed orbits R. Mickens, 2000, pp. 181-219.

The general methodology of NSFD has its own set of fundamental postulates that are consistent with one another and cannot be derived from the mathematical framework used to analyse standard numerical procedures. These postulates are as follows:

- dynamic consistency;
- construction of denominator functions;
- non-local representations of functions.

The mathematical structure of the equation will determine how the problems relating to these ideas turn out.

Dynamical Consistency

The application of dynamic consistency depends on the specific characteristics or attributes of a system of equations and varies among them. The notion of DC is being introduced with the intention of using it as a general principle to impose limitations on the mathematical forms that may arise when developing a NSFD scheme. It has the principal importance of establishing the limitation for the denominator functions and non-local forms in the differential equations.

Let consider one or more properties of the differential equation and/or its solutions have. The most important properties of differential equation, describing phenomena from sciences and engineering may include:

P1 positivity of solutions;

P2 boundedness of solutions;

P3 monotonicity of solutions;

P4 number and stability of fixed-points;

P5 overall order of the differential equation;

P6 conservation laws;

P7 special symmetries;

P8 asymptotic behavior;

P9 bifurcations;

P10 integer valued dependent variables;

P11 existence of special solutions (traveling waves, solitons, rational, limit cycles and other periodic solutions).

Definition 7.1.1 (of dynamic consistency)
Consider the differential equations

$$\frac{dx}{dt} = f(x, t, \lambda), \quad x(0) = x_0, \tag{7.1}$$

where $\lambda = (\lambda_1, \lambda_2, \ldots, \lambda_m)$ is the set of parameters characterizing the mathematical model. Let a discrete finite difference representation of (7.1) be

$$x_{k+1} = F(x_k, t_k, h, \lambda), \tag{7.2}$$

where $h = \Delta t$, $t + k = hk$, and x_k is an approximation to $x(t_k)$. Then, the discrete model (7.2) is dynamically consistent (DC) with (7.1) with respect to the property P, if it and/or its solutions also have property P.

A given differential equation can possess one or more of those properties and a valid finite difference scheme must incorporate all the essential properties of the original differential equations. Then, it follows that the existence of numerical instabilities is an indication that some "physical principle" underlying the dynamics of the original differential equation is not included in the discrete model R. Mickens, 2000, pags. 181-219.

Denominator Functions

The discretization of the derivatives is a key component of the NSFD methodology. The first derivative, for example, takes the form:

$$\frac{dx(t)}{dt} \rightarrow \frac{x_{k+1} - \psi(h)x_k}{\phi(h)}, \tag{7.3}$$

where $\phi(h)$ and $\psi(h)$ are respectively the "numerator" and "denominator" functions. Generally speaking, $\phi(h)$ and $\psi(h)$ share the following mathematical properties and are dependent on the time step size, h:

$$\psi(h) = 1 + \mathcal{O}(h^2), \quad \phi(h) = h + \mathcal{O}(h^2) \tag{7.4}$$

To simplify, it is considered $\psi(h) = 1$ and, then it is only evaluated $\psi(h)$ for a given equation or system of equations. The problem of how $\phi(h)$ is calculated is addressed in Mickens R. Mickens, 2020, sec. 9.6. But, generally is $\phi(h)$ is determined

by solving the equations of form

$$\frac{dx}{dt} = ax, \tag{7.5}$$

and, then $\phi(h)$ is determined so that the solution of equation (7.5) is also the solution of one of the following numerical methods:

$$\frac{x_{k+1} - x_k}{\phi_1(h,a)} = ax_k, \tag{7.6}$$

$\phi_1(h,a) = \frac{\exp(ah)-1}{a}$, or

$$\frac{x_{k+1} - x_k}{\phi_1(h,a)} = ax_{k+1}. \tag{7.7}$$

$\phi_1(h,a) = \frac{1-\exp(-ah)}{a}$. In the scenario where $a = 0$ (i.e., no linear term appears), h is the only denominator function.

Nonlocal Discretization of Functions

The non-local discretization is an evaluation of the functions appearing in the differential equation at more than one computational lattice point. It will ensure dynamic consistency when discretizing a differential equation regarding a certain proper of the differential equation or its solutions. It takes a thorough understanding of the differential equation and the behaviour of its solutions to choose the right non-local discretizations. For example, it my be required to use $x \to 2x_k - x_{k+1}$ rather than $x \to x_k$. For x^2 and x^3, we can have the following non-local discretizations:

$$x^2 \to 3x_k^3 - x_k^2 x_{k+1} \quad \frac{x_{k+1} + x_k + x_{k-1}}{3} x_k \tag{7.8}$$

$$x^3 \to \frac{x_{k+1} + x_{k-1}}{2} x_k^2 \tag{7.9}$$

Exact Finite Difference Schemes

The exact schemes for an equation are schemes designed in such a way to produce a difference scheme that its discrete solution is equal to the exact solution at the mesh points. The exact solution is then plugged into the standard numerical scheme to obtain correction factors that ensure that the solution of the ordinary differential equation is equal to solutions of the difference equation on a computational grid. Their application requires us to know the solution of the differential equation and can only be applied for those equation having some solution.

Now, we consider the differential equation

$$\frac{dy}{dt} = f(y,t,\lambda),\ y(t_0) = y_0 \tag{7.10}$$

and the corresponding discrete model,

$$y_{k+1} = g(\lambda, h, y_k, t_k), \;\; t_k = hk \tag{7.11}$$

Definition 7.1.2
Equations (7.10) and (7.10) are said to have the same general solution if and only if

$$y_k = y_{t_k} \tag{7.12}$$

for arbitrary values of h.

Definition 7.1.3 (of exact difference scheme)
An exact difference scheme is one for which the solution to the difference equation has the same general solution as the associated differential equation.

Method of Sub-Equations

For many differential equations there are not exact schemes, since they do not possess a general solution. Then, the sub-equations approach is used. The idea behind the sub-equation methodology is that some sub-equations of principal differential equations may admit the exact finite difference schemes. So, the exact schemes of the sub-equations can be combined in such a way to construct NSFD schemes, R. Mickens, 2020, section 9.8.

Definition 7.1.4 (of sub-equation)
Let a differential equation consist of $N \geq 3$ terms. A sub-equation is any differential equation formed by including any $(N-1)$ of fewer terms of the original differential equation.

7.1.2 Nonstandard modeling rules

Then the constructions process of NSFD schemes must be in agreement with some following basic rules R. Mickens, 2005:

Rule 1 the orders of the discrete derivatives should match the orders of the corresponding derivatives that appear in the differential equations;

Rule 2 discrete representations for derivatives must, in general, have nontrivial denominator functions;

Rule 3 nonlinear terms should, in general, be replaced by non-local discrete representations;

Rule 4 special conditions that hold for either the differential equation and/or its solutions should also hold for the difference equation model and/or its solutions;

Rule 5 it is imperative that the solutions of the finite difference equations match exactly with the solutions of the differential equations.

7.1.3 Best finite difference schemes

Since there is no general solution for any arbitrary differential equation, it makes it impossible to construct an exact discrete model for an arbitrary differential equation. Mickens developed modelling rules that, when associated with the sub-equations method, enable the construction of finite difference schemes that are not exact, but have certain highly desired properties and solve a number of issues pertaining to numerical instabilities. The sub-equations approach allows us to construct the finite difference schemes that will not be exact schemes, but they will possess certain very desirable properties and will eliminate a number of problems related to numerical instabilities.

Although the deterministic process for creating NSFD schemes is flexible, there are a general set of steps to be taken R. Mickens, 2020:

- begin by confirming the "correctness" of the differential equations provided;
- check the equations to see what parameters show up, along with their signs and potential values;
- in terms of the parameters, determine the dependent and independent variables' physical scales. The initial and/or boundary conditions may be important to the process in some circumstances;
- examine the relevant sub-equations and establish the circumstances in which the solutions to them provide insight into the behavior of the solutions to the entire set of differential equations;
- examine qualitative and quantitative characteristics of the differential equations in as much detail as possible;
- make a list of the essential qualities you would like to see included in the finite difference scheme based on the findings in previous point;
- determine the denominator functions;
- to determine the non-local mathematical structure of the nonlinear terms in the differential equations, use knowledge and expertise;
- make sure your discretization has included every one of the previously chosen properties in a way that is dynamically consistent;
- this cycle can be repeated if needed.

The best finite difference schemes will be constructed as a result of applying the earlier steps. There is no guarantee that the optimal finite difference scheme

for a differential equation is an exact scheme. Nonetheless, they present the possibility of obtaining models with finite differences that lack the common numerical instabilities.

Definition 7.1.5 (of the best finite difference scheme)
A discrete model of a differential equation constructed in accordance with the five modeling rules **Rules 1-5** is known as a best finite difference scheme or nonstandard finite difference scheme.

The five listed rules, in many cases associated with the sub-equations approach, have been applied to construct the best schemes in a variety of kind of differential equationsR. Mickens, 1994, 2005, 2020. However, there is no clear methodology on the process of choosing the form of best the finite difference scheme among others, since a differential equation can admit more than one best finite difference equation R. Mickens, 2020, section 3.4. To enable a unique selection, more details regarding the characteristics of the differential equation solutions are required. However, the number of dynamically consistent properties incorporated into a given finite difference scheme determines its validity and numerical accuracy; a difference scheme with more dynamically consistent features is thought to be significantly better.

7.1.4 The nonstandard methods for PDEs

The literature on nonstandard schemes for general partial differential equations, particularly those with variable coefficients, is relatively sparse. However, the nonstandard modeling rules are applied in the same way as for ordinary differential equations described, for example R. Mickens, 2020. The definition of a dynamic consistent numerical method 7.1.1, is formulated in terms of ordinary differential equations, but it is extended to the partial differential equations.

The non-local considerations can be extended to PDEs as for example:

$$u(x,t) \to \frac{u_{m+1}^k + u_m^k + u_{m-1}^k}{3} x_k^2, \quad u_m^{k+1} \tag{7.13}$$

$$u(x,t)^2 \to u_m^{k+1} x_{m-1}^k, \quad \frac{u_{m+1}^k + x_{m-1}^k}{2} u_m^k \tag{7.14}$$

$$u(x,t)^3 \to \frac{u_{m+1}^k + u_m^k + u_{m-1}^k}{3} (u_m^k)^2 \tag{7.15}$$

The sub-equations approach is very crucial in developing NSFD schemes for PDEs. In R. E. Mickens, 2007, the NSFD was developed for linear convection-diffusion equation,

$$u_t + a u_x = D u_{xx} \tag{7.16}$$

with a and D constants. The equation (7.16) has three sub-equations which are:

$$u_t + au_x = 0, \quad u_t = Du_{xx}, \quad au_x = Du_{xx}. \tag{7.17}$$

The exact finite difference schemes for the first and last sub-equations were combined to create the NSFD, in order to ensure that the common term au_x has the same discretization. For the Black-Scholes partial differential equation

$$\frac{\partial U}{\partial t} = D\frac{\partial^2 U}{\partial x^2} + (r - D)\frac{\partial U}{\partial x} - rU, \tag{7.18}$$

very popular in financial mathematics for modeling and understanding financial markets, the NSFD scheme was derived in R. Mickens, 2020, section 11.11 also applying the method of sub-equations. The equation (7.18) has the following sub-equations:

$$\frac{\partial U}{\partial t} = -rU \tag{7.19}$$

$$D\frac{\partial^2 U}{\partial x^2} - rU = 0 \tag{7.20}$$

$$\frac{\partial U}{\partial \tau} - (r - D)\frac{\partial U}{\partial x} = 0 \tag{7.21}$$

$$(r - D)\frac{\partial U}{\partial x} = rU \tag{7.22}$$

$$(r - D)\frac{\partial U}{\partial x} = -D\frac{\partial^2 U}{\partial x^2} \tag{7.23}$$

$$\frac{\partial U}{\partial t} = D\frac{\partial^2 U}{\partial x^2}. \tag{7.24}$$

For the PDE (7.18) there are six sub-equations (7.19)–(7.24), but, in general, we cannot use all of them R. Mickens, 2020. Initially, the exact finite difference scheme is derived for the sub-equation

$$\frac{\partial U}{\partial t} = -rU, \tag{7.25}$$

that is

$$\frac{U^{k+1} - U^k}{\phi(\Delta t, r)} = -rU^{k+1}, \quad \phi(\Delta t, r) = \frac{\exp(r\Delta t) - 1}{r}, \tag{7.26}$$

where $U^k = U(t_k); k = 0, 1, 2, \cdots; t_k = (\Delta t)k)$. The exact finite difference schemes for the equation (7.18) were found to match the term (7.26) with the corresponding term, which was found to be the NSFD.

$$\frac{U_m^{k+1} - U_m^k}{\phi(\Delta t, r)} = \frac{-r}{B}(U_{m+2}^k - 2U_{m+1}^k + U_m^k) + \frac{-Ar}{B}(U_{m+1}^k - U_m^k) - rU_m^{k+1}. \tag{7.27}$$

A and B obtained by constructing the exact finite difference scheme for the sub-equation (7.23). Additionally, a nonlinear, generalized version of the Black-Scholes pricing PDE has been solved using this methodology.Arenas et al., 2013.

On Ehrhardt and Mickens, 2013, an explicit nonstandard scheme for Black Scholes equation was developed based on (7.19)–(7.22) sub-equations and the condition to guaranty the positivity were determined.

Attention must be taken when we deal with partial differential equations in higher dimensions, especially when the coefficients in each direction have other direction variables. In this case, the nonstandard algorithm is not an a direct extension of the one dimensional case and additional Laplacian operators must be introduced R. Mickens, 2000, pp. 109-151 . On the other hand, we think one can relax this problem by applying the theory of splitting operators, since the addition of more Laplacian operators can be computationally expensive.

7.2 The nonstandard numerical method for the PDE model

We develop a nonstandard numerical scheme base on splitting the PDE (6.9)-(6.10) in two partial differential equation. In y direction (fixed x), we have the hyperbolic equation (6.9), with the initial condition $V(x,y,0) = \psi(y) = tick \times (K - y_T)^+$. Then, we construct nonstandard numerical method using the non-local modeling rule.

The main idea on applying the non-local modeling rule, is to get an monotone numerical method. The monotone property means an positive preserving numerical method, that is, if the initial condition of the numerical method is non-negative, then the solution at last step is also non-negative.

$$v_j^0 \geq 0 \ \ \forall j \Rightarrow v_j^n \geq 0, \ \ \forall j, n. \tag{7.28}$$

For the downwind scheme developed for hyperbolic direction in section 5.3, the monotone scheme is

$$\frac{V_{j,k}^{n+1} - V_{j,k}^n}{\Delta\tau} - f_j \frac{V_{j,k+1}^n - V_{j,k}^{n+1}}{\Delta y} = 0 \tag{7.29}$$

The computational domain is $[x^{min}, x^{max}] \times [y^{min}, y^{max}] \times [\tau_0, \tau_f]$. The grid points of the discrete domain are equally spaced in time and in the spatial direction x, being the time step and the space steps given respectively by

$$\Delta\tau = \frac{\tau_f - \tau_0}{N_\tau}, \qquad \Delta x = \frac{x^{max} - x^{min}}{N_x}, \qquad \Delta y = \frac{y^{max} - y^{min}}{N_y}.$$

Therefore the discretized computational domain is

$$\{(x_j, y_k, \tau_n), j = 0, \ldots, N_x; k = 0, \ldots, N_y; n = 0, \ldots, N_\tau\}$$

with

$$x_j = x^{min} + j\Delta x; \;\; y_k = y^{min} + k\Delta y; \;\; \tau_n = \tau_0 + n\Delta\tau.$$

The approximated solution of $V(x, y, \tau)$ in y direction is denoted $V^n_{j,k} \approx V(x_j, y_k, \tau_n)$ and the values of the function $f(x)$ is denoted respectively by $f_j = f(x_j)$. Note that x_j is fixed. Then, we can rewrite the monotone scheme 7.29 as

$$(1 + \frac{\Delta\tau}{\Delta y} f_j) V^{n+1}_{j,k} = V^n_{j,k} + \frac{\Delta\tau}{\Delta y} f_j V^n_{j,k+1} \tag{7.30}$$

from where by taking $\nu_j = \frac{\Delta\tau}{\Delta y} f_j$, we get the monotone numerical method,

$$V^{n+1}_{j,k} = \frac{1}{(1 + \nu_j)} (V^n_{j,k} + \nu_j V^n_{j,k+1}). \tag{7.31}$$

In x direction, we have a convection diffusion equation (6.10) with coefficients depending only on time t and space x variable. Then we can follow the methodology presented on Kojouharov and Chen, 1999; Kojouharov and Chen-Charpentier, 2004, based on sub-equations methodology to construct a nonstandard numerical scheme.Then, the sub-equations of (6.10) are:

$$\frac{\partial V}{\partial t} = -rV \tag{7.32}$$

$$\frac{1}{2}\sigma^2_\tau \frac{\partial^2 V}{\partial x^2} - rV = 0 \tag{7.33}$$

$$\frac{\partial V}{\partial \tau} + \gamma(x, \tau)\frac{\partial V}{\partial x} = 0 \tag{7.34}$$

$$\gamma(x, \tau)\frac{\partial V}{\partial x} = -rV \tag{7.35}$$

$$\gamma(x, \tau)\frac{\partial V}{\partial x} = \frac{1}{2}\sigma^2_\tau \frac{\partial^2 V}{\partial x^2} \tag{7.36}$$

$$\frac{\partial V}{\partial t} = \frac{1}{2}\sigma^2_\tau \frac{\partial^2 V}{\partial x^2}. \tag{7.37}$$

As stated in R. Mickens, 2020, we can not use all the sub-equations. Our choice of the sub-equations to use for constructing the NSFD method for equation (6.10), is motivated by the findings of Kojouharov and Chen R. Mickens, 2000, pp. 55-106. There, the exact time stepping scheme was constructed for the convection-reaction part of the transport equation, and, it has enabled to follow the transport and track sharp fronts more accurately than with the standard numerical schemes.

First, the exact time-stepping scheme will be developed for the convection–reaction

part and the standard numerical methods will be used for solving the remaining diffusion part. An exact time-step scheme is a type of numerical scheme for which the numerical solution is the same to the solution of the corresponding equations in the mesh points. Lubuma and Patidar, Lubuma and Patidar, 2005 have used an exact time-steps scheme in solving a singular perturbed convection-reaction equation in the context of NSFD schemes. In Arenas et al., 2013, the authors have also used a similar approach in solving a nonlinear Black-Scholes equation. These NFDS provide numerically stable algorithms for approximating solutions of differential equations.

Now, let us consider the convection-reaction equation

$$\frac{\partial V}{\partial \tau} - \gamma(x,\tau)\frac{\partial V}{\partial x} = -rV, \tag{7.38}$$

Let $V(x,y,0) = \psi(x,y)$ be the initial condition for the equation (7.38) where $\psi(x,y)$ is a given function. Using the method of characteristics, the partial differential equation (7.38) can be solved and get the solution of the form Kojouharov and Chen, 1999,

$$V(x,y) = \psi(s_x,y)\exp^{(-r\tau)}, \tag{7.39}$$

where $s_x = x(0)$ is the initial condition of the ordinary differential equation

$$\frac{dx(\tau)}{d\tau} = -\gamma(x,\tau), \tag{7.40}$$

where $\gamma = -kx + q(\tau)$, and $q(\tau) = k\theta(\tau) - \theta'(\tau) - \lambda\sigma$. Then, we use the integrator factor $\exp(-k\tau)$ to solve the integral

$$\frac{dx(\tau)}{d\tau} = kx - q(\tau). \tag{7.41}$$

Hence, we get

$$x\exp(-k\tau) = \int(-\exp(-k\tau)q(\tau))d\tau \tag{7.42}$$

and

$$x\exp(-k\tau) = -Q(\tau) + C, \tag{7.43}$$

so,

$$x(\tau) = \exp(k\tau)(-Q(\tau) + C), \tag{7.44}$$

where $Q(\tau)$ is a continuous function such that $Q'(\tau) = q(\tau)$. By using the initial condition $x(0) = s_x$, the constant of integration C becomes

$$C = s_x + Q(0). \tag{7.45}$$

Substituting (7.45) into the equation (7.44), we get

$$x(\tau) = \exp(k\tau)(-Q(\tau) + s_x + Q(0)), \tag{7.46}$$

and, finally we obtain

$$s_x = x(\tau)\exp(-k\tau) + Q(\tau) - Q(0). \tag{7.47}$$

Substituting s_x into the equation (7.39), we obtain the general solution

$$V(x, y, \tau) = \psi(x(\tau)\exp(-k\tau) + Q(\tau) - Q(0), y)\exp^{(}-r\tau), \tag{7.48}$$

Theorem 7.2.1
The exact time-step scheme for equation (7.38) is given by

$$\frac{V(x, y, \tau + \Delta\tau) - V(\bar{x}, y, \tau)}{\varphi(\Delta\tau)} = -rV(\bar{x}, y, \tau), \tag{7.49}$$

where

$$\varphi(\Delta\tau) = \frac{1 - \exp(-r\Delta\tau)}{r} \tag{7.50}$$

and

$$\bar{x} = x\exp(-k\Delta t) + [Q(\tau + \Delta\tau) - Q(t)]\exp(kt). \tag{7.51}$$

Proof. Let us evaluate the solution (7.48) at time $\tau + \Delta\tau$, such that $\tau + \Delta\tau \in [0, \tau_f]$. We have,

$$\begin{aligned}
V(x, y, \tau + \Delta\tau) &= \psi(xe^{-k(\tau+\Delta\tau)} + Q(\tau + \Delta\tau) - Q(0), y)e^{-r(\tau+\Delta\tau)} \\
&= \psi(xe^{-k(\tau+\Delta\tau)} + Q(\tau + \Delta\tau) - Q(t) + Q(t) - Q(0), y)e^{-r(\tau+\Delta\tau)} \\
&= \psi([xe^{-k\Delta\tau} + (Q(\tau + \Delta\tau) - Q(t))e^{k\tau}]e^{-k\tau} + Q(t) - Q(0), y) \cdot \\
&\quad \cdot e^{-r(\tau+\Delta\tau)} = \\
&= \psi(\bar{x}e^{-k\tau} + Q(t) - Q(0), y)e^{-r(\tau+\Delta\tau)} = V(\bar{x}, y, \tau)e^{-r\Delta\tau} \\
&= V(\bar{x}, y, \tau)e^{-r\Delta\tau} - V(\bar{x}, y, \tau) + V(\bar{x}, y, \tau)
\end{aligned} \tag{7.52}$$

from here,

$$V(x, y, \tau + \Delta\tau) = V(\bar{x}, y, \tau)(e^{-r\Delta\tau} - 1) + V(\bar{x}, y, \tau) \tag{7.53}$$

where $\bar{x}$ is the backtrack point associated with the point x at time $\tau + \Delta\tau$,

$$\bar{x} = x\exp(-k\Delta t) + [Q(\tau + \Delta\tau) - Q(t)]\exp(kt). \tag{7.54}$$

Finally, by passing the second term in the right hand side of the equation (7.53) to left hand we get

$$\frac{V(x,y,\tau+\Delta\tau)-V(\bar{x},y,\tau)}{\varphi(\Delta\tau)}=-rV(\bar{x},y,\tau)$$

where

$$\varphi(\Delta\tau)=\frac{1-\exp(-r\Delta\tau)}{r}.$$

□

The left-hand side of (7.49) can be viewed as a nonstandard difference approximation of the characteristic derivative $\frac{DV}{D\tau}=\frac{\partial V}{\partial\tau}-\gamma\frac{\partial V}{\partial\tau}$ and the right-hand side a non-local modeling of the linear reaction term.

Let us recall the computational domain $[x^{min},x^{max}]\times[y^{min},y^{max}]\times[\tau_0,\tau_f]$. The grid points of the discrete domain are equally spaced in time and in the spatial direction x, being the time step and the space steps given respectively by

$$\Delta\tau=\frac{\tau_f-\tau_0}{N_\tau},\qquad \Delta x=\frac{x^{max}-x^{min}}{N_x},\qquad \Delta y=\frac{y^{max}-y^{min}}{N_y}.$$

Therefore, the computational domain is

$$\{(x_j,y_k,\tau_n), j=0,\ldots,N_x; k=0,\ldots,N_y; n=0,\ldots,N_\tau\}$$

with

$$x_j=x^{min}+j\Delta x;\;\; y_k=y^{min}+k\Delta y;\;\; \tau_n=\tau_0+n\Delta\tau.$$

The approximated solution of $V(x,y,\tau)$ is denoted by $V_{j,k}^n\approx V(x_j,y_k,\tau_n)$ and the values of the functions $f(x)$ and $\gamma(x,\tau)$ are denoted by $f_j=f(x_j)$ and $\gamma_j^n=\gamma(x_j,\tau_n)$, respectively. Note that y_k is fixed.

We consider that $V(x,y,t)\in C^{4,2}$, and we define the first derivatives and second derivatives as,

$$\frac{\partial V(x_j,y_k,\tau_n)}{\partial\tau} = \frac{V(x_j,y_j,\tau_{n+1})-V(x_j,y_k,\tau_n)}{\varphi(\Delta\tau)}+O(\Delta\tau) \tag{7.55}$$

$$\frac{\partial^2 V(x_j,y_k,\tau_n)}{\partial x_j^2} = \frac{V(x_{j+1},y_k,t_n)-2V(x_j,y_k,t_n)+V(x_{j-1},y_k,t_n)}{\Delta x^2}+ +O((\Delta x)^2) \tag{7.56}$$

where, $\varphi(\Delta\tau)=O((\Delta\tau)^2)$.

To complete the discretization of the equation (6.10), we will apply the central approximation (7.56) to the second order derivative to deduce,

$$\frac{V(x_j, y_k, \tau_{n+1}) - V(\bar{x}_j, y_k, \tau_n)}{\varphi(\Delta\tau)} - \frac{\sigma^2}{2\Delta x^2}\delta_x^2 V_{j,k}^n = -rV(\bar{x}_j, y_k, \tau_n). \tag{7.57}$$

Then,

$$V_{j,k}^{n+1} = (1 - r\varphi(\Delta\tau))V^n(\bar{x}_j, y_k) + \frac{\sigma^2\varphi(\Delta\tau)}{2\varphi(\Delta x)}\delta_x^2 V_{j,k}^n. \tag{7.58}$$

whre $1 \leq j \leq N_x - 1$, y_k fixed, and $V^n(\bar{x}_j, y_k) = V(x\exp(-k\Delta t) + [Q(\tau + \Delta\tau) - Q(t) - Q(0)]\exp(kt), y_k, t_n)$.

At the nodes $j = 0$ and $j = N_x$ we have, the Dirichelet and Neuman boundary conditions, respectively. The implematntation is the same as in section 5.3.2.

The solution in the points $V^n(\bar{x}_j, y_k)$ is calculated using the following approximation Arenas et al., 2013,

$$V^n(\bar{x}_j, y_k) = V_{j,k}^n + \frac{\bar{x}_j - x_j}{\Delta x}(V_{j+i,k}^n - V_{j,k}^n), \qquad 1 \leq j \leq N_x, \tag{7.59}$$

$$V^n(\bar{x}_0, y_k) = V_{0,k}^n. \tag{7.60}$$

Now, let us substitute (7.59) into (7.58), the explicit nonstandard finite scheme for equation (6.10) take the form,

$$V_{j,k}^{n+1} = (1 - r\varphi(\Delta\tau))[V_{j,k}^n + \frac{\bar{x}_j - x_j}{\Delta x}(V_{j+i,k}^n - V_{j,k}^n)] + \frac{\sigma^2\varphi(\Delta\tau)}{2\varphi(\Delta x)}\delta_x^2 V_{j,k}^n, \tag{7.61}$$

from where we get,

$$\begin{aligned} V_{j,k}^{n+1} &= (\frac{\bar{x}_j - x_j}{\Delta x} - r\varphi(\Delta\tau)\frac{\bar{x}_j - x_j}{\Delta x} + \frac{\sigma^2\varphi(\Delta\tau)}{2\varphi(\Delta x)})V_{j+i,k}^n + \\ &+(1 - r\varphi(\Delta\tau) - \frac{\bar{x}_j - x_j}{\Delta x} + r\frac{\bar{x}_j - x_j}{\Delta x}\varphi(\Delta\tau) - \frac{\sigma^2\varphi(\Delta\tau)}{\varphi(\Delta x)})V_{j,k}^n + \\ &+\frac{\sigma^2\varphi(\Delta\tau)}{2\varphi(\Delta x)}V_{j-1,k}^n. \end{aligned} \tag{7.62}$$

We can see that the positive condition for the numerical scheme is

$$1 - r\varphi(\Delta\tau) - \frac{\bar{x}_j - x_j}{\Delta x} + r\frac{\bar{x}_j - x_j}{\Delta x}\varphi(\Delta\tau) - \frac{\sigma^2\varphi(\Delta\tau)}{\varphi(\Delta x)} > 0,$$

Since ,

$$\frac{\bar{x}_j - x_j}{\Delta x} + \frac{\sigma^2\varphi(\Delta\tau)}{2\varphi(\Delta x)} \geq r\varphi(\Delta\tau)\frac{\bar{x}_j - x_j}{\Delta x}.$$

7.2.1 Convergence analysis

Consistency

We recall that the concept of consistency of numerical methods means that the exact solution of the finite difference scheme, approximates the exact solution of the partial differential equation.

In Y direction, we are dealing with first order downwind scheme. If $v \in C^{(4,2,2)}(\Omega)$ we have,

$$\frac{v_{j,k}^{n+1} - v_{j,k}^{n}}{\Delta\tau} = \frac{\partial v_{j,k}^{n}}{\partial\tau} + O(\Delta\tau), \tag{7.63}$$

$$\frac{v_{j,k+1}^{n} - v_{j,k}^{n+1}}{\Delta y} = \frac{\partial v_{j,k}^{n}}{\partial y} + O(\Delta y + \frac{\Delta\tau}{\Delta y}). \tag{7.64}$$

The truncation error for the monotone downwind method is

$$T_{j,k}^{n} = \frac{\partial v_{j,k}^{n}}{\partial\tau} + O(\Delta\tau) - f_j\left(\frac{\partial v_{j,k}^{n}}{\partial y} + O(\Delta y + \frac{\Delta\tau}{\Delta y})\right)$$

Then, we conclude that the order of accuracy is $O(\Delta y + \frac{\Delta\tau}{\Delta y}, \Delta\tau)$.

Now let us avaluate in X direction. We assume that the analytical solution of the partial differential equation (6.10) belong to $C^{(4,2,2)}(\Omega)$. Then, for the exact solution $V(x, y, \tau)$, with $\bar{V}_{j,k}^{n+1} = V(x_j^{n+1}, y_k, \tau_{n+1})$ and $\bar{V}_{j,k}^{n} = V(\bar{x}_j^{n}, y_k, \tau_n)$ the truncation error of the nonstandard method (7.62) at time-level $n+1$ is

$$T_{j,k}^{n} = \frac{V_{j,k}^{n+1} - \bar{V}_{j,k}^{n}}{\varphi(\Delta\tau)} - \frac{\sigma^2}{2\Delta x}\delta_x^2 V_{j,k}^{n} + r\bar{V}_{j,k}^{n}. \tag{7.65}$$

By definition,

$$\begin{aligned} T_{j,k}^{n} = {} & \frac{V_{j,k}^{n+1} - V_{j,k}^{n}}{\varphi(\Delta\tau)} - \left(\frac{\partial V(x_j, y_k, \tau^{n+1})}{\partial\tau} - \gamma^{n+1_j}\frac{\partial V(x_j, y_k, \tau^{n+1})}{\partial x}\right) + \\ & -\left(\frac{\sigma^2}{2\Delta x}\delta_x^2 V_{j,k}^{n} - \frac{1}{2}\sigma^2\frac{\partial^2 V}{\partial x^2}\right) - \left(r\bar{V}_{j,k}^{n} - rV_{j,k}^{n+1}\right) \end{aligned} \tag{7.66}$$

By using the Taylor series expansions and the Mean Value Theorem, we deduce, after some computation, the following

$$T_{j,k}^{n} = O(\frac{\partial^2 V^*}{\partial x^2}\Delta\tau) + O(\|\frac{\partial^4 V^{n+1}}{\partial x^4}\|_\infty \Delta x^2) + O(\|\frac{\partial R}{\partial z}(V_{j,k}^{n+1}, \dot{)}\|_\infty \frac{\partial V^*}{\partial t}\Delta\tau), \tag{7.67}$$

where $\frac{\partial V^*}{\partial t}$ and $\frac{\partial^2 V^*}{\partial t^2}$ are some evaluations of the first and the second tangential derivatives along the characteristic segment between (x_j, y_j, τ_{n+1}) and $(\bar{x}_j, y_k, \tau_n)$, respectively.

Stability

Let us recall the "frozen coefficient" approach and the Fourier analysis method. Then, the symbol of the amplification factor for the monotone downwind scheme is

$$\rho(x_j, y_k, \xi) \quad = \quad \frac{1}{1+\nu_j}(1+\nu_j e^{i\xi_y})$$

Then, using the corresponding polar form of the complex number, we get,

$$\rho(x_j, y_k, \xi) \quad = \quad \frac{1}{1+\nu_j}(1+\nu_j(\cos(\xi_y)+i\sin(\xi_y))).$$

Then,

$$\rho(x_j, y_k, \xi)^2 \quad = \quad \frac{1}{(1+\nu_j)^2}[(1+\nu_j\cos(\xi_y))^2+\nu_j^2\sin^2(\xi_y)].$$

From where we deduce,

$$\rho(x_j, y_k, \xi)^2 \quad = \quad \frac{1}{(1+\nu_j)^2}(1+\nu_j\cos(\xi_y)+\nu_j^2).$$

Lets consider $\nu_j < 1$. Since $\cos(\xi_y) < 2$, we deduce $\nu_j\cos(\xi_y) < 2\nu_j$. Then $(1+\nu_j\cos(\xi_y)+\nu_j^2) < (1+\nu_j)^2$. From where we can conclude that

$$\rho(x_j, y_k, \xi)^2 \quad \leq \quad 1.$$

The amplification factor for the nonstandard numerical method (7.62) is given by

$$\begin{aligned}\rho(x_j, y_k, \xi) \quad = \quad & (\frac{\bar{x}_j - x_j}{\Delta x} - r\varphi(\Delta\tau)\frac{\bar{x}_j - x_j}{\Delta x} + \frac{\sigma^2\varphi(\Delta\tau)}{2\Delta x^2})e^{i\xi_x} + \\ & +(1 - r\varphi(\Delta\tau) - \frac{\bar{x}_j - x_j}{\Delta x} + r\frac{\bar{x}_j - x_j}{\Delta x}\varphi(\Delta\tau) - \frac{\sigma^2\varphi(\Delta\tau)}{\Delta x^2}) + \\ & +\frac{\sigma^2\varphi(\Delta\tau)}{2\Delta x^2}e^{-i\xi_x}. \end{aligned} \tag{7.68}$$

Using the corresponding polar form of the complex number, we get,

$$\begin{aligned}\rho(x_j, y_k, \xi) \quad = \quad & (1 - r\varphi(\Delta\tau) - \frac{\bar{x}_j - x_j}{\Delta x} + r\frac{\bar{x}_j - x_j}{\Delta x}\varphi(\Delta\tau) - \frac{\sigma^2\varphi(\Delta\tau)}{\Delta x^2}) + \\ & +(\frac{\bar{x}_j - x_j}{\Delta x} - r\varphi(\Delta\tau)\frac{\bar{x}_j - x_j}{\Delta x} + \frac{\sigma^2\varphi(\Delta\tau)}{\Delta x^2})\cos(\xi_x) + \\ & +(\frac{\bar{x}_j - x_j}{\Delta x} - r\varphi(\Delta\tau)\frac{\bar{x}_j - x_j}{\Delta x^2})i\sin(\xi_x). \end{aligned} \tag{7.69}$$

For simplicity, let us denote

$$\nu_1 = (1 - r\varphi(\Delta\tau) - \frac{\bar{x}_j - x_j}{\Delta x} + r\frac{\bar{x}_j - x_j}{\Delta x}\varphi(\Delta\tau) - \frac{\sigma^2\varphi(\Delta\tau)}{\Delta x^2})$$

$$\nu_2 = (\frac{\bar{x}_j - x_j}{\Delta x} - r\varphi(\Delta\tau)\frac{\bar{x}_j - x_j}{\Delta x} + \frac{\sigma^2\varphi(\Delta\tau)}{\Delta x^2})$$

$$\nu_3 = (\frac{\bar{x}_j - x_j}{\Delta x} - r\varphi(\Delta\tau)\frac{\bar{x}_j - x_j}{\Delta x^2}).$$

Then,

$$\rho(x_j, y_k, \xi)^2 = (\nu_1 + \nu_2\cos(\xi_x))^2 + \nu_3^2\sin^2(\xi_x) \tag{7.70}$$

If, $\nu_1 + \nu_2 \leq 1$, then

$$\rho(x_j, y_k, \xi)^2 \leq \nu_1^2 + \nu_2^2\cos^2(\xi_x) + \nu_3^2\sin^2(\xi_x). \tag{7.71}$$

Since $\frac{\phi(\Delta\tau)}{\Delta x} > 0$, then

$$\rho(x_j, y_k, \xi)^2 \leq \nu_1^2 + \nu_2^2\cos^2(\xi_x) + \nu_2^2\sin^2(\xi_x). \tag{7.72}$$

Therefore,

$$\rho(x_j, y_k, \xi)^2 < \nu_1^2 + 2\nu_2^2 \tag{7.73}$$

Now, if we set $\nu_2 < 1$, we deduce

$$\rho(x_j, y_k, \xi)^2 < (1 + r\phi(\Delta\tau))^2 - 2\nu_2^2 + 2\nu_2^2. \tag{7.74}$$

Therefore,

$$\rho(x_j, y_k, \xi)^2 < 1 + r\phi(\Delta\tau) \tag{7.75}$$

7.2.2 Test problem: stability and convergence rate

For the test problem, we also take the function from Section 5.3.2 to analyze the performance of the strang splitting nonstandard numerical method. The source term is added to the equation in x direction with fixed y variable and take the form of (6.18).

Recall the computational domain defined as $0 \leq x \leq 1/2$, $0 \leq y \leq 1$ and $0 \leq \tau \leq 1/2$. The initial condition for a European put option is given by (5.15). The coefficients in the equations functions (6.9) and (6.10) are given by,

$$f(x) = (x - x_{ref})^+, \quad \gamma(x, \tau) = k(\theta(\tau) - x) + \theta'(\tau) - \lambda\sigma,$$

with

$$\theta(\tau) = \frac{74}{50} + \frac{19}{50}\sin\left(\frac{\pi(\tau - 6)}{6}\right)$$

and the respective test values

$$K = \frac{1}{2}, \quad x_{ref} = \frac{1}{4}, \quad r = 0.02, \quad \sigma = \frac{55}{50}, \quad \lambda = 0.8, \quad k = 3.$$

The discrete norms to measure the numerical errors,

$$E_\infty(\tau_n) = \max_{1\le j\le N_x, 1\le k\le N_y} (V(x_j, y_k, \tau_n) - V^n_{j,k}),$$

$$E_2(\tau_n) = \left(\Delta x \Delta y \sum_{j=1}^{N_x} \sum_{k=1}^{N_y} \left(V(x_j, y_k, \tau_n) - V^n_{j,k} \right)^2 \right)^{1/2}.$$

Next, we present the results for the nonstandard numerical method 7.62. It is an monotone downwind scheme in y direction. In x direction, it uses a nonstandard numerical method based on the sub-equations approach. We are able to run the experiments for the final time we have chosen $\tau_n = 0.1$.

TABLE 7.1: Convergence rate of the numerical method with $\Delta x = 1/1024$, $\Delta\tau = 0.5 * dx^2$, $\tau_n = 0.1$.

Δy	E_∞	E_2	R_∞	R_2
1/8	3.6329e-04	6.7583e-05		
1/16	2.1436e-04	3.8483e-05	0.76	0.81
1/32	1.1317e-05	1.9552e-05	0.92	0.98
1/64	5.5232e-05	9.3687e-06	1.03	1.05
1/128	2.5956e -05	3.7750e-06	1.06	1.09

TABLE 7.2: Convergence rate of the numerical method with $\Delta\tau = 1/128$, $\Delta y = \Delta x$, $\tau_n = 0.1$.

Δx	E_∞	E_2	R_∞	R_2
1/8	3.6349e-04	6.7483e-05		
1/16	2.1446e-04	3.8483e-05	0.76	0.81
1/32	1.1307e-04	1.9451e-05	0.92	0.98
1/64	5.5232e-05	9.3587e-06	1.03	1.05
1/128	2.5957e-05	3.7650e-06	1.06	1.09

TABLE 7.3: Convergence rate of the numerical method with $\Delta\tau = 1/128$, $\Delta y = (\Delta x)^2$, $\tau_n = 0.1$.

Δx	E_∞	E_2	R_∞	R_2
1/8	3.3657e-04	3.34234e-05		
1/16	1.0880e-04	8.9950e-06	1.62	1.89
1/32	2.9959e-05	2.3931e-06	1.86	1.91
1/64	8.01906e-06	6.0572e-07	1.90	1.98
1/128	1.9972e-06	1.4757e-07	2.00	2.03

The Tables 7.1-7.3, show the results of the convergence of the nonstandard numerical method combined with the operator splitting equations. We can see that, the results are in accordance with the theoretical results. In y direction it is first order accuracy and in x direction it is second order accuracy. Then, we can use the method as an alternative to calculate the approximated values of European rainfall options, with less computational effort.

Chapter 8

Final remarks

We have presented a model to price rain weather derivatives. The model is derived by applying the widely used methodology based on the partial differential approach, that assumes the self-financing portfolio principle. The discounted conditional expectation is used to determine the weather option price. In order to ensure that movements in the derivative are balanced by changes in a multiple of the underlying, option valuation typically depends on the underlying quantity being used to hedge the position of the option. This allows the portfolio to be assumed to be risk-free. We use a variant of Black and Scholes analysis to derive unique prices, that is Feynman-Kac formula. A two-dimensional convection diffusion equation is derived where the spatial variables are the rainfall index and rainfall quantities. The partial differential equation has several variables that need to be estimated, such as, the rate of mean reversion k, the long term mean $\theta(t)$ of the process and the volatility σ. These variables are estimated in the context of an Ornstein-Uhlenbeck process for the random variable precipitation. A suggestion on how to estimate these parameters, based on precipitation data, has been included.

A numerical method has been suggested to determine the price of the option as a solution of the partial differential equation that is convection dominant. It makes an accurate numerical approximation very difficult, since there is an excessive number of nonphysical oscillations. Modified numerical methods, which are special cases of finite-difference schemes and nonstandard finite difference schemes and operator splitting approaches, have been proposed. These numerical methods are explicit and therefore are conditionally stable. However, the appropriate regions of stability are given. In addition, the model is described by an initial boundary value problem and appropriate boundary conditions have been suggested. Regarding the boundary conditions, our approach is different from what we can find in literature. This approach takes in consideration the financial interpretation of the model and also the fact that, from the mathematical point of view, it is convenient that they are compatible with the terminal condition.

Two explicit numerical methods are suggested in chapter 5. The methods are

based on Lax-Wendrof schemes and upwind-downwind schemes. We show by numerical experiments that the methods are able to handle the convection dominance problems. The operator splitting approach is developed in chapter 6, as an alternative to solving numerically the partial differential equations with less additional cost associated with the direct extensions of finite difference methods. The numerical experiments showed the effectiveness of the approach. The nonstandard finite difference scheme combined with the operator splitting approach is developed in chapter 7. The numerical solutions of the rainfall European options are evaluated based on concept of exact schemes and nonstandard modeling rules which tend to preserve all the underlying physical properties for the corresponding underlying problem, such as discontinuity, as well as positivity and stability . It also includes the use of more complicated denominator functions, allowing us take large time steps without sacrificing the solution's accuracy of the nonstandard method. The numerical experiments show the effectiveness of the numerical method.

Test cases based on real data of the precipitation are presented in chapter 5. We have used the monthly precipitation as the unit of time because it has shown a more appropriate fit for the seasonal component $\theta(t)$. The unit of time is a key factor in determining a model for the dynamics of the rainfall process, and then get meaningful values of the weather derivative contract. However, similar test cases can be done using day as the unit of time.

8.1 Future work

We can consider extensions of this research in various interesting directions.

The model for rainfall weather variables proposed in this research is based on the assumption that the dynamics of monthly rainfall process follows Ornstein-Uhlenbeck process, which belongs to the class of mean reverting process. Then, different mean reverting models can be tested for historical data as well as the inclusion of more complex dynamic models of the behaviour of rainfall process. However, the model used here, seems to catch properly the dynamics of the monthly rainfall process on the two locations in study. Furthermore, if a day is taken as a unit of time for rainfall data, the censored mean reverting process can be tested.

The methodology used here to derive the model of European option price is based on the assumption of the self-financing portfolio principle. The risk-free portfolio is achieved by consider the market price of risk which has to be extracted from the quoted rainfall contract in the market. However, there are not enough negotiated contracts in order to be used. Another direction could be to consider an approach that uses a correlated underlying asset. Then, the correlation between rainfall and other commodity contracts also needs to be investigated and modeled.

Regarding the numerical methods developed in this research, it would be interesting to analyse the positive conditions of the nonstandard numerical method developed. Would be interesting also to compare between the fitted exponential schemes and the nonstandard numerical methods. Both of them are based on the theory of exact schemes, and are appropriate for boundary layer problems, that is, problems with rapidly increasing or decreasing solutions such as convection-dominated PDEs. Furthermore, the nonstandard numerical methods combined with the operator splitting approaches open a new range of numerical methods to consider in the future.

References

Alaton, P., Djehiche, B., & Stillberger, D. (2002). On modelling and pricing weather derivatives. *Applied mathematical finance*, *9*(1), 1–20.

Alexandridis, A., & Zapranis, A. (2013). *The weather derivatives market*. Springer.

Allen, E. (2007). *Modeling with itô stochastic differential equations* (Vol. 22). Springer Science & Business Media.

Araújo, A., Das, A., & Sousa, E. (2014). A numerical approach to study the kramers equation for finite geometries: Boundary conditions and potential fields. *Journal of Physics A: Mathematical and Theoretical*, *48*(4), 045202.

Arenas, A., González-Parra, G., & Caraballo, B. (2013). A nonstandard finite difference scheme for a nonlinear black–scholes equation. *Mathematical and Computer Modelling*, *57*(7-8), 1663–1670.

Balter, A., & Pelsser, A. (2018). Pricing and hedging in incomplete markets with model uncertainty. *Netspar Discussion Paper*, (01/2015-002).

Basawa, I., & Rao, B. (1980). Asymptotic inference for stochastic processes. *Stochastic Processes and their Applications*, *10*(3), 221–254.

Benth, F., & Saltyte-Benth, J. (2012). *Modeling and pricing in financial markets for weather derivatives* (Vol. 17). World Scientific.

Bibby, B., & Sørensen, M. (1995). Martingale estimation functions for discretely observed diffusion processes. *Bernoulli*, 17–39.

Björk, T. (1998). *Arbitrage theory in continuous time*. Oxford university press, New York.

Björk, T. (2009). *Arbitrage theory in continuous time*. Oxford university press.

Brix, A., Jewson, S., & Ziehmann, C. (2002). Weather derivative modelling and valuation: A statistical perspective. *Climate Risk and the Weather Market. Risk Books, London*, 127–150.

Brockwell, P., Davis, R., & Fienberg, S. (1991). *Time series: Theory and methods: Theory and methods*. Springer Science & Business Media.

Broni-Mensah, E. (2012). *Numerical solutions of weather derivatives and other incomplete market problems* (Doctoral dissertation). The University of Manchester (United Kingdom).

Cabrera, B., Odening, M., & Ritter, M. (2013). Pricing rainfall futures at the cme. *Journal of Banking & Finance*, *37*(11), 4286–4298.

Cao, M., & Wei, J. (2004). Weather derivatives valuation and market price of weather risk. *Journal of Futures Markets: Futures, Options, and Other Derivative Products*, *24*(11), 1065–1089.

Carmona, R., & Diko, P. (2005). Pricing precipitation based derivatives. *International Journal of Theoretical and Applied Finance*, *8*(07), 959–988.

Cerny, A. (2009). *Mathematical techniques in finance: Tools for incomplete markets*. Princeton University Press.

Chen, Y. (2017). Numerical methods for pricing multi-asset options. *University of Toronto, Toronto*, 1–75.

Chidzalo, P., Ngare, P. O., & Mung'atu, J. K. (2023). Pricing weather derivatives under a tri-variate stochastic model. *Scientific African*, *21*, e01768.

Coe, R., & Stern, R. (1982). Fitting models to daily rainfall data. *Journal of Applied Meteorology and Climatology*, *21*(7), 1024–1031.

Coles, S., Pericchi, L., & Sisson, S. (2003). A fully probabilistic approach to extreme rainfall modeling. *Journal of Hydrology*, *273*(1-4), 35–50.

Cox, D., & Isham, V. (1988). A simple spatial-temporal model of rainfall. *Proceedings of the Royal Society of London. A. Mathematical and Physical Sciences*, *415*(1849), 317–328.

Davidson, A., & Levin, A. (2014). *Mortgage valuation models: Embedded options, risk, and uncertainty*. Oxford University Press.

Delbaen, F., & Schachermayer, W. (2006). *The mathematics of arbitrage*. Springer Science & Business Media.

The deutscher wetterdienst. (n.d.). https://www.dwd.de (accessed November 2022)

Dischel, R., & Barrieu, P. (2002). *Financial weather contracts and their application in risk management*. Risk Books.

Duffy, D. J. (2006). *Finite difference methods in financial engineering: A partial differential equation approach*. John Wiley & Sons.

Duffy, D. (2004). A critique of the crank nicolson scheme strengths and weaknesses for financial instrument pricing. *70+ DVD's FOR SALE & EXCHANGE*, 333.

Duffy, D. (2022). *Numerical methods in computational finance: A partial differential equation (pde/fdm) approach*. John Wiley & Sons, Limited.

Ehrhardt, M., & Mickens, R. E. (2013). A nonstandard finite difference scheme for convection–diffusion equations having constant coefficients. *Applied Mathematics and Computation*, *219*(12), 6591–6604.

Emmerich, C., Günther, M., & Nelles, M. (2005). *Modelling and simulation of rain derivatives* (Doctoral dissertation). MS thesis, University of Wuppertal, Wuppertal, Germany.

Feng, Y., & Kitzmiller, D. (2006). A short-range quantitative precipitation forecast algorithm using back-propagation neural network approach. *Advances in Atmospheric Sciences*, *23*, 405–414.

Foufoula-Georgiou, E., & Guttorp, P. (1986). Compatibility of continuous rainfall occurrence models with discrete rainfall observations. *Water Resources Research*, *22*(8), 1316–1322.

Geiser, J. (2015). Recent advances in splitting methods for multiphysics and multiscale: Theory and applications. *Journal of Algorithms & Computational Technology*, *9*(1), 65–93.

Geyser, J. (2004). Weather derivatives: Concept and application for their use in south africa. *Agrekon*, *43*(4), 444–464.

Glasbey, C., & Nevison, I. (1997). Rainfall modelling using a latent gaussian variable. *Modelling longitudinal and spatially correlated data*, 233–242.

Haan, C., Allen, D., & Street, J. (1976). A markov chain model of daily rainfall. *Water Resources Research*, *12*(3), 443–449.

Hageman, L., & Young, D. (2012). *Applied iterative methods*. Courier Corporation.

Hamisultane, H. (2008). Which method for pricing weather derivatives? *HAL, archives-ouvertes.fr*, (halshs-00355856).

Hannachi, A. (2014). Intermittency, autoregression and censoring: A first-order ar model for daily precipitation. *Meteorological Applications*, *21*(2), 384–397.

Haug, E. (2007). The complete guide to option pricing formulas. *(No Title)*.

Hess, G., Leslie, L., Guymer, A., & Fraedrich, K. (1989). Application of a markov technique to the operational, short-term forecasting. *Australian Meteorological Magazine*, *37*(2).

Hirsch, C. (1988). *Numerical computation of internal & external flows: Fundamentals of numerical discretization*. John Wiley & Sons, Inc.

Hirsch, C. (2007). *Numerical computation of internal and external flows: The fundamentals of computational fluid dynamics*. Elsevier.

Hull, J. (2009). *Options, futures and other derivatives*. Upper Saddle River, NJ: Prentice Hall.

Hull, J. (2012). *Risk management and financial institutions* (Vol. 733). John Wiley & Sons.

Iacus, S. (2009). *Simulation and inference for stochastic differential equations: With r examples*. Springer Science & Business Media.

Iacus, S. (2011). *Option pricing and estimation of financial models with r*. John Wiley & Sons.

Karatzas, I., & Shreve, S. (1988). *Brownian motion and stochastic calculus*. Springer Verlag, New York.

Karatzas, I., & Shreve, S. (1998). *Methods of mathematical finance* (Vol. 39). Springer.

Katz, R. (1977). Precipitation as a chain-dependent process. *Journal of Applied Meteorology (1962-1982)*, 671–676.

Kavvas, M., & Delleur, J. (1981). A stochastic cluster model of daily rainfall sequences. *Water Resources Research*, *17*(4), 1151–1160.

Kedem, B., Pavlopoulos, H., Guan, X., & Short, D. (1994). A probability distribution model for rain rate. *Journal of Applied Meteorology and Climatology*, *33*(12), 1486–1493.

Kelman, J. (1977). *Stochastic modeling of hydrologic, intermittent daily processes* (Doctoral dissertation). Colorado State University. Libraries.

Kermiche, L., & Vuillermet, N. (2016). Weather derivatives structuring and pricing: A sustainable agricultural approach in africa. *Applied Economics*, *48*(2), 165–177.

Klebaner, F. (2005). Introduction to stochastic calculus with applications, monash university, australia.

Kojouharov, H., & Chen, B. (1999). Nonstandard methods for the convective-dispersive transport equation with nonlinear reactions. *Numerical Methods for Partial Differential Equations: An International Journal*, *15*(6), 617–624.

Kojouharov, H., & Chen-Charpentier, B. (2004). Nonstandard eulerian lagrangian methods for multi-dimensional reactive transport problems. *Applied numerical mathematics*, *49*(2), 225–243.

Leobacher, G., & Ngare, P. (2011). On modelling and pricing rainfall derivatives with seasonality. *Applied Mathematical Finance*, *18*(1), 71–91.

LeVeque, R. J. (2007). *Finite difference methods for ordinary and partial differential equations: Steady-state and time-dependent problems*. SIAM.

Li, P. (2018). Pricing weather derivatives with partial differential equations of the ornstein–uhlenbeck process. *Computers & Mathematics with Applications*, *75*(3), 1044–1059.

Li, P. (2021). The valuation of weather derivatives using one sided crank–nicolson schemes. *Computational Economics*, *58*(3), 825–847.

Li, P., Lu, X., & Zhu, S.-P. (2020). Pricing weather derivatives with the market price of risk extracted from the utility indifference valuation. *Computers & Mathematics with Applications*, *79*(12), 3394–3409.

Little, M., McSharry, P., & Taylor, J. (2009). Generalized linear models for site-specific density forecasting of uk daily rainfall. *Monthly weather review*, *137*(3), 1029–1045.

Lubuma, J. M.-S., & Patidar, K. C. (2005). Contributions to the theory of non-standard finite difference methods and applications to singular perturbation problems. In *Advances in the applications of nonstandard finite difference schemes* (pp. 513–560). World Scientific.

Malawi-weatherhedge-foodsecurity. (n.d.). https://documents1.worldbank.org/curated/en/945561468302479116/pdf/81171-Malawi-WeatherHedge-FoodSecurity-2015.pdf (accessed November 2023)

Managing climate risk with cme. (n.d.). https://www.cmegroup.com/education/articles-and-reports/managing-climate-risk-with-cme-group-weather-futures-and-options.html (accessed November 2023)

Mandel, M. (2007). Censoring and truncation—highlighting the differences. *The American Statistician*, *61*(4), 321–324.

Margrabe, W. (1978). The value of an option to exchange one asset for another. *The journal of finance*, *33*(1), 177–186.

Mickens, R. (1994). *Nonstandard finite difference models of differential equations*. world scientific.

Mickens, R. (2000). *Applications of nonstandard finite difference schemes*. World Scientific.

Mickens, R. (2005). *Advances in the applications of nonstandard finite difference schemes*. World Scientific.

Mickens, R. (2020). *Nonstandard finite difference schemes: Methodology and applications*. World Scientific.

Mickens, R. E. (2007). Calculation of denominator functions for nonstandard finite difference schemes for differential equations satisfying a positivity condition. *Numerical Methods for Partial Differential Equations: An International Journal*, *23*(3), 672–691.

Miyahara, Y. (2011). *Option pricing in incomplete markets: Modeling based on geometric lévy processes and minimal entropy martingale measures* (Vol. 3). World Scientific.

Morton, K. W. (1996). Numerical solution of convection-diffusion problems. *(No Title)*.

Nasa power data access viewer. (n.d.). https://power.larc.nasa.gov/data-access-viewer/ (accessed November 2022)

Nhangumbe, C., Fredericks, E., & Canhanga, B. (2020). Lie symmetry analysis on pricing weather derivatives by partial differential equations. *Algebraic Structures and Applications: SPAS 2017, Västerås and Stockholm, Sweden, October 4-6*, 875–901.

Nhangumbe, C., & Sousa, E. (2024). Numerical solutions of an option pricing rainfall weather derivatives model. *Computers & Mathematics with Applications*, *153*, 43–55.

Noven, R., Veraart, A., & Gandy, A. (2015). A lévy-driven rainfall model with applications to futures pricing. *AStA Advances in Statistical Analysis*, *99*, 403–432.

Odening, M., Musshoff, O., & Xu, W. (2007). Analysis of rainfall derivatives using daily precipitation models: Opportunities and pitfalls. *Agricultural Finance Review*, *67*(1), 135–156.

Oksendal, B. (2000). *Stochastic differential equations: An introduction with applications*. Springer Verlag, New York.

Oksendal, B. (2003). *Stochastic differential equations: An introduction with applications*. Springer Verlag, Berlin.

Park, J. W., Genton, M. G., & Ghosh, S. K. (2007). Censored time series analysis with autoregressive moving average models. *Canadian Journal of Statistics*, *35*(1), 151–168.

Pavlopoulos, H. (1991). *Statistical inference for optimal thresholds*. University of Maryland, College Park.

Pavlopoulos, H., & Kedem, B. (1992). Stochastic modeling of rain rate processes: A diffusion model. *Communications in statistics. Stochastic models*, *8*(3), 397–420.

Pirrong, C., & Jermakyan, M. (2001). The price of power: The valuation of power and weather derivatives. *Working Paper, Oklahoma State University*.

Pirrong, C., & Jermakyan, M. (2008). The price of power: The valuation of power and weather derivatives. *Journal of Banking & Finance*, *32*(12), 2520–2529.

Rajagopalan, B., Lall, U., & Tarboton, D. G. (1996). Nonhomogeneous markov model for daily precipitation. *Journal of Hydrologic Engineering*, *1*(1), 33–40.

Ramirez, M., de Campos Velho, H., & Ferreira, N. (2005). Artificial neural network technique for rainfall forecasting applied to the sao paulo region. *Journal of hydrology*, *301*(1-4), 146–162.

Richtmyer, R. (1967). Kw morton differential methods for initial-value problems john wiley & sons inc. *New York*.

Risk net. first south african weather derivatives contract. (n.d.). https://www.risk.net/exchanges/1506167/gensec-structures-first-south-african-weather-derivatives-contract (accessed November 2023)

Roache, P. (1998). Fundamentals of computational fluid dynamics(book). *Albuquerque, NM: Hermosa Publishers*.

Rodriguez-Iturbe, I., Cox, D., & Isham, V. (1987). Some models for rainfall based on stochastic point processes. *Proceedings of the Royal Society of London. A. Mathematical and Physical Sciences*, *410*(1839), 269–288.

Sheppard, R. (2007). *Pricing equity derivatives under stochastic volatility: A partial differential equation approach* (Doctoral dissertation). University of the Witwatersrand.

Smith, R., & Schreiber, H. (1973). Point processes of seasonal thunderstorm rainfall: 1. distribution of rainfall events. *Water Resources Research*, *9*(4), 871–884.

Sod, G. (1985). *Numerical methods in fluid dynamics: Initial and initial boundary-value problems* (Vol. 1). Cambridge University Press.

Sousa, E. (2009). On the edge of stability analysis. *Applied Numerical Mathematics*, *59*(6), 1322–1336.

Stoppa, A., & Hess, U. (2003). Design and use of weather derivatives in agricultural policies: The case of rainfall index insurance in morocco. *International Conference "Agricultural Policy Reform and the WTO: Where are we heading", Capri (Italy)*.

Tang, W., & Chang, S. (2016). A semi-lagrangian method for the weather options of mean-reverting brownian motion with jump–diffusion. *Computers & Mathematics with Applications*, *71*(5), 1045–1058.

Todorovic, P., & Woolhiser, D. A. (1975). A stochastic model of n-day precipitation. *Journal of Applied Meteorology (1962-1982)*, 17–24.

Tong, Z., & Liu, A. (2021). A censored ornstein–uhlenbeck process for rainfall modeling and derivatives pricing. *Physica A: Statistical Mechanics and its Applications*, *566*, 125619.

Topper, J. (2005). *Financial engineering with finite elements*. John Wiley & Sons.

Tsakiris, G., Pangalou, D., & Vangelis, H. (2007). Regional drought assessment based on the reconnaissance drought index (rdi). *Water resources management*, *21*, 821–833.

Unami, K., Abagale, F., Yangyuoru, M., Alam, A., & Kranjac-Berisavljevic, G. (2010). A stochastic differential equation model for assessing drought and flood risks. *Stochastic environmental research and risk assessment*, *24*(5), 725–733.

Unesco report: World distribution of arid regions. (n.d.). https://unesdoc.unesco.org/ark:/48223/pf0000032661 (accessed November 2023)

Vardi, Y. (1985). Empirical distributions in selection bias models. *The Annals of Statistics*, 178–203.

Varga, R. (1962). Matrix iterative analysis. englewood cliffs, nj: Prenticehall.

Weather products. (n.d.). https://www.cmegroup.com/trading/weather/ (accessed November 2023)

Wilks, D. (1998). Multisite generalization of a daily stochastic precipitation generation model. *journal of Hydrology*, *210*(1-4), 178–191.

Williams, P. (1997). Modelling seasonality and trends in daily rainfall data. *Advances in neural information processing systems*, *10*.

Wilmott, P. (2013). *Paul wilmott on quantitative finance*. John Wiley & Sons.

World bank. 2022. poverty and shared prosperity 2022. (n.d.). https://open-knowledge.worldbank.org/entities/publication/a33782e6-415e-5699-a9a8-4a50dc4ae3bc (accessed November 2023)

World bank. agriculture and ruraldevelopment. (n.d.). https://www.worldbank.org/en/programs/knowledge-for-change/brief/agriculture-and-rural-development (accessed November 2023)

Zeger, S. L., & Brookmeyer, R. (1986). Regression analysis with censored autocorrelated data. *Journal of the American Statistical Association*, *81*(395), 722–729.

Zeng, L. (2000). Pricing weather derivatives. *The Journal of Risk Finance*, *1*(3), 72–78.